RAILWAY INTERFERENCE MANAGEMENT

TLM Modelling in Railway Applications

by

Adesegun A. Ogunsola

A Doctoral Thesis

Submitted in partial fulfilment of the *requirements for the award of*

Doctor of Philosophy

of

Loughborough University

June 2008

ABSTRACT

RAILWAY INTERFERENCE MANAGEMENT

TLM Modelling in Railway Applications

by Adesegun. A. Ogunsola

This thesis deals with the application of analytical and numerical tools to Electromagnetic Compatibility (EMC) management in railways. Analytical and numerical tools are applied to study the electromagnetic coupling from an alternating current (AC) electrified railway line, and to study the electrical properties of concrete structure - a widely used component within the railway infrastructure. An electrified railway system is a complex distributed system consisting of several sub-systems, with different voltage and current levels, co-located in a small area.

An analytical method, based on transmissions line theory, is developed to investigate railway electromagnetic coupling. The method is used to study an electrified railway line in which the running rails and earth comprise the current return path. The model is then modified to include the presence of booster transformers. The analytical model can be used to study the railway current distribution, earth potential and electromagnetic coupling - inductive and conductive coupling - to nearby metallic structures. The limiting factor of the analytical model is the increasing difficulty in resolving the analytical equation as the complexity of the railway model increases.

A large scale railway numerical model is implemented in Transmission Line Matrix (TLM) and the electromagnetic fields propagated from the railway model is studied. As this work focuses on the direct application of TLM in

railway EMC management, a commercially available TLM software package is used. The limitation of the numerical model relates to the increased computation resource and simulation time required as the complexity of the railway model increases.

The second part of this thesis deals with the investigation of the electrical properties of concrete and the development of a dispersive material model that can be implemented in numerical simulators such as TLM. Concrete is widely used in the railway as structural components in the construction of signalling equipment room, operation control centres etc. It is equally used as sleepers in the railway to hold the rails in place or as concrete slabs on which the whole rail lines are installed. It is thus important to understand the contribution of concrete structures to the propagation of electromagnetic wave and its impact in railway applications.

An analytical model, based on transmission line theory, is developed for the evaluation of shielding effectiveness of a concrete slab; the analytical model is extended to deal with reinforced concrete slab and conductive concrete. The usefulness and limitation of the model is discussed. A numerical model for concrete is developed for the evaluation of the effectiveness of concrete as a shield. Initially, concrete is modelled as a simple dielectric material, using the available dielectric material functionality within TLM.

It is noted that the simple dielectric model is not adequate to characterise the behaviour of concrete over the frequency range of interest. Better agreement is obtained with concrete modelled as a dispersive material having material properties similar to that exhibited by materials obeying Debye equation. The limitations of the dispersive material model are equally discussed.

The design of conductive concrete is discussed, these have application in the railway industry where old existing structures are to be converted to functional rooms to house sensitive electronic system. A layer of conductive concrete can be applied to the façade to enhance the global shielding of the structure.

TABLE OF CONTENTS

LIST OF FIGURES

Figure *Page*

LIST OF TABLES

ACKNOWLEDGMENTS

The work that has been presented in this thesis could not have been possible without the support and encouragement of many people. Here, I would like to take the opportunity to thank them all.

First, I wish to express my gratitude to Dr Simon C. Pomeroy, my thesis supervisor, for the stimulating scientific discussions and encouragement. I am often impressed with the way in which he directed my focus and by the enthusiasm with which he used analogies from related fields to explain those things about TLM that baffled me.

I would like to thank Robert Seager of the Department of Electrical and Electronics for his invaluable time and discussions on the use of Microstripes™. I also would like to thank Prof Ugo Reggiani and Dr Leonardo Sandrolini, of the University of Bologna, Italy, for their friendship and shared academic interest in 'Electromagnetic Shielding".

I also have to thank Prof C.C. Okoro, Dr Ike Mowete and Dr Frank Okafor of the Department of Electrical and Electronics Engineering, University of Lagos, Nigeria for their support. I would like to thank my colleagues at Parsons Group International, especially Dr Alan Rumsey and Paul Thomas, for giving me the space to be me.

I would like to thank Ibiyemi Olaitan, Andrew Akoto and Dr Ajala, *we never know how high we are till we are asked to rise and then if we are true to plan, our statures touch the skies.* It's been a long mile.

To my father, Adepoju Ogunsola, for his encouragement and support throughout this academic journey. You have always been there.

Finally, I wish to thank my children Adeola and Jadesola for being a great source of inspiration and to my wife, Folashade, for her support, her faith in me, and her ability to put things into perspective.

Adesegun A Ogunsola

DEDICATION

This thesis is dedicated to

Fadekemi and Adefunke Ogunsola

That we might clasp, ere closed, the book of faith
And make the writer on a fairer leaf
Inscribe our names, or quite obliterate

Ah! Lord, could you and I with fate conspire
To mend this sorry scheme of things entire
Would we not shatter it to bits, and then
Remould it nearer to the heart's desire?

Omar Khayyam (1048 – 1131)

To My Late Sister and Mother

LIST OF SYMBOLS

ω	Angular frequency
ω_r	Relaxation frequency
μ_0	Magnetic permeability of vacuum and air
μ_r	Relative magnetic permeability
σ	Conductivity
ρ	Resisitvity
ε_r	Relative permittivity
ε^*	Complex permittivity
ε'	Real part of the complex permittivity
ε''	Imaginary part of the complex permittivity
L	Separation distance between the load (train) and the feeder station
L''	Separation distance between the load (train) and a Booster Transformer
x	Horizontal distance along the equivalent rail
γ	Propagation constant
C	Conductance
I	Current
I_c	Catenary current
I_r	Rail current
k	Coupling factor
I_0	Modified Bessel functions of the first kind and zero order
I_1	Modified Bessel function of the first kind and first order
K_0	Modified Bessel function of the second kind and zero order

K_1	Modified Bessel function of the second kind and first order
V	Voltage
V_E	Impressed earth potential in the earth
Z_0	Characteristics Impedance
Z_m	Mutual Impedance
Z_A, Z_B	Earthing Impedance at the end points of a conductor
Y	Admittance

Chapter 1

INTRODUCTION

The railway as a form of transport was first introduced in the United Kingdom in the year 1803. Increasing demands for stronger engines and higher speed together with the development of electrical motors led to the demand for electrified railways. The first electric traction system used in the United Kingdom (in 1890) was a third rail 600V DC traction system. Due to the limitations of this system and the ever-increasing demand for efficiency, power and higher speeds AC electric traction systems were introduced.

In the United Kingdom, the AC traction system is a single-phase system with overhead catenary and the running rails used for traction return current and signalling purposes. The system operates at power frequency of 50 Hz and a voltage of 25 kV. The 25 kV 50 Hz AC traction supply was first introduced in the United Kingdom in the 1950's. The ability to connect single-phase traction loads to the transmission system (132kV) supplied by the National Grid, without the requirement for special equipment or instructions to minimize traction loads under certain outage conditions, was a major factor in its implementation. The power supply process in this system consist of three stages:

- Catenary supply power from the feed station to the train;
- Current collection from the catenary to the train;
- Current return from the train location back to the feed station.

Chapter 2 covers the significance of the running rail, its impact on the electrification system as well as its safety implication. At this stage of the

thesis, it is worth mentioning that the running rails are used for signalling as well as for electrification purposes.

An electrified railway is an electromagnetically complex installation due to its physical size, the interaction between its constituent parts and the electromagnetic interference coupling mechanisms between these parts [1]. The railway should operate in a safe manner and should not pose any hazard to people. Electromagnetic Compatibility (EMC) as applied to the railway has three main areas of impact, the first being the effect on the railway environment, the second is its effect on signalling and communications equipment and the third is the ability of railway equipment to withstand the severe environment within which it has to operate.

1.1 The Relevance of Signalling

From the earliest days of railways, it was realised that some form of signalling would be required to control the movement of trains [2]. Signalling is the essential element in the control of train movements, being the link between the controller and the train crew. Railway signalling has developed from hand signals of the early 1800's through increasingly complicated mechanism to modern electronic techniques.

The railway signalling systems are designed to perform the following functions [3]:

- Maintain a safe distance between trains on the same track;
- Safe guard the movement of trains at junctions, and at crossings which could be taken by another;
- Regulate the passage of trains according to the service density and speed required;

- Ensure the safety of trains in the event of a failure.

While the railway signalling system has been developed to provide for the safe movement of mixed types of trains in conditions of high traffic density and increasing speed, equipment failure can still occur occasionally. To effectively assure signalling EMC, an understanding of the interference phenomena in the railway environment, the method of coupling into signalling installation and the sensitivities of signalling installation is required. Signalling installations are exposed to hazards of electromagnetic fields created by large currents (typically 2 kA to 6.8 kA for 750V DC powered trains and 300 A for 25 kV AC) and the effects of the currents themselves, which frequently are not contained by the return conductors and flow through the earth, causing local voltages.

1.2 Research Stimulus

The European Directive on EMC, 2004/108/EC[1], has a wide-ranging implication and repercussion for manufacturers of electrical, electronics apparatus and systems from both a product and legal perspective. The EMC Directive does not contain any standards or technical description, but gives generic legal and technical directions. The details of complying with the Directive are embodied in national laws and European standards. These standards are prepared to contribute to the effective opening of railway public procurement contracts to free competition, railway interoperatibility [4] and safe operation of rail networks.

The product specific standard, EN 50121, has been prepared so that the EMC Directive can be applied to railways and covers the emission and

[1] The EMC Directive 89/336/EEC was repealed on the 20th July 2007 and replaced with by a new EMC Directive, 2004/108/EC which came into force on the same day.

immunity aspect of EMC. The scope of EN 50121 covers inductive and conductive coupling mechanism with limits set from 9 kHz to 1 GHz, low frequency electromagnetic interference phenomena are not covered in much detail and limits are not set above 1 GHz[2] [5]. The omission of low frequency interference phenomena from EN 50121 implies that EMI due to traction return current remains untreated. It is fair to mention that certain low frequency interference phenomena are covered in other EU Directives and standards. For example, low frequency inductive coupling in telephone cables parallel to the railway are covered under the Radio-communication ITU-R recommendations (formerly CCITT Directive) [6] - [10]. However, there does not appear to be any regulation in force covering conductive coupling through earth for AC systems. Stray current effects in DC systems are covered in EN 50122 Part 2.

The EMC Directive and standards do not address the issue of safety or the impact of EMC on safety. However, the protection against line conductors and indirect contact from a safety point of view is dealt with in EN 50122 Part 1. No values for rail to earth resistance are given in this document but touch voltages originating from rail potential are adequately covered. The mode of failures and dangers due to traction return current following an unwanted path are also covered, however the focus of the standard is only on metallic contact between different systems. EN 50122-1 does not deal with any EMC related coupling mechanism.

For interference problems associated with return paths, the point of intersection between safety and EMC is extremely important. How does the earthing arrangement between the railway and signalling installation (in close

---

[2] The 2006 Edition of EN 50121 Part 4, now contains radiated immunity requirements up to 2.5 GHz.

proximity) effect railway EMC? What is the impact of the earthing arrangement on maintaining safety of the railway? How does the electrical properties of concrete slabs/structures or earth impact the electromagnetic coupling in a railway installation? What is the effect of low frequency interference on nearby buried metallic conductors and how can EMC and safety of the railway be assured in the presence of low frequency electromagnetic interference sources? The deployment of multi-system locomotives (e.g. Eurostar) and the implementation of common train control system across Europe (e.g. European Train Control System) for international traffic within Europe [4], [11] has emphasized the necessity for the development of formal techniques for assessing EMC and safety.

The traditional means of EMC assurance involves performing qualification test in accordance with test methods prescribed in product standards for railway applications, EN 50121. However, as mentioned above, this series of standards does not include evaluation of low frequency interference phenomena. For the purpose of safety assurance, the demonstration of *due diligence,* is achieved by demonstrating that the said product has been designed with an understanding of the electromagnetic environment in which the product is destined for and that all precautions have been taken to ensure compliance with the protection requirements of the EMC Directive.

In railway terms, due diligence is an assessment of the risk and that the risk has been reduced to As Low As Reasonably Practicably (ALARP). Due to the complexity of the railway and the cost associated with railway EMC approval, numerical techniques can be applied to address EMC related issues provided the model reflects the installation scenario and that the model can be validated against measurements. This will be particularly useful when applied to assess the risk of electromagnetic interference during the design phase of a railway project. However, the application of electromagnetic modelling to

large distributed systems such as railway installation is computationally challenging, more so when dielectric materials such as concrete structures/slabs and ground are included in the numerical model.

1.3 Objective and Scope of Work

While the European Railway industry is moving towards a common operational platform enabling inter-European rail traffic, the focus of this thesis will be on the AC electrified system found in the UK (i.e. 25 kV at 50 Hz). The main objectives of this research described in this thesis can be summarised as follows:

- Describe the physics of the coupling mechanism from the track to nearby buried metallic conductors;
- Use numerical techniques to quantify the coupling mechanism (inductive coupling) and assess the suitability of such techniques for inclusive in EMC and Safety Conformity arguments as part of a System Safety Case;
- Study the impact of concrete structures/slabs as a propagation medium within the railway environment;

A comparison of both analytical and numerical techniques for evaluating the coupling mechanism will be undertaken. With respect to low frequency coupling, the research will focus on the frequency range of a few Hz up to 9 kHz, however the case study will be limited to the fundamental frequency. The analysis will be restricted to inductive coupling from the track to nearby buried metallic conductors. For concrete slabs, the electrical properties from 30 MHz to 1 GHz would be investigated.

1.4 Structure of Thesis

The thesis can be divided into four parts. There are eight chapters, a number of which can be read in non-consecutive order. In particular, the chapters

covering the analytical and numerical analysis can be referred to in any sequence. Following the introductory chapter, the remaining seven chapters fall into three parts: Chapters 2 and 3, cover background literature on railway and railway EMC management processes, Chapters 4 to 6 covers analytical and numerical analysis of low frequency coupling in railway, Chapter 7 cover analytical and numerical simulations of concrete slabs/structures, while Chapter 8 presents the conclusions and discussions.

1.5 Achievements

Electromagnetic Compatibility (EMC) management in railway is an important system assurance activity that cannot be ignored. The railway as a complex system consist of high energy sources in close proximity to sensitive signalling and communication circuits. For an electrified railway, the power supply rails and/or overhead line provide an effective electromagnetic coupling mechanism by which electromagnetic interference from the train impacts the correct and safe operation of safety critical systems. Furthermore, the use of the running rails for railway signalling provides an effective means of coupling electromagnetic fields into wayside installations as well as into nearby buried metallic structures.

With the design and build cost of a Light Rail Transport (LRT) costing between £15 - £30 million per km route, and the cost of an in-situ EMC test on the railway costing about £100,00 per day there is a desire to apply EMC engineering tools during the design phase with the view of optimising the design and ensuring electromagnetic compatibility.

Analytical and numerical methods are powerful tools for an EMC Engineer. These can be used to simulate the behaviour of a system, in different system configurations, during the design phase of a railway project lifecycle having

the advantage of avoiding bad design, post installation retrofit costs etc. However, applying this tools to a complete railway system is an extremely difficult task due to the large problem space being modelled. Despite this, this research focused on the application of analytical and numerical tools for EMC Management in railways.

In the course of the research performed in this thesis, the following achievements were made:

- A theoretical framework was developed describing the low frequency electromagnetic coupling from an ac electrified railway line to nearby buried metallic structures (§4). This was achieved by detailed description of the current distribution between the conductors of the current return path.

- An analytical model was developed describing the current distribution between conductors of the current return path, earth potential and electromagnetic to nearby buried metallic structures (§4.4)

- A large scale railway model was developed for use TLM, for the assessment of the electromagnetic fields and coupling from an electrified railway to nearby installations (§6). The 10 km railway model did not include booster transformers, sleepers, ballast etc. These infrastructure elements can easily be included in the model at the expense of increase computation time and resource.

- An analytical model was developed to assess the ability of concrete to attenuate electromagnetic waves (§7.2 and §7.2.2). The model was expanded to include the analysis of reinforced concrete (§7.2.1) and conductive concrete (§7.3). The model assumes that the concrete structure is infinite and ignores discontinuities in the concrete

structure. The model analyses the impact of moisture content on the ability of concrete structures to attenuate electromagnetic waves.

- A concrete material model suitable for use in numerical simulators, in particular TLM, was developed (§7.2.3). The model was used to predict the shielding effectiveness of concrete over a wide frequency range and the results obtained with the material model was in good agreement with those obtained via measurement. To implement this model, the measured complex permittivity data would have to be used.

1.6 References

[1] Holmes, R. "*EMC of electrified railways*", Electric Railways in a United Europe, IEE Conference, March 1995, Pg. 131 – 135.

[2] Kichenide, G. M and Williams, A. " *British Railway Signalling*", 3rd Edition, 1975, Pg. 7

[3] Nock, O. S. "*Railway Signalling*", ISBN: 0713637498, March 1980, Pg. 1

[4] Council Directive, 89/336/EEC, " *Council Directive on the approximation of the laws of the Member States relating to Electromagnetic compatibility (EMC)*", OJ L139 of May 1989

[5] Dell' Aquila *et al*, "*Investigation of low frequency EMI produced by inverters feed linear inductor motor drives in railway system*", 4th European Symposium on Electromagnetic Compatibility, EMC Europe 2000, Brugge, September 2000.

[6] *Directives concerning the protection of telecommunication lines against harmful effects from electric power and electrified railway lines. Vol. 1: Design, construction and operational principles of telecommunication, power and electrified railway facilities.* CCITT, 1989.

[7] *Directives concerning the protection of telecommunication lines against harmful effects from electric power and electrified railway lines. Vol. 2: Calculating induced voltages and currents in practical cases.* CCITT, 1989

[8] *Directives concerning the protection of telecommunication lines against harmful effects from electric power and electrified railway lines. Vol. 3: Capacitive, inductive and conductive coupling: physical theory and calculation methods.*

CCITT, 1989

[9] *Directives concerning the protection of telecommunication lines against harmful effects from electric power and electrified railway lines. Vol. 4: Inducing currents and voltages in electrified railways systems.* CCITT, 1989

[10] *Directives concerning the protection of telecommunication lines against harmful effects from electric power and electrified railway lines. Vol. 6: Dangers and disturbance.* CCITT, 1989

[11] Council Directive, 96/48/EEC, " *Council Directive on the interoperability of the trans-European high speed rail system*", 1996

[12] Green, D. R. M. "*Certifying railway systems for the EC Directive on EMC*", Railway Traction and Braking, Railtech '96, 1996.

[13] BS EN 50121 –1: 2006, *"Railway Applications – Electromagnetic Compatibility, Part 1: General"*, August 2006.

[14] BS EN 50121 – 2: 2006, *"Railway Applications – Electromagnetic Compatibility, Part 2: Emission of the whole railway system to the outside world"*, August 2006.

[15] BS EN 50121 – 3 –1: 2006, *"Railway Applications – Electromagnetic Compatibility, Part 3-1: Rolling Stock – train and complete vehicle"*, August 2006.

[16] BS EN 50121 – 3 – 2: 2006, *"Railway Applications – Electromagnetic Compatibility, Part 3-2: Rolling Stock – rolling stock apparatus"*, August 2006.

[17] BS EN 50121 – 4: 2006, *"Railway Applications – Electromagnetic Compatibility, Part 4: Emission and Immunity of Signalling and Telecommunications apparatus"*, August 2006.

[18] BS EN 50121 – 5: 2006, *"Railway Applications – Electromagnetic Compatibility, Part 5: Fixed Power Supply Installations"*, August 2006

[19] Statutory Instruments 2006 No. 3142, "*The Electromagnetic Compatibility Regulations 2006*", HMSO, 2006.

[20] ERTMS/ETCS Class 1 Specification for an European Train Control System, ERTMS Core SRS Assessment Group, European Railway Agency, April 2000.

Chapter 2

AN OVERVIEW OF THE RAILWAY ENVIRONMENT

2.1 Power Supply Arrangement

A single-phase AC system operating at a fundamental frequency of 50 Hz and a voltage of 25 kV is employed in the UK for AC electrification. This system is used on all main line routes; in addition to this, DC electrification using the third rail configuration is also used on the main line. This configuration operates on a reduced voltage of 750 V DC. London Underground, however employs a fourth rail configuration for DC electrification, two rails (positive and negative) are used for a 660 V DC supply. Most urban transport trains use a third or fourth rail system.

Power is nominally supplied from the public network via substations where conversion from the three phase 50 Hz voltage to single-phase voltage takes place. In some European countries where a reduced frequency supply is used, i.e. 16 2/3 Hz, it is at this stage that the frequency conversion takes place. To ensure the continuity of the supply to the substation, high voltage feed to the substation is normally arranged from two sources of supply or by a double circuit 132 kV 50 Hz three-phase transmission line. The power supply arrangement will typically include two single phase transformer (10 or 12.5 MVA 132/25 kV), generally one leg of the 25 kV winding of the 132/25 kV transformer is earthed at the substation. Return feeders then connect the earthed end to all rails of the electrified rail opposite to the feeding post. Typically, substations are spaced 50 – 90 km apart, in the UK however, a spacing of 40 km is recommended [1]. Figure 2.1, depicts a typically power supply arrangement.

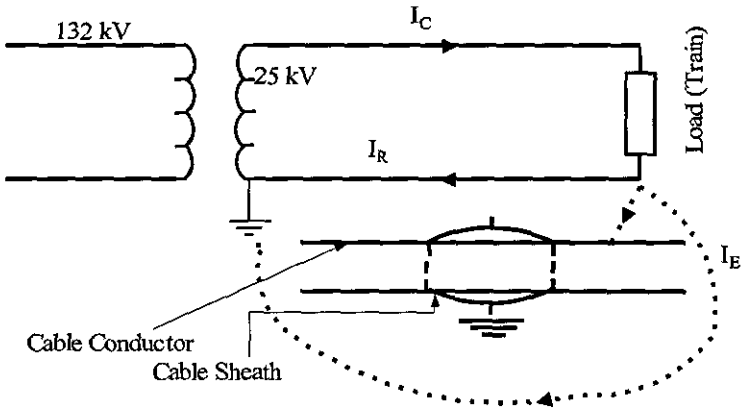

Figure 2.1: A typical power arrangement showing nearby buried conductor

2.2 Power Supply from the Catenary to the Load (Train)

The foremost function of electric traction is to keep the traction unit fed with the energy it requires. In AC electrification systems, current is supplied to the traction via an overhead wire (also referred to as the overhead catenary). The catenary consists of a suspension wire and a contact wire, which are suspended on masts. The two wires are connected by densely spaced bonds or droppers. The contact wire is a solid grooved copper or cadmium copper conductor with a cross-sectional area typically between 100 -107 mm^2, while the suspension wire is a standard cadmium copper conductor with a cross-section area typically between 50 – 65 mm^2. The dropper spacing is 9 m except the first and second droppers, which are 2.25 m and 6.75 m from the support respectively. Figure 2.2 shows a typical single catenary system employed on 25 kV AC electrification. For higher speed traffic, more complicated supporting arrangements between the suspension and catenary wires are employed.

The catenary current will split between the two conductors according to the impedance of the system. Current collection from the overhead catenary is achieved by a sliding pantograph. This current collection configuration involving the pantograph produces both mechanical and electromagnetic interference issues. The industry has been interested in the optimum design of the pantograph as well the catenary – pantograph combination as a source of high frequency interference. Fujiwara *et al* [2] presented a method for estimating the arc discharge rate using noise current flowing through the pantograph, while Lucca in [3] and [4] presents electrical models for calculating the radiated field produced by the pantograph – contact wire combination. The pantograph – catenary contact as a source of radio frequency interference is further discussed in [5].

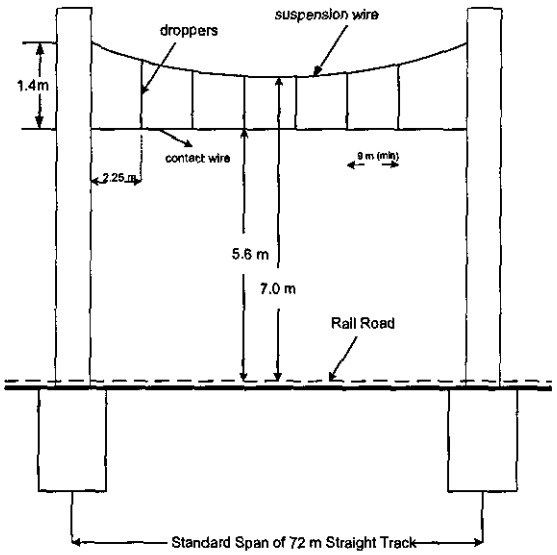

Figure 2.2: Typical single catenary system employed on 25 kV AC electrification

The feeder stations are normally run in parallel with the catenary operated as a continuous grid. Typical impedance for a catenary at 50 Hz is given as 0.169 + 0.612 Ω/ km in [6].

2.3 Return Current Path

The rails, being conductive and in contact with the wheels, form a means whereby electric current can flow to or from a vehicle from any point on the track. In AC electrification systems, the pantograph (fitted on the vehicle) collects the required traction current from the overhead lines and the return current passes via the wheels of the vehicle to the running rails and back to the supply point, completing the electric circuit. The use of the running rail as the return path for current is a special phenomenon in railway electrification, as the running rails are also used for signalling purposes.

In the following sub-sections, a simplistic description of the electrification installation involving the running rails is given. In the description presented, the following assumptions have been made:

- The train is assumed to be fed from one feeder station; and
- Only one train is present

2.3.1 Current Return via Running Rails Only

Figure 2.3, shows a simple arrangement whereby current is collected by the pantograph and flows from the vehicle to the feeder station via the running rails. In this type of installation, the rails are not earthed intentionally but achieve electrical contact with the earth by the use of sleepers and ballast. Due to the close proximity of the rail to earth, the return current will leak to ground within short distances and returns to the substation through its earth.

Electrically, the system just described, can be analysed as a transmission line with earth return, when the train is sufficiently far from the feeding station.

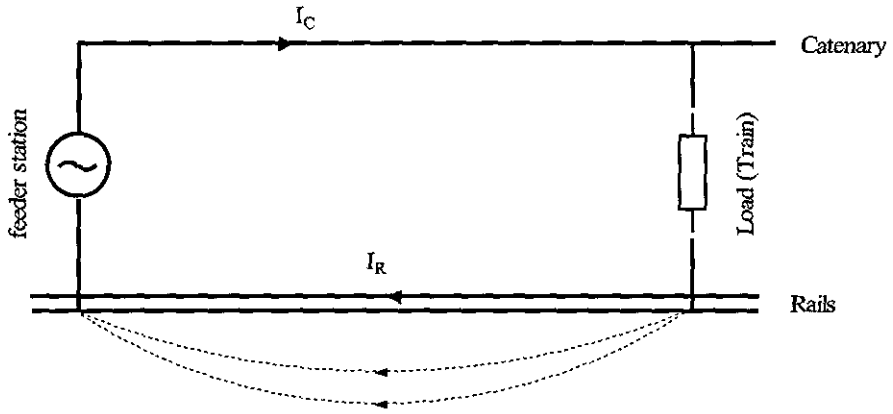

Figure 2.3: Current return via running rail only

The use of rail for traction current return presents two scenarios, (a) a system where both rails are used for return current paths and, (b) one where only one rail is used for return current path and the other for signalling. Although this arrangement is simple, the disadvantage is the loss of current to earth, which forms an unbalanced circuit. The effect of this unbalance is that by magnetic induction, the traction current may lead to induced voltages in neighbouring parallel conductors, such as signalling cables. The percentage of current return through the earth is dependent on the inductive coupling between the catenary and the rails, the rail leakage resistance to earth and the earth resistivity. This system is generally used in areas with high earth conductivity.

2.3.2 Systems with Booster Transformers (BT)

As discussed above, the simple arrangement of the overhead wire and the running rail for AC single-phase system of railway electrification forms an

unbalanced circuit. This results in the return current, which flows through the vehicle to the rail, to leak to earth. This leakage current may cause interference with nearby buried metallic conductors. To minimise the interference due to ground currents, a typical approach is to constrain the return current to flow through a restricted path (i.e. the running rail). In the railway, this is achieved by the use of booster transformers (BT). Booster transformers are, in effect, power current transformers with unity ratio (i.e. 1:1 current transformers) and are used with their primary windings connected in series with the overhead line (contact wire). The secondary windings of the transformer are connected directly to the running rails (this set-up is known as the *rail return configuration*) or to a special return conductor (this set-up is known as the *return conductor configuration*). Current flowing through the primary requires to be balanced by an equal amount in the secondary and, therefore a reduction in current flowing via stray path is achieved. Figure 2.4(a) shows a typical BT connection.

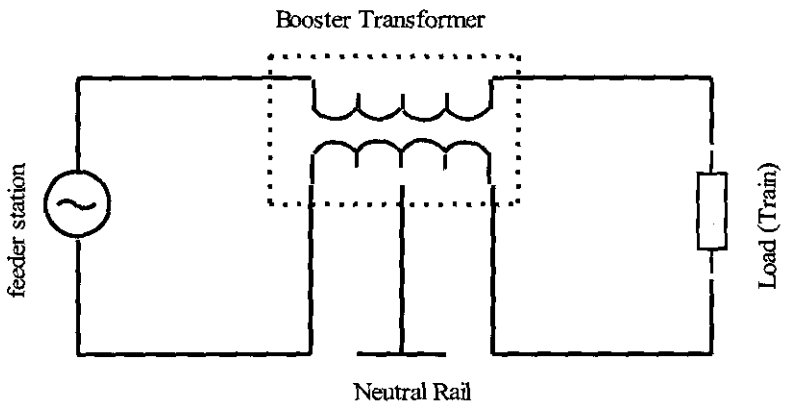

Figure 2.4(a): A Typical Booster Transformer Connection

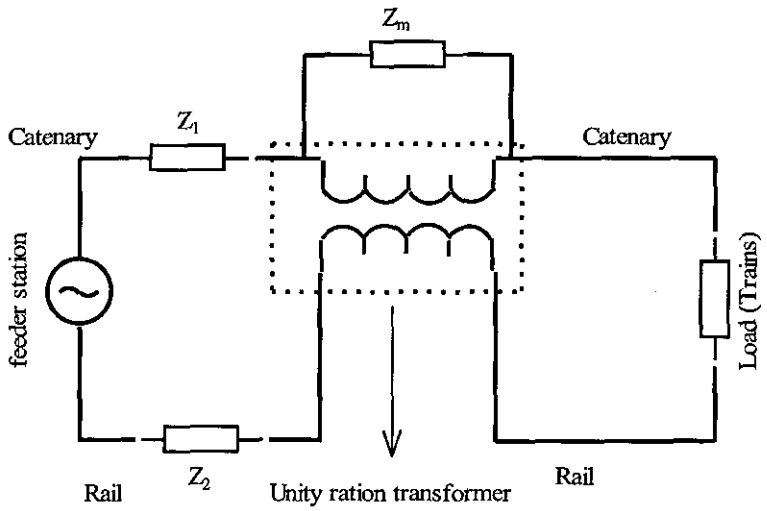

Figure 2.4(b): Equivalent circuit for the catenary and Booster Transformer

From Figure 2.4(a) and 2.4(b), it can be seen that the load on the secondary winding, which governs the voltage drop across the windings, is, in the simplest case the running rails. The secondary circuit is closed by imaginary conductors from points at zero potential on either side of the transformer.

2.3.2.1 Rail Return Configuration

As shown in Figure 2.5, the primary is connected in series with the contact line and the secondary winding in series with the running rails. Induced voltage in the secondary constrains the return current to flow through the rails. The transformers are spaced approximately 3.2 km apart. The BT spacing is governed by the touch voltage limits, of 60 V for a continuous duration greater than 300 seconds, specified in [7]. For large catenary currents the transformer can become saturated and unable to generate the

necessary electromotive force to collect current from the earth. The advantage of this arrangement is the reduction of earth currents, zero rail potential can be also be achieved between the train and the feeder station.

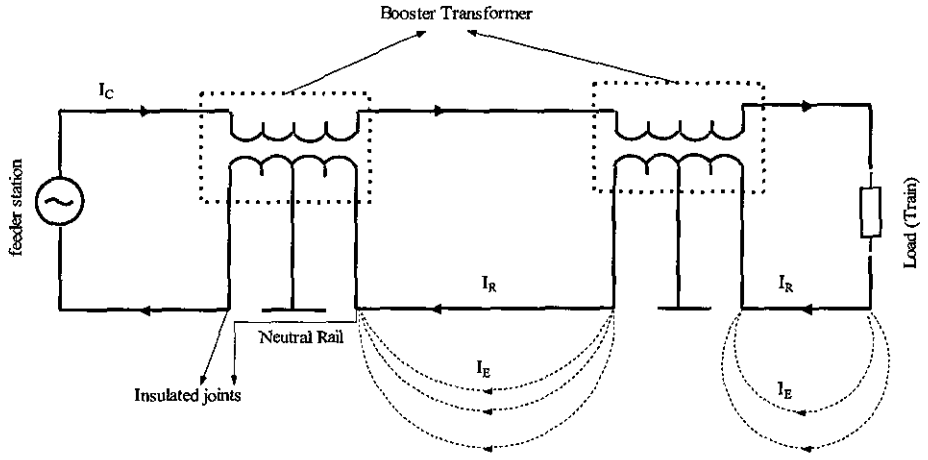

Figure 2.5: Rail Return Configuration with Booster Transformer (BT)

2.3.2.2 Return Conductor Configuration

As shown in Figure 2.6, the running rails are connected to a return conductor midway between booster transformers, the primary of the transformer is connected in series with the catenary and the secondary winding is connected in series to the return conductor. In this configuration, the rails are relieved of the return current, which now flows through the return conductor to the feeder station. Placing the return conductor (also called return feeder) close to the contact wire reduces the tendency of magnetic coupling between the power line and nearby signalling cables. The return conductors are normally insulated conductors and are suspended on the catenary pole, as shown in Figure 2.6. The return conductor configuration is more effective when compared to the rail return configuration. Booster transformers connected in this configuration can be spaced at larger intervals. The return conductor

configuration can be configured in one of two ways: (a) with continuous rails and, (b) with discontinuous rails.

In a discontinuous rail system, the insulated joints in the rails and the neutral rail are configured as in Figure 2.6. This configuration forces current to flow through the BT secondary and enables the rails to be used for signalling. The mid-point of the BT secondary winding is connected to the neutral rail. The traction current is injected into the rails at the position of the train, and will flow in the rails and earth to the closest down lead from the return conductor to the rails. From this point on, the current will flow in the return conductor. For sections where there are no trains, the rail current will be approximately zero.

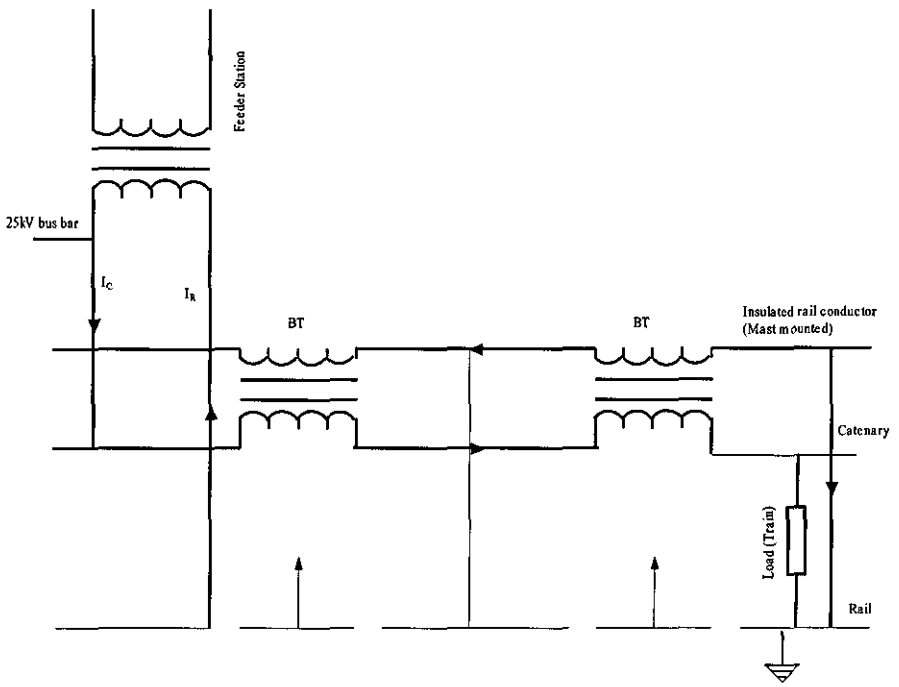

Figure 2.6: Return Conductor Configuration with BT

The main difference between a continuous rail system and a discontinuous rail system is the earthing arrangement. In a continuous rail system, the earthing arrangement includes an insulated earth wire. The earth wire is placed in a cable trough located on the Cess side of the rail. In practice, the rail closest to the Cess is connected at regular intervals to the earth wire. The only connection between the two rails is a 50 Hz bond per track circuit. The earth wire is connected to earth through the foundation of the catenary mast. The ground wire can be continuous or sectioned.

2.3.3 Auto-Transformers – an overview

In regions of low population density, where adequate points of common coupling are available where substations are to be sited, it might be beneficial to increase the operating voltage of the railway rather than upgrade the national mains or construct new transmission lines. Increasing the operating voltage of the railway, results in a reduction of the longitudinal impedance and voltage drop. To retain the nominal catenary voltage of 25 kV, autotransformers (AT) are used to generate a second voltage, phase shifted by 180° (i.e. – 25 kV), which is then fed via a second line – feeder – to the catenary supports.

The Autotransformer (AT), also referred to as the 2 × 25 kV system, converts the catenary – rail plus earth current into a balanced type catenary/ inverter feeder type current. ATs have one winding, connected between the catenary and an adjacent feeder wire. The rails are connected to an intermediate point on the winding, which is the mid-point when the AT ratio is unity. The substations are 50 kV and the traction system is 25 kV. At distances of approximately 10 km, both the catenary and the feeder lines are linked using ATs of approximately one-third of the substation transformer power. In each AT section, train current is supplied from adjacent transformer. The current

distribution is governed by the voltages across the windings and the Ampere-turn balance in the transformer cores. There is a finite rail voltage caused by return current from the train, which flows as far as the adjacent ATs. For ideal transformers and perfect rail-earth admittance conditions, no rail current will flow in unoccupied sections. The advantages of using ATs in AC-supplied traction systems include longer spacing between substations and reduction of induced voltages in telecommunications circuits.

2.3.4 The Rail

The railway track provides a path on which the trains run, and which directs trains in the appropriate direction at junctions. The rails are also used for signalling purposes to detect the position of trains and to perform other relevant signalling requirements. In the systems described above, the rail was either the only metallic conductor or part of a circuit by which traction current returns to the feeder station. Mechanically, the rails are supported on sleepers whose function is to hold the rails in position. The sleepers are themselves held in position by ballast. Since the primary function of the rails is to provide a path on which the trains' runs, its mechanical properties and not its electrical properties are considered most important.

Rails exist in two designs with different cross sectional shapes. For many years a rail section known as the *Bullhead* was used. The advantage of this design was the ability to use the other surface should the other become worn out. The modern design known as the *Flatbottom*, is now the industry standard. All track replacement projects in the UK, especially on the West Coast Modernisation Route (WCMR) and on London Underground involve the use of *Flatbottom* rails.

Both rail designs are available in different weights, the heavier the traffic the more substantial the rail section required. A very common flatbottom rail in use is known as UIC 54, UIC stands for the Union Internationale des Chemins de Fer (i.e. International Union of Railways), while 54 refers to the mass in kg per metre. Currently, UIC 60 rails are being installed in the UK.

The rails are held in place the correct distance apart by sleepers, which are arranged transversely under the rails. For many years sleepers were cut out of wood, but modern sleepers are of reinforced concrete, which has a substantially longer life. Steel sleepers are now being installed in the UK. The sleepers are held in place by ballast, which consist of stone chips. In metro railway, via duct and suicide pits are generally reinforced concrete structures.

The key electrical parameters of the rail are its resistivity, ρ, which typically has a values of 22 –25 $\mu\Omega$m; its relative permeability, μ_r with typical values of 50 – 350 depending on steel quality. The rail impedance is non-linear and depends on the magnitude of the current and on frequency. A typical conductor rail would have a resistance of 0.0015 Ω/km and an insulation resistance of 60,000 Ω/km in dry conditions, falling to some 3000 Ω/ km after a heavy rain [9].

2.4 Telecommunications and Signalling Systems

2.4.1 Telecommunications

The railway requires a comprehensive telecommunications system linking signalling centres, railway offices, and workshop etc for both voice and data. In addition, there are extra facilities required by the signalling system. In recent re-signalling projects, i.e. North Stafford Alliance on the WCMR, every signal has a signal post telephone, so that a driver stopped at a signal can talk

to the signaller to ascertain the situation, and be given instructions as appropriate. In a lot of areas direct radio communication between the signaller and the driver is also provided; phones are also provided in the areas of points, to allow easy communication for testers and maintainers. GSM-R communication specific for the railway is also employed for train control [10]. In the UK, both analogue and digital telecommunication systems are used, with increasing migration to digital systems.

From an interference point of view, it is the long telecommunication cable, which are either buried in the ground (approximately 1m from the running rail) or laid in cable routes installed alongside the railway that is of concern. The cable route usually consists of concrete troughing laid in the ground on one side of the track. The troughing is supplied with loose lids that are placed on top of the troughing. The cables are either fibre optic or paired copper cables.

2.4.2 Signalling Systems

The signalling system is an essential part of the railway, its principal task is to ensure that trains run safely. The signalling system also affects the sort of service that can be run on a section of railway. The principal elements of a signalling system are:

- Track circuiting; which ensures that trains on a particular section of a track remains detected, observed and protected;
- Interlocking (and route holding) which ensures the safe passage of trains from one signal to the next;
- Multiple aspect colour light signals to give simple and clear indication to the drivers in all weather conditions;

- An audible warning system, which warns the driver to make a brake application which will bring the train to rest when a signal displays a red aspect, and to enforce such application automatically if the audible warning is ignored.

2.4.2.1 Train Detection System

An essential requirement in signalling is the need to determine whether a defined section of the track is clear of traffic, or has any vehicle (stationary or moving) on it. One method of achieving this is by track circuit, using electrical circuits in the rails, another method is the use of axle counters.

Track circuits are used to detect the presence of trains and the presence of, some types of, broken rails. A track circuit is composed of three main parts; the supply circuit, the track and the return circuit. Voltage is applied across the rails, in the absence of a train on the rail; the applied voltage will reach the return circuit and will be sensed by the relay. If the rail is occupied (i.e. the rails are short circuited) the applied voltage will not reach the return circuit and the relay senses no voltage (resulting in a proceed aspect being shown). This principle applies if one of the rails is broken. Thus, the basic fail – safe design is one whereby the relay is energized as long as the track circuit is clear and de-energized otherwise.

Adjacent track circuits are separated from each other by insulated joints in the rails, thus stopping the adjacent track circuits from affecting each other. However, due to the imperfect insulator combination of the rail – sleeper – ballast (especially one contaminated by spillage), current flow is possible between rail sections. There are several types of track circuits, with AC and DC track circuits being the most widely used in the UK. These can be either single insulated, double insulated or non-insulated configured. Typically, single and double configurations can be used for AC or DC track circuits,

while non-insulated track circuits are operated with AC in the audio frequency range. In single insulated track circuits, one of the rails is used for traction return current, while both rails form part of the signalling system. In double insulated track circuits, the track return circuits is split equally between the two rails and insulated joints are employed in both rails.

2.5 Earthing and Bonding

Earthing and bonding arrangements in electrified railways are necessary to meet the railway and statutory requirements on safety, track potential and interface with other trackside electrical equipment. The principle requirements are:

- Protection against electrical hazards for railway users in contact with the system;
- Equipment protection against harmful voltages;
- System earthing / return path for traction current; and
- Definite and low impedance return path for fault currents.

For AC electrification, there are three principal approaches to earthing and bonding on AC electrified railways. In the first approach, the running rails are used as the return current path, with the rails of each track inter-bonded and the tracks cross-bonded to reduce the impedance of the return path, either directly or, where both rails must also carry signalling circuits, via impedance bonds. An additional non-insulated earth wire is provided, linking all masts and lineside structures. The second approach, commonly used in the UK, is the use of Booster Transformers (BT) (refer to Section 2.3 for a detailed discussion on BTs). The earthing and bonding arrangements remains the same as described above, with the difference that virtually all of the return current now returns to the feeder station via the BT and insulated return

conductors. The return conductors are connected to the rails either directly or via impedance bonds, approximately mid way between BT locations and at feeder stations. The third approach centres on the Autotransformer (AT) configuration discussed in Section 2.3.3. In this approach, the running rails are earthed and are connected to the common terminal of the two windings.

In general, the running rails when bonded or laid on metallic sleepers provide an earth as good as or better than special earthing stations obtained by burying one or more earthing electrodes in the ground. Thus, all mechanical and electrical equipment including traction masts, portals, e.t.c are cross-bonded to traction earth, especially when the lineside equipment is within 2m of any part of the traction circuit. When a modern 25 kV AC system runs through bored tunnels where earth resistivity is high, copper earth wire is used which is connected at both ends of the tunnels to earthing stations and to traction rails.

Traditionally, two earths system are implemented on the railway, one for power and the other for signalling. The principle behind this strategy is the prevention of conducted interference from power circuits impacting the performance of signalling circuits, as such the main the purpose of the earthing system from a signaller view point is the protection of equipment rather than the protection of staff. The Health and Safety at Work Act [12], however requires the risk to be re-assessed and mitigated in accordance with the ALARP principles, with an emphasis on protection of staff. To this effect, recent railway projects [13] have implemented a Common Bonding Network (CBN) earthing system to mitigate the risk due to two earth systems in close proximity, where a separation distance of 2m between the earth systems cannot be maintained.

The CBN earthing system is a system of interconnecting, intentionally or fortuitously, the conductive parts of an installation, and may include the structural steel works, reinforcing rods, and cable sheathing. These connections form an irregular mesh of low impedance paths for high frequency currents. The irregularity of the mesh ensures that resonant frequencies do not occur on all return paths, minimising the overall mesh impedance. Interconnection of the CBN to the station' earthing system will improve both the safety and EMI characteristics of the installation. Further deliberate interconnection between these will extend the effective operational frequency range of the signalling and communication equipment.

2.6 Summary

An overview of the railway environment has been presented. The description has focused on the main components of an AC electrified railway that influences the propagation of electromagnetic waves and the flow of leakage currents. The use of the rails as a return path for current as well as for railway signalling purposes is discussed. The potential victim circuits are described and as the impact of the leakage currents to these circuits. A description is given of the method employed in the industry to reduce inductive voltage drop and limit the flow of current to earth through the use of Booster Transformer or Autotransformers.

2.7 References

[1] RT/E/S/21036, "*25 kV Booster Transformer for AC Electrified Lines*", Railtrack Line Specification, March 1998.

[2] Fujiwara, O.; Yamashita, K. and Azakami, T. "*A proposal for estimating pantograph discharge rate using noise currents*", EMC Zurich 1989, Pg. 441 – 445.

[3] Lucca, G. "*Electromagnetic field produced by Sliding Contact Between Pantograph and Contact Wire of an Electrified Traction Line*", 4th

European Symposium on Electromagnetic Compatibility, EMC Europe 2000, Brugge, September 2000, Pg. 3 – 8.

[4] Lucca, G. "*Radiation from a traction line due to arcs between a pantograph and the contact wire*", Proc. of the 13th International Zurich Symposium on Electromagnetic Compatibility", February 1999, Pg. 197 – 202.

[5] Borsero, M., Farino, G. and Vizio, G. "RF *Disturbance Field Produced by the Pantograph – Catenary Contact*", International Symposium on Electromagnetic Compatibility, EMC'98 ROMA, September 1998, Pg. 46 – 51.

[6] Millard, A.; Taylor, I. A. and Weller, G. C., "*AC electrified railways – protection and distance to fault measurements*", Electric Railways in a United Europe, March 1995, IEE Conference, Pg. 73 – 77.

[7] EN 50122 – 1, "*Railway Applications – Fixed Installations. Power Provisions Relating to Electrical Safety and Earthing*", 1998

[8] EN 50122 – 2, "*Railway Applications – Fixed Installations – Part 2: Protective provisions against the effects of stray currents caused by D.C. traction systems*" 1998

[9] BR13422, "*50 Hz single phase AC electrification, immunisation of signalling & telecommunication systems against electrical interference*", British Railway Board, Issue 1, 1973.

[10] ERTMS/ETCS Class 1 Specification for an European Train Control System

[11] Attardo, F. and Di Stefano, M. "*EMI from AC traction Lines: Field Measurements on Telecommunication Cables*", EMC Zurich 1989, Pg 553 – 558.

[12] Health and Safety at Work Act, HMSO, UK, ISBN: 0105437743, 1974.

[13] A. Ogunsola, "JNUP-A-SRA-PLN-00002, *JNUP Earthing and Bonding Plan*", Jubilee and Northern Line Upgarde Project, Tubelines Limited, 2004.

[14] Griffin, A. J. "*Methods of improving the voltage regulation on 25 kV electric railways*", Main Line Railway Electrification, International Conference on, 1989, Pg 252 – 259.

[15] Stuart, M. "*25 kV AC Electrification Constraints*", Conference on Electric Railway for a New Century, IEE, September 1987, Pg 199 – 203

[16] Williment, P. T. "*East Coast Main Line Electrification – 25 kV AC system Design*", Main Line Railway Electrification, International Conference on, IEE, 1989, Pg 306 – 310.

[17] GL/RT1254, "*Electrified Lines. Traction Bonding*", Railway Group Standard, Issue 1, April 2000.

[18] RT/E/PS/11765, "Impedance *Bonds*", Railtrack Line Product Specification, Issue 1, December 2000.

Chapter 3

INTERFERENCE MANAGEMENT IN THE RAILWAY

3.1 Electromagnetic Interference

Electromagnetic interference (EMI) has become a major problem for railway equipment suppliers and railway operators. The railway operator and maintainer must ensure that the electromagnetic compatibility of the railway is maintained such that it does not impact operations or cause interference to its neighbours. The equipment supplier must assure that the equipment is adequately immune from self-generating electrical noise plus that anticipated within the railway environment. In addition, the equipment supplier must ensure that the installed equipment will meet all applicable emission regulations. More importantly, in the event of mal-operation due to electromagnetic interference the equipment must be designed to "fail-safe". Assuring electromagnetic compatibility (EMC) has become more difficult due to the proliferation of modern telecommunication, signalling and electrification technology [1].

For an interference problem to exist, there must be a noise source, victim and a path for the energy to be transferred from the source to the victim. In this context, the victim is any equipment where the interference problem occurs. Figure 3.1 depicts the interference model. Effective interference control usually involves all three of these elements. The noise may be transferred from a source to the victim by either conductor (conducted emission) or a dielectric (induced or radiated emission). In this context, transfers by induction implies predominatly electric field or magnetic field coupling (near field) whereas radiation implies electromagnetic waves (far field) coupling.

Intra-system interference normally results from conducted or induced energy transfers, whereas intersystem interference normally results from radiated energy transfers.

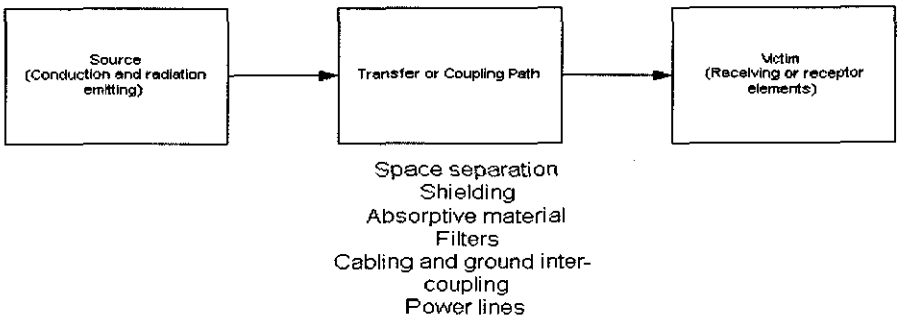

Figure 3.1: Interference Model

The railway environment consists of numerous electrical and power sources resulting in an electromagnetic environment spanning a wide frequency range. Some of the special features of the railway environment are highlighted below:

- A variety of power supply configuration supplying high power to loads;
- Close proximity and area of source and victim circuits;
- Method of power transfer to moving trains;
- A fluctuating and imprecise system of current flow to and from the trains;
- High single-phase loads which may cause imbalance in the three-phase systems;
- The possibility of simultaneous generation of interference from several sources;

- Moving sources within the same zone of influence;
- The variability of noise level due to weather conditions;
- Trackside installation subject to high ambient profile;
- Safety critical nature of the railway.

3.2 Sources and Victims of Interference

Numerous sources of electromagnetic interference exist in the railway; these can broadly be categorized as intra-system and inter-system sources of interference. Intra-system interference within the railway includes, for example, traction power supply and traction drives to signalling installation, and coupling between parallel DC and AC traction systems. Inter-system interference in this context is the electromagnetic interaction between the railway and its neighbour, and is exampled by the generation of earth current causing corrosion or interference to sensitive systems outside the railway environment, or the degradation of performance of railway telecommunication and signalling installations due to sources external to the railway.

Electrified railways can generate electrical noise over a wide frequency band by a variety of mechanism giving rise to complex amplitude and time varying signature as a trainset travels along the installation. The electrical noise generated by a trainset will depend upon the operation of the vehicle and the noise can be enhanced by system resonance and interaction with other trainsets operating on the route. The electromechanical interaction between the contact wire and the pantograph is a source of radio frequency interference [2]. This interference is due to high voltage spark breakdown when the pantograph is raised or lowered and high current arcing during operation. Typically, high current low voltage sources such as fields produced by traction currents and pantograph arcing generate induction or near

magnetic fields, whereas low current high voltage sources from switching, spark breakdown and arc formation create (far) electric fields. AC and DC fed traction drives are also a source of electromagnetic noise.

While signalling installation is generally considered to be a victim (in a railway context) it can also function as a source of radio frequency interference with reference to equipment located outside the railway environment. This is exampled by:

- Power and audio frequency track circuits with modulated carriers signals which can form long loop[3] transmitters;
- Signalling transponders which can function as localized radio frequency transmitter (e.g. Eurobalise and balise);
- The wheel – rail contact zone, which when diverting low power track circuit current can act as a transitory interference source.

3.3 Signalling Interference Issues

Railway signalling equipment must co-exist with a variety of other electrical systems and in some cases, share common electrical conductors. It is possible that these conductors will lie on the ground, close to each other. In some cases the protective insulating layer of these signalling cables may be damaged and the signalling equipment may be susceptible to induced electromagnetic interference from neighbouring signalling equipment or power supply systems. Electric traction faults, or the general environment in the form of lightning strikes, may cause interference to signalling equipment.

---

[3] The typically loop length between the transmitter and receiver end of a Jointless Track Circuit (JTC) is about 80m

Electromagnetic interference may cause degradation of performance in signalling equipment. Signalling equipment are designed to: perform [1]:

- Operate without suffering wrong-side failures;
- Operate without suffering an unacceptable level of right-side failures;
- Not suffer permanent damage except in extreme circumstances;
- Operate without endangering live.

The dominant mechanism of interference from traction supplies will depend on the type of supply used. Alternating current (AC) produces a large and fluctuating electromagnetic field, which may cause inductive and electrostatic interference in its locality. AC traction system in the UK uses a voltage of 25kV 50 Hz, which may be supplied directly from the public network or from the railway's dedicated supply. The AC traction supply can have significant distortion, which may produce harmonics of the fundamental frequency. The AC currents will induce a voltage in parallel circuits, the magnitude of which will depend on the spatial location of the traction and signalling conductors, and the magnitude of the traction current. Direct current (DC) produces minimal inductive fields but will propagate conductive interference over a large area. They are usually derived from rectified AC mains supply; as such, any non-linearities in the rectification will produce AC components.

The running rails, which may have other electrical circuits, connected to them, are also used for traction return purposes. They run parallel to lineside conductors, and are in contact with the ground. By virtue of their location and usage, the running rails may have a voltage generated along and across them, or may be raised to a voltage with respect to earth. This voltage may be applied to signalling equipment attached to the rails or in contact with them.

Some of the interference problems experienced by signalling installations in the railway environment are listed below [3]:

- Induced voltages in short signalling cables resulting in false lighting of lights;
- Induced voltages in long signalling cables;
- Over-voltages coming into the system through track circuit, power supply or other channels;
- Magnetic saturation in track circuits components due to non-symmetric conduction of current from the rails;
- Interference in track circuit due to harmonic content in the traction return current.

3.4 EMC Management

From the 1st January 1992, all electrical and electronic equipment "placed on the market" and "taken into service" within the European Economic Area (EEA) are required to comply with the objectives of the European Communities EMC Directive, 89/336/EEC[4] [4], agreed in May 1989. The Directive applies to both new and existing designs i.e. those currently under development and existing designs, which are still in production and being marketed. The Directive was amended in 1992 and enacted into UK Law by Statutory Instrument 1992 No 2372[5] [6].

Before the introduction of the EMC Directive, the Wireless and Telegraphy Act of 1949 largely governed EMC issues in the UK. In the UK railway

---

[4] The EMC Directive 89/336/EEC has been repealed from the 20th July 2007 and replaced with a new EMC Directive, 2004/108/EC which came into force on the same day.

[5] This Statutory Instrument has now been superseded by SI 2006: No. 3418

industry, Industry initiative and Company standards such as, Railway Industry Application (RIA) standards and Railway Group Standards were the only accepted standards. Statutory Instrument 1992 No. 2372 repeals Section 12A of the Wireless and Telegraphy Act [7] and Section 78 of the Telecommunications Act of 1984 [8].

The objectives defined by the EMC Directive are mandatory, whilst standards themselves are not binding and are only defined as a means of demonstrating that compliance with the objectives has been achieved. The objectives of the EMC Directive are encompassed by the protection requirements placed on electrical and electronic equipment, which must be designed, manufactured and installed to ensure:

- The electromagnetic disturbance it generates does not exceed a level allowing radio and telecommunication equipment and other equipment to operate as intended;
- The equipment has an adequate immunity level of intrinsic immunity of electromagnetic disturbance to enable it to operate as intended.

It is worth mentioning that whether or not the EMC Directive applies, the protection requirements stated above are nothing more than good engineering practice that all suppliers of equipment destined for the railway environment should follow. The product EMC standard for electrical and electronic equipment destined for the railway environment is the EN 50121 series of standards. EN 50121 has five parts [9] - [14], which are reviewed below:

EN 50121-1: 2006 This part gives a description of the electromagnetic behaviour of a railway. It specifies the performance criteria for the whole set of standards but only in very

broad terms. A management process to achieve EMC at the interface between the railway infrastructure and the trains is provided.

EN 50121-2: 2006 This part sets the emission limits at radio frequency from the railway to the outside world. It defines test methods and gives information on typical field strengths likely to be measured. This part is focused on the broadband emissions from traction units and the Overhead Line Equipment (OLE).

EN 50121-3-1: 2006 This part specifies the emission and immunity requirements for traction stock, train-sets and hauled stock. Some aspects are similar to EN 50121-2 but there is an emission test to assess the interference of the stock on telecommunication lines. There are no immunity tests defined for rolling stock. It is recognized however that field strengths of 20V/m are to be expected.

EN 50121-3-2: 2006 This part specifies the emission and immunity requirements for electrical and electronic apparatus to be fitted on rolling stock. The immunity levels have been set to provide "adequate" immunity under normal operating conditions. Extreme conditions, e.g. fault conditions, are not addressed but it is recognized that special requirements may be specified.

EN 50121-4: 2006 This part specifies the emission and immunity requirements for electrical and electronic apparatus

	for signalling and telecommunications apparatus. Like EN 50121-3-2, the immunity levels have been set to provide "adequate" immunity under normal operating conditions
EN 50121-5: 2006	This part specifies the emission and immunity requirements for electrical and electronic apparatus for fixed installations associated with power supply.

In addition to the above mentioned standards, a number of Railway Group Standards [18] – [30] exists which have been developed in an attempt to address the electromagnetic environment and compatibility issues within the United Kingdom's railway environment. These standards are code of practice, containing susceptibility limits and methods for demonstrating compatibility with specific infrastructure assets. In some cases, the susceptibility limits have been translated into line current values and validated by testing. In most cases, permissible limits are taken directly from approved safety cases or system assurance documents.

3.4.1 EMC-Safety Related Issues

For any system, which could pose a hazard to people or property if incorrectly controlled and/ or designed, safety questions must invariably be addressed, and these questions must include the issue of safety in the face of external electromagnetic disturbance. Safety in the railway can be sub-divided into two areas: (1) functional safety [32], [34] which is directly related to apparatus performing a safety related function and (2) personal safety issues, which may lead to degradation of health of railway users (and maintainers) and/or loss of life.

In the UK, Network Rail (formerly Railtrack) has overall responsibility for overseeing safety on the mainline infrastructure, similar responsibilities rest with other infrastructure owners (i.e. London Underground and Dockland Light Railway). It discharges these responsibilities via a formal set of procedures, which provides a systematic basis for the safe management of change. These procedures are detailed in a series of documents entitled "*Engineering Safety Management*" [35], known in the railway industry as the 'Yellow Book". The aim of these documents is to ensure that any change to be introduced on the railway is managed safely and that the safety arrangements are adequate for the proposed undertaking. It is required that the safety implications of any proposed change be shown to be acceptable before implementation of that change. Proposed changes are formally defined and submitted with safety justification to a change management system. It is the responsibility of the change instigator to ensure that the potential hazards and risks has been identified, assessed and shown to be As Low As Reasonably Practicable (ALARP). This justification is provided in the form of a Safety Case, a document that provides the prime assurance that all hazards and risks have been assessed and shown to be ALARP.

The Safety Case must contain considerations of EMC issues and its impact on the safe operation of the railway. Electromagnetic coupling or interactions, which are relevant and pose a threat to personal safety should be identified and assessed during the hazard identification stage and included in the Safety Case. Electromagnetic interference or coupling that only result in a degradation of performance without resulting in a safety hazard or risk to personal safety is dealt with under the EMC Directive and should not be included in the Safety Case. Thus complying with the EMC Directive does not necessarily imply that a *change* is safe nor does it ensure the safe operation of the railway.

3.4.2 Railway EMC Route to Compliance

Manufacturers (including distributors of imports from outside the EEA) are required to provide a declaration that their equipment complies with the protection requirements of the directive. The EMC Directive, 2004/108/EC, in Annex IV, specifies only one route to compliance; this is in contrast to the three routes specified in the repelled EMC Directive 89/336/EEC.

Compliance with the essential requirement is to be demonstrated by the procedure described in Annex II or at the manufacturer' discretion as stated in Annex III. A manufacturer is required to perform an EMC assessment, in which all electromagnetic phenomena, which potentially could interact with the apparatus in its intended environment of use, are to be identified and addressed in order to meet the protection requirements. The EMC assessment should take into consideration all possible configurations of the apparatus.

In essence, self-certification is the primary route for demonstrating compliance with the EMC Directive. It is the simplest method and is achieved by satisfying relevant standards, which is likely to be demonstrated through either in-house testing or contracting the tests to an independent test house. In the absence of a European Standard, compliance with an existing national standard will suffice if the particular standard is accepted by the Commission and published in the Official Journal of the European Community (OJEC). Presumption of conformity is limited to the scope of the standard(s) applied and the relevant essential requirements covered by the standard(s) [33].

Conformity has to be demonstrated through "Technical Documentation" regardless of whether or not products are manufactured in compliance with

harmonised standards. The Technical documentation should demonstrate conformity with the protection requirements of the EMC Directive, and may include a report from a Notified Body to support the statement of compliance.

A common theme in EMC technical documentation is the demonstration of due diligence, this is an argument that the said product has been designed with an understanding of the electromagnetic environment in which the product is destined for and that all precautions have been taken to ensure compliance with the protection requirements of the EMC Directive.

In railway terms, due diligence is an assessment of the risk and that the risk has been reduced to ALARP. Thus, increasingly the "TD" is becoming an important part of the safety case (the remits of the safety case is discussed in Section 3.4.1. and in detailed in [36] - [39]). Due to the complexity of the railway and the cost associated with railway EMC approval, computational techniques can be applied to address EMC related issues provided the model reflects the installation scenario and that the model can be validated against measurements.

3.5 Summary

The electric railway is a complex distributed system comprising of many sources of electromagnetic interference in close proximity to sensitive signalling and telecommunication equipment. The management of EMC in a railway environment is not a trivial task; it requires a system engineering approach, a good understanding of railway system assurance principle, and a detailed appreciation of the applicable national and international standards – and the technical rationale underpinning the requirement contained within them.

The EMC management principles is therefore centred around the ensuring that the railway remains safe during all life cycle phases and modes of operations, and that it is demonstrably compliant to statutory requirements on EMC.

3.6 References

[1] Ogunsola, A. and Pomeroy, S. "*EMC Assurance and Safety Critical Apparatus in a Railway Environment*", The 2003 IEEE International Symposium on Electromagnetic Compatibility, Istanbul, Turkey, May 2003.

[2] Lucca, G. *"Electromagnetic Field Produced by Sliding Contact between Pantograph and Contact Wire of an Electrified Traction Line*", EMC Europe 2000, Bruges, Pg 3-8.

[3] Hill, R. J. "*Electric railway traction. VI. Electromagnetic compatibility disturbance and equipment susceptibility*", Power Engineering Journal, Vol. 11, Issue 1, Feb. 1997, Pg 31 – 39.

[4] Council Directive, 89/336/EEC, " *Council Directive on the approximation of the laws of the Member States relating to Electromagnetic compatibility (EMC)*", OJ L139 of May 1989

[5] Council Directive, 2004/108/EC, "*Council directive on the approximation of the laws of the Member States relating to Electromagnetic Compatibility and repealing Directive 89/336/EEC*", OJ L 390/24 of December 2004.

[6] Statutory Instruments 2006 No. 3418, "*The electromagnetic Compatibility Regulations 2006*", HMSO, December 2006.

[7] Wireless Telegraphy Act , Public Acts, HMSO, UK 1949

[8] Telecommunications Act, Public Acts, HMSO, UK, 1984

[9] EN 50121 –1: 2006, *"Railway Applications – Electromagnetic Compatibility, Part 1: General"*, July 2006.

[10] EN 50121 – 2: 2006, *"Railway Applications – Electromagnetic Compatibility, Part 2: Emission of the whole railway system to the outside world"*, July 2006.

[11] EN 50121 – 3 –1: 2006, *"Railway Applications – Electromagnetic Compatibility, Part 3-1: Rolling Stock – train and complete vehicle"*, July 2006

[12] EN 50121 – 3 – 2: 2006, *"Railway Applications – Electromagnetic Compatibility, Part 3-2: Rolling Stock – rolling stock apparatus"*, July 2006

[13] EN 50121 – 4: 2006, *"Railway Applications – Electromagnetic Compatibility, Part 4: Emission and Immunity of Signalling and Telecommunications apparatus"*, July 2006

[14] EN 50121 – 5: 2006, *"Railway Applications – Electromagnetic Compatibility, Part 5: Fixed Power Supply Installations"*, July 2006

[15] NR/GN/SIG/50001, "*Methodology for the demonstration of compatibility between rolling stock and infrastructure*", Network Rail Group Standard, Issue 1, February 2003.

[16] NR/SP/SIG/50002, "*Methodology for the demonstration of compatibility with single rail reed track circuits on the AC railway*", Business Process Document, Network Rail, Issue 2, February 2007.

[17] NR/SP/SIG/50003, "*Methodology for the demonstration of compliance with double rail reed track circuit on the DC railway*", Business Process Document, Network Rail, Issue 2, February 2007.

[18] NR/E/C/50004, "*Methodology for the demonstration of compatibility with DC (AC immune) Track Circuit*", Business Process Document, Network Rail, Issue 2, April 2007.

[19] NR/GN/SIG/50005, "*Methodology for the demonstration of compatibility with 50 Hz single rail track circuits*", Network Rail, Issue 1, February 2003.

[20] NR/SP/SIG/50006, "*Methodology for the demonstration of compatibility with 50 Hz double rail track circuit*", Business Process Document, Network Rail, , Issue 1, 2006.

[21] NR/GN/SIG/50007, "*Methodology for the demonstration of compatibility with HVI track circuits*", Network Rail Group Standard, Issue 1, February 2003.

[22] NR/GN/SIG/50008, " *Methodology for the demonstration of compatibility with T121 track circuits*", Network Rail Group Standard, Issue 1, February 2003.

[23] NR/GNSIG/50009, " *Methodology for the demonstration of compatibility with FS 2600 track circuits on the DC railway*", Network Rail Group Standard, Issue 1, February 2003.

[24] NR/L2/SIG/50010, "*Methodology for the demonstration of electrical compatibility with train detection system in use on non-electrified lines*", Network Rail Group Standard, Issue 1, December 2007.

[25] NR/SP/SIG/50011, "*Methodology for the demonstration of compatibility with axle counter*", Business Process Document, Network Rail, Issue 1, April 2006.

[26] NR/SP/SIG/50012, "*Methodology for the demonstration of compatibility with TPWS track sub-system*", Business Process Document, Issue 2, April 2006.

[27] NR/GN/SIG/50013, "*Methodology for the demonstration of compatibility with interlockings*", Network Rail Group Standard, Issue 1, February 2003.

[28] NR/GN/SIG/50014, "*Methodology for the demonstration of compatibility with lineside equipment*", Network Rail Group Standard, Issue 1, February 2003.

[29] NR/SP/SIG/50015, "*Methodology for the demonstration of compliance with Reed FDM systems on the AC and DC railways*", Business Process Document, Network Rail, Issue 2, February 2007.

[30] NR/SP/TEL/50016, " *Methodology for the demonstration of compatibility with telecommunication systems*", Business Process Documents, Network Rail, Issue 3, April 2006.

[31] 2-01018-001, "*Electromagnetic Compatibility*", London Underground Category 1 Standard, Issue A2, July 2004.

[32] IEC 61000-1-2, "*Electromagnetic Compatibility (EMC) – Part 1-2, General – Methodology for the achievement of the functional safety of electrical and electronics equipment with regards to electromagnetic phenomena*", 2001.

[33] Marshman, C. A, "*The Impact of the New EMC Directive 2004/108/EC for the Railway Industry*", Workshop on EMC Management and Assurance in Railway, 18th International Zurich Symposium on EMC, Munich 2007

[34] IEC 61508 Parts 1 - 7, "*Functional safety of electrical/ electronics/ programmable electronic safety-related systems*", IEC, Geneva, 2000.

[35] Engineering Safety Management, Issue 3, Yellow Book, Vol. 1 & 2, Railtrack, 2000.

[36] Pilkington, S. D. J and Lee, A. R. "*The development of safety cases for mass transit signaling and control projects – Jubilee Line case study*", Developments in Mass Transit Systems, Inter. Conference on, IEE, April 1998, Pg. 254 – 259.

[37] Hessami, A. G. "*Optimal management of safety – a system approach*", Developments in Mass Transit Systems, Inter. Conference on, IEE, April 1998, Pg. 254 – 259.

[38] Geyer, T. A. W. et al, "*Channel Tunnel Safety Case: Development of the Risk Criteria*", Electric Railways in a United Europe, International Conference on, 1995, Pg. 164 –167.

[39] Bond, A. E, "*UK Implementation of the EMC Directive*", Proc. Instn. Elec. Engrs, Part A, Sci Meas. Technol, July 1994, 141(4), Pg 234 – 243

[40] *General Specification for Interference Testing for Electronic Equipment used on Traction and Rolling Stock*, BRB/LU/Ltd, RIA technical Specification, Railway Industry Association, No. 18, 1990

[41] Allan, J and Armstrong, D. S." *The New European Electromagnetic Compatibility Standards for Railway"*, Proc. Instn Mech. Engrs., Part F: Journal of Rail & Rapid Transit, Vol. 212, No. F2, 1998, Pg 135 – 144.

[42] Marshman, C, "On *track for compliance [railway, EMC]*", IEE Review, Vol. 45, Issue 6, 18 Nov 1999, Pg 260 – 262.

[43] Frasco, L. A, "*EMC commissioning and safety certification of AC rail transit vehicle*", Developments in Mass Transit Systems, 1998. Inter. Confer. On (Conf. 453), 1998.

[44] Davidson, W. "Radiated *emissions from contact shoes*", EMC in Electric Traction and Signalling, IEE Colloquium on, 1995, Pg 3/1 – 3/6.

[45] Armstrong, D. S. "*The Standards are coming hurrah! Hurrah? [Railway EMC]*", EMC in Electric Traction and Signalling, IEE Colloquium on, 1995, Pg 5/1 – 5/4.

[46] Holmes, R. "*Electromagnetic compatibility of electrified railways*", Electric Railways in a United Europe, International Conference on, 1995,
Pg 131 – 135.

[47] Armstrong, D. S "*EMC aspects of electrified railways at high frequencies*", EMC in Large Systems, IEE Colloquium on, 1994, Pg 7/1 – 7/4.

[48] Hadrian, W. "*The Electromagnetic Environment in the Area of Railway Stations at 16,66 Hz*", EMC Zurich 1989, Pg 577 – 580.

[49] Cheng, K. W. E *et al*, "*Railway EMC Environment and Measurement*", Computers in Railways VII. Seventh International Conference on Computers in Railways, COMPRAIL 2000, Italy, Pg 323 – 331.

[50] Amendolara, A *et al*, "Electromagnetic *Compatibility in Railway Systems: Standard and Application*", Inter. Symp. On Electromagnetic Compatibility, EMC'96 ROMA, Pg 627 – 632.

[51] Fasoli, C and Cau, G. "*A Survey on Electromagnetic Compatibility Standards in the Railway Fields: Problems and Perspectives*", 16th Conf. on Transportation Systems. Automation in Transportation '96. Pg 100 – 103.

[52] Solbiati, G. L. "*Managing the EMC between an AC Railway Line and the External World*", Industrial Applications in Power Systems, Computer Science and Telecommunications, 8th Mediterranean

Electrotechnical Conference, IEEE Part 2, 1996, Pg 839 – 841.

Chapter 4

LOW FREQUENCY COUPLING AND TRANSMISSION LINE THEORY

4.1 Introduction

The analysis of low frequency coupling from a railway line to nearby buried metallic structures is achieved by solving the current distribution between different conductors of the (current) return path. A solution of earth potential created by leakage currents from the rails, along the route of the buried metallic structure, is also required for conductive coupling assessment. These solutions are required for the evaluation of rail potential and for the determination of step and touch voltages. A review of analytical methods for solving current distribution as applied to railway environment is given in this chapter. In the analysis given, it is assumed that the load consists of one train and that power is supplied by one feeder station. The catenary mast is assumed to be a wooden mast, thus leakage from the rails flow through the sleepers and the ballast. The earth is assumed homogenous and all conductors are assumed uniform over their respective lengths.

4.2 Earth – Rail Current Distribution

The railway AC electrification system consists of long length of parallel conductors. The catenary - rail/ground configuration can be represented as two coupled transmission lines. In such a system, energy transfer takes place through the surrounding electric and magnetic fields, which are perpendicular to the longitudinal direction. The primary line distributed components are the self and mutual impedance and admittance. A remote earth reference is necessary to define these equivalent impedance and admittances. In an AC

electrified railway, current is carried by the running rails, the catenary and the ground.

4.2.1 Running Rails

As discussed in Section 2.3, the simplest AC traction system is one in which the current return path consist of the running rails only. In this configuration, the return path comprises the running rail in parallel with the ballast and the earth, resulting in the return current flowing in all three parallel paths. *Longitudinal currents in the ballast will be negligible compared to the currents* in the rails and earth, due to its high resistivity.

The rail - earth loop can be considered as a leaky transmission line with series resistance and leakage conductance with respect to earth. For this analysis, it is assumed that both rails are used for return current and for simplicity are regarded as one equivalent rail. Due to the mutual coupling between the *catenary – earth loop and the rail – earth loop, some current is forced to flow* in the rails (induced current), while the remaining current will flow through earth (injected current). The injected current will not flow to earth immediately but tends to leak over some distance due to the finite conductance between the rails and earth. The distance is defined by the parameters of the configuration and is known as the *current transfer zone.* If the railway is long enough, there will be a zone in the centre (middle) where no rail to earth current leakage occurs, this zone is known as the *stationary zone.*

As shown in Figure 4.1, the injected current will flow through both sides of the injection point; it will also be collected from both sides of the feeding point. The current flow is dependent on the parameters and distances in the system, however for infinitely long rails and distances between the feeding

and load points it is reasonable to assume that the current will split in equal parts.

The distribution of rail current and voltage may be calculated from the transmission line equations:

$$I(x) = \left[A\exp(-\gamma x) - B\exp(\gamma x)\right]$$
$$V(x) = Z_0\left(A\exp(-\gamma x) + B\exp(\gamma x)\right) \qquad [4.1]$$

where Z_o is the characteristic impedance, γ is the propagation constant and the constants A and B are determined from boundary conditions which require continuity of both conductors current and potential at series or shunt discontinuities, except at a source point.

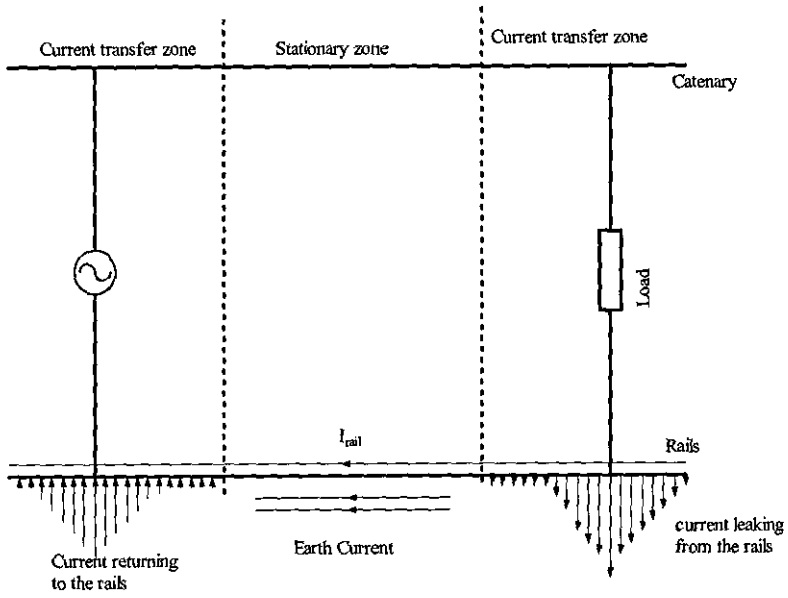

Figure 4.1: The zones of the railway line

A thorough treatment of this subject using wave propagation theory is given by Sunde [1], in which the rails are treated as ground conductors with inductance and shunt sources at both ends. In the proceeding analysis, principles of transmission line theory apply; in addition to the application of transmission line theory, quasi-static behaviour is assumed.

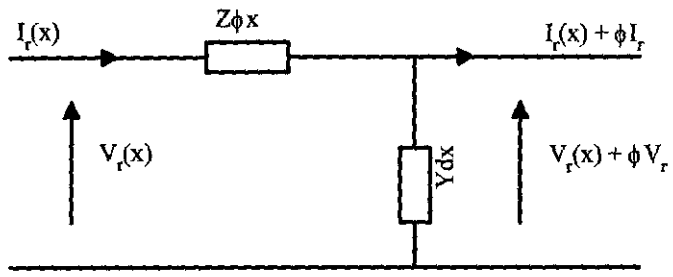

Figure 4.2: An infinitesimal part of the rail-earth loop

Where:

$V_r(x)$ = Rail potential with respect to remote earth
$I_r(x)$ = Rail current

The following differential equations can be written for the rail -- earth loop (Figure 4.2) taking into account the inductive coupling to the catenary [2]:

$$\frac{dV_r}{dx} + I_r Z_{rr} + I_c Z_{cr} = 0 \qquad [4.2]$$

$$\frac{dI_r}{dx} + V_r Y_{re} = 0 \qquad [4.3]$$

where:

Z_{rr} is the series impedance per unit length if the rail - earth loop, Z_{cr} is the mutual coupling impedance between the catenary and earth, I_c is the catenary current, $V_r(x)$ is the rail potential with respect to remote earth and Y_{re} is the shunt admittance from the rail - earth loop per unit length.

Solving the equation above gives the following solution

$$V_r = V_1 \exp(\gamma x) + V_2 \exp(-\gamma x) \qquad [4.4]$$

$$I_r = I_1 \exp(\gamma x) + I_2 \exp(-\gamma x) + CI_c \qquad [4.5]$$

where γ, is the propagation constant describing the wave propagation on a conductor or in a medium and is given as: $\gamma = \sqrt{Y_{re}Z_{rr}} = \alpha + j\beta$; where α is the attenuation per unit length and β is the phase shift of the propagating wave per unit length. From [4.2] to [4.5], the following relations can be determined:

$$C = \frac{Z_{cr}}{Z_{rr}} = -k \qquad [4.6]$$

$V_1 = Z_0 I_1$ and $V_2 = Z_0 I_2$, where $Z_0 = \sqrt{Z_{cr}/Y_{re}}$ and is the characteristic impedance of the rail. k is the coupling factor describing the catenary - rail inductive coupling. Inserting the above relations into [4.4] and [4.5], the following are obtained:

$$V_r(x) = -Z_0 I_1 \exp(\gamma x) + Z_0 I_2 \exp(-\gamma x) \qquad [4.7]$$

$$I_r(x) = I_1 \exp(\gamma x) + I_2 \exp(-\gamma x) - kI_c \qquad [4.8]$$

The rail current can be split into two parts; an induced current and an injected current. The induced current can be found by inserting the following boundary conditions into [4.7] and [4.8]: $V_0 = -i_0 Z_0$ and $V_L = i_L Z_o$, resulting in an induced current given as:

$$i_{r(induced)} = -\frac{1}{2} I_c k \left[2 - \exp(-\gamma x) - \exp(-\gamma L + \gamma x) \right] \qquad [4.9]$$

where L is the length of the running rail.

The injected current can be obtained by assuming that $k = 0$ (i.e. there is no induction) and by inserting the boundary conditions, $i_0 = -0.5 I_c$ and $\mathrm{V_L} = I_L Z$ for $x = 0$ (at the feeding point) and inserting the boundary conditions $i_L = -0.5 I_c$ and $\mathrm{V_0} = I_0 Z$ at $x = L$ (at the load point).

The two parts are added to give the injected current component for the whole line:

$$I_r\big|_{injected} = -\frac{1}{2} I_c \left[e^{-\gamma x} + e^{-\gamma (L-x)} \right] \qquad [4.10]$$

The injected current flows out from the load point and in towards the feeding point in both directions, as shown in Figure 4.3.

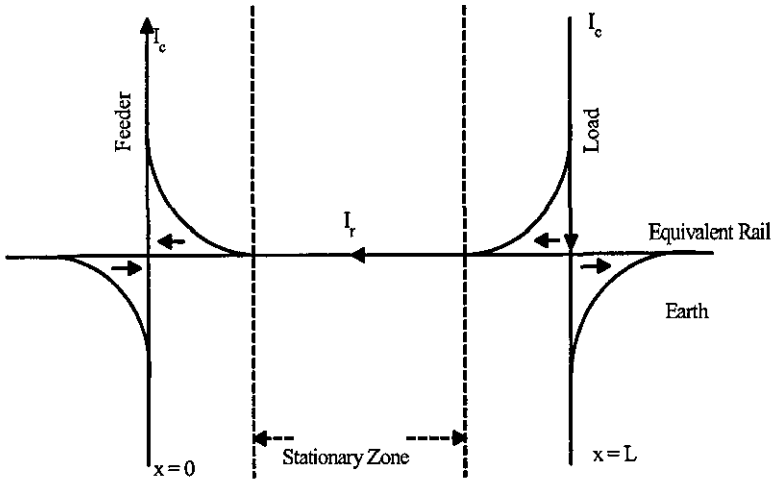

Figure 4.3: Current flow in a railway system

The total rail current is the sum of [4.9] and [4.10], and is given below as:

$$I_r(x) = -kI_c - \frac{1}{2}(1-k)I_c\left[e^{-\gamma x} + e^{-\gamma(L-x)}\right] \qquad [4.11]$$

The constant part of the rail current of [4.11], kI_c, flows only between the feeding point and the load, where there is no earth potential. With reference to Figure 4.1, this is in the *stationary zone*. The variable part of the rail current of [4.11], $-\frac{1}{2}(1-k)I_c\left(e^{-\gamma x} + e^{-\gamma(L-x)}\right)$ flowing partly outside the feeder and load point.

4.2.2 Series Discontinuity due to Booster Transformers (BT)

In the previous analysis, a continuous rail was assumed, however when Booster Transformers (BT) are used the rails are broken at each transformer location. As a result, [4.11] would need to be modified to account for the

discontinuity and thus current flow. A BT can be described as an ideal unity current transformer, thus the rail current must be equal to the catenary current at the transformer location (i.e. same magnitude but opposite phase as the catenary current).

Referring to Figure 2.5, the section between two BTs is referred to as the transformer section. In the following analysis, it is assumed that the train is located outside the transformer section. For this situation, the catenary current and the mutual coupling between the catenary and the equivalent rail are as described for a continuous rail. The impact of rail series impedance is considered negligible, thus the constant part of the rail current is given as: $-kI_c$. Since the injection and collection points of the circuit will now be at the BT locations and the equivalent rail is discontinuous at these locations, the variable part of the current will no longer flow to both sides of the injection point. Using the following boundary conditions; $I_r(x)\big|_{variable} = -(I_c - kI_c)$ and $I_r(L')\big|_{variable} = -(I_c - kI_c)$ in [4.12], the variable part of the current can be solved:

$$I_r\big|_{variable} = I_1 e^{\gamma x} + I_2 e^{-\gamma x} \qquad [4.12]$$

The total current is obtained by adding the constant and variable component of the current and is given below as (where L' is the distance between two BTs)

$$I_r(x) = -I_c\left[k + (1-k)\frac{Cosh\left(\gamma(\frac{L'}{2} - x)\right)}{Cosh\left(\gamma\frac{L'}{2}\right)}\right] \qquad [4.13]$$

For a non-ideal transformer, the exciting current, I', which has a finite value, is supplied to the primary windings of the transformer through the catenary and returns to the feeding station via earth. Equation [4.13], is therefore not sufficient to describe the total current since the boundary conditions characterizing the variable rail current differ.

For this situation, the following boundary conditions apply: $I_r(0)\big|_{variable} = -\left[(I-k)I_c - I'\right]$ and $I_r\left(L'\right)\big|_{variable} = \left[(1-k)I_c - I'\right]$. The total current is then given as:

$$I_r(x) = -I_c\left[k + \left(1-k-\frac{I'}{I_c}\right)\frac{Cosh\left(\gamma(\frac{L'}{2}-x\right)}{Cosh\left(\gamma\frac{L'}{2}\right)}\right] \qquad [4.14]$$

In railway applications it is of interest to determine the rail current at a distance from the load to the closest BT. This situation is illustrated in Figure 4.4, where L' is the distance from the BT to the train.

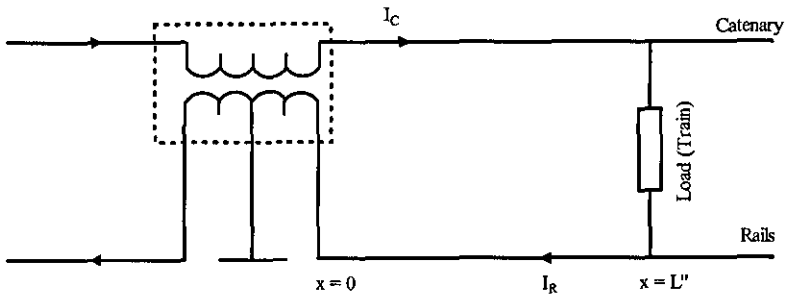

Figure 4.4: Schematic of train in BT section

The constant part of the rail current will be the same as described in previous analysis. The variable part of the current is again determined from [4.12] with the following boundary conditions: $I_r(0)\big|_{variable} = -(1-k)I_c$ and $I_r(L")\big|_{variable} = -0.5(1-k)I_c$. It is assumed that the BTs are ideal and that the injected rail current splits equally at $x = L^*$. The total current for this condition is given as:

$$I_r(x) = -I_c\left[k + (1-k)\left|\frac{Cosh\left[\gamma\left|\frac{L^*}{2} - x\right|\right]}{Cosh\left[\gamma\frac{L^*}{2}\right]} - \frac{1}{2}\frac{Sinh(\gamma x)}{Sinh(\gamma L^*)}\right|\right] \qquad [4.15]$$

and for a non-ideal BT, [4.15] becomes:

$$I_r(x) = -I_c\left[k + (1-k-\frac{I'}{I_c})\left|\frac{Cosh\left[\gamma\left|\frac{L^*}{2} - x\right|\right]}{Cosh\left[\gamma\frac{L^*}{2}\right]} - \frac{1}{2}\frac{Sinh(\gamma x)}{Sinh(\gamma L^*)}\right|\right] \qquad [4.16]$$

4.3 Earth Potential near Tracks

The earth potential is influenced by the distribution of current in the ground. The current distribution will be different for alternating and direct current. Direct current has a tendency to spread out, while alternating current is kept closer to the supply by electromagnetic coupling. For low frequency AC problems, DC approximations can be assumed to give a fair approximation to the actual earth potentials. The principles of DC distribution of current around a point source can be applied to the railway problem if the equivalent rail is viewed as a series of small sections, short enough to be regarded as a point source. In doing so, it becomes possible to apply the principle of

superposition theory in determining the earth potential provided the system can be considered linear.

The starting point therefore, with respect to deriving an expression for the earth potential is an analysis of a simple hemispherical earth electrode as shown in Figure 4.5

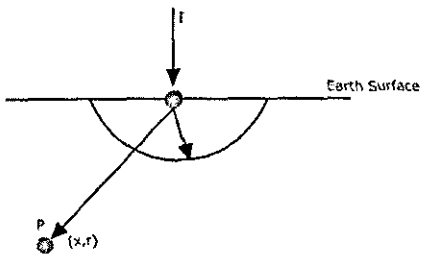

Figure 4.5: Earth potential around a hemispherical electrode

Assuming the earth is homogenous, the current distribution around the hemispherical electrode is given as:

$$i = \frac{I}{2\pi r^2} \qquad [4.17]$$

where r is the distance from the injection point to the observation point P, and the electric field is given as:

$$E = \rho i = \rho \frac{I}{2\pi r^2} \qquad [4.18]$$

where ρ is the resistivity of earth. The potential at the observation point is obtained by integrating [4.18] from the centre of the hemisphere to the observation point with respect to remote earth:

$$V(r) = \int_{r}^{\infty} E dr = \int_{r}^{\infty} \rho \frac{I}{2\pi r^2} dr = \rho \frac{I}{2\pi r} \qquad [4.19]$$

The current injected into the ground from a small piece of the equivalent rail is the derivative of the longitudinal rail current. The distance from the injecting piece of rail to the observation point can be described by the coordinates of the point and injecting rail, this is shown schematically in Figure 4.6.

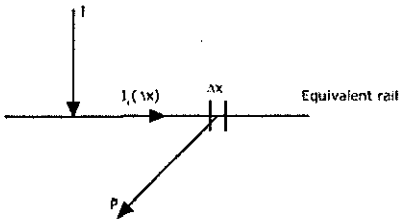

Figure 4.6: The railway line as series of infinitely small sections

An expression for the earth potential presented by Machczynski [3], is given below:

$$V(x) = -\frac{1}{2\pi\sigma} \int_{-\infty}^{\infty} \frac{dI_0(\Delta x)}{d(\Delta x)} \frac{1}{S_{\Delta x}} d\Delta x \qquad [4.20]$$

where $S_{\Delta x} = \sqrt{(x - \Delta x)^2 + r^2}$.

The earth potential at a given point is a function of the leakage current, however the earth potential will be greatly influenced by the leakage currents in the proximity to the observation point. Inserting the expression for earth current in [4.20], gives the earth potential at the observation point:

$$V(p) = \frac{(1-k)I_c\gamma}{2\pi\sigma}\left[\int_{-\infty}^{0}\frac{-e^{\gamma\Delta x}}{S_{\Delta x}}d\Delta x + \int_{0}^{L}\frac{-e^{\gamma\Delta x}+e^{-\gamma(L-\Delta x)}}{S_{\Delta x}}d\Delta x + \int_{L}^{\infty}\frac{e^{\gamma(L-\Delta x)}}{S_{\Delta x}}d\Delta x\right] \quad [4.21]$$

Sunde [4] and Machczynski [5] both provide analytic approximations to [4.21].

4.3.1 Series Discontinuity – Earth Potential

Equation [4.13], defines the total rail current for an ideal series discontinuous system. An expression for earth potential can be obtained by inserting [4.13] into [4.20], to give:

$$V(x) = \frac{-I_c(1-k)\gamma}{2\pi\sigma Cosh\left(\frac{\gamma L'}{2}\right)}\int_{0}^{L'}\frac{Sinh\left[\gamma\left\{\frac{L'}{2}-\Delta x\right\}\right]}{S_{\Delta x}} \quad [4.22]$$

This describes the earth potential for a single transformer section. The influence of neighbouring transformer sections on the earth potential is given as:

$$V(x)=\frac{(1-k)I_c\gamma}{2\pi\sigma Cosh\left(\gamma\frac{L'}{2}\right)}\left[\int_{-\Delta x-\xi}^{-\xi}\frac{Sinh\left[\gamma\left(\frac{L'}{2}-\Delta x-\left(L'+\xi\right)\right)\right]}{S_{\Delta x}}d\Delta x+\right.$$
$$\left.\int_{0}^{L'}\frac{Sinh\left[\gamma\left(\frac{L'}{2}-\Delta x\right)\right]}{S_{\Delta x}}d\Delta x+\int_{L'+\xi}^{2L'+\xi}\frac{Sinh\left[\gamma\left(\frac{L'}{2}-\Delta x+\left(L'+\xi\right)\right)\right]}{S_{\Delta x}}d\Delta x\right] \quad [4.23]$$

Where ξ is the length of the neutral rail of the transformer.

The current pattern will be the same for each elementary transformer section, to account for this in [4.23], $\Delta x=\Delta x\pm(L'+\xi)$. Consequently, the earth potential pattern along the line will be repetitive.

4.4 Coupling from Railways to Buried Metallic Conductor

The induced current in a metallic buried conductor can be due to impressed electromotive force concentrated at certain points and/or due to a distributed electric field in the axial direction along the conductor. The distributed electric field is caused by varying magnetic field surrounding a nearby AC conductor by potential gradients in the earth along the buried metallic structure.

The analysis of coupling to long power and communication lines has been described by Carson [6], Sunde [1], Machczynski [3] and Vance [7] using transmission line models. In this section, the inductive and conductive components are treated separately although the basic equivalent circuit is the same and in principle allows for a combined treatment. In practice, the total coupling influence in a buried metallic conductor is found by adding the inductive and conductive components vectorially.

An element of an extended buried metallic conductor of differential length with inductive and conductive influence is shown in Figure 4.7, where $Edx = \left(-j\omega A - \nabla V\right)dx$.

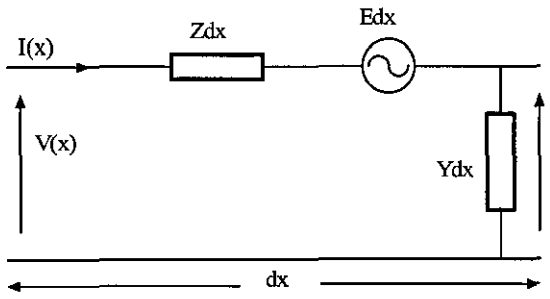

Figure 4.7: Coupling to buried metallic conductor circuit

4.4.1 Conductive Coupling

The figure above presents a convenient starting point for the analysis of conductive interference to an extended buried metallic conductor. In this scenario, the gradient of the scalar potential, $-\nabla V_E$, is the only component of the electric field.

$$E\left(x\right) = -\nabla V_E \qquad [4.24]$$

Where V_E is the impressed potential in the earth adjacent to the conductor, in railway system the source will be the leakage currents from the rails. Thus, Figure 4.8 gives a better representation of the conductive coupling circuit.

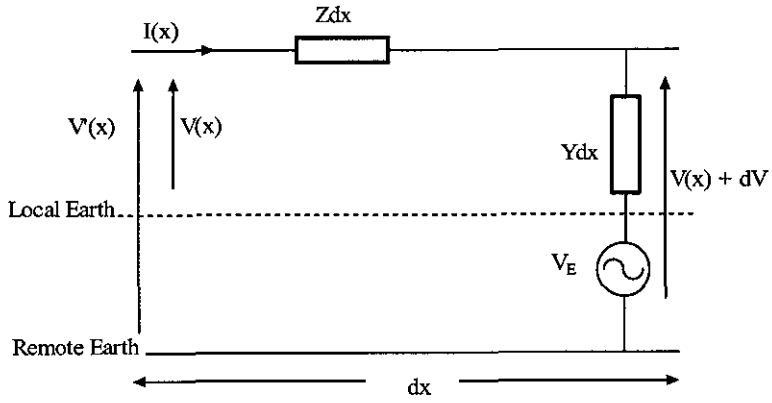

Figure 4.8: Conductive Coupling Circuit

Sunde [1] and Krakowski [8] provided expressions for the conductively coupled current and potential in an infinitely long buried conductor due to an impressed earth potential $V_E(x)$, in the following form [5]:

$$V(x) = \frac{\gamma}{2}\left[e^{-\gamma x}\int_{-\infty}^{x} V_E(v)e^{\gamma v}dv + e^{\gamma x}\int_{x}^{\infty} V_E(v)e^{-\gamma v}dv\right] \qquad [4.25]$$

$$I(x) = \frac{Y}{2}\left[e^{-\gamma x}\int_{-\infty}^{x} V_E(v)e^{\gamma v}dv - e^{\gamma x}\int_{x}^{\infty} V_E(v)e^{-\gamma v}dv\right] \qquad [4.26]$$

Where γ is the propagation constant of the buried metallic conductor defined as $\gamma = \sqrt{ZY}$. In obtaining these expressions, the per unit length parameters are assumed constant over the entire length of the metallic conductor. If the earth return circuit is of finite length and terminated through the earthing impedance at its end point, the current excited in the circuit may be written in the form [5]:

$$I(x)\Big|_{finite} = I(x) + I'(x) \qquad [4.27]$$

$$I'(x) = Ae^{-\gamma x} + Be^{\gamma x} \qquad [4.28]$$

Where A and B are arbitrary constants and I(x) the excited current in an infinitely long conductor given by [4.26]. The current is no longer constant along the conductor, and consequently potentials with respect to earth along the conductor will occur. The potential may be obtained from:

$$\begin{aligned} V(x)\Big|_{finite} &= V_E(x) - \frac{1}{Y}\frac{dI(x)\Big|_{finite}}{dx} \\ &= V(x) - \frac{1}{Y}\frac{dI'(x)}{dx} \end{aligned} \qquad [4.29]$$

Where V(x) is given by [4.25]. The current and potential along the conductor of finite length can be derived as the solution of [4.25] and [4.26] with the following boundary conditions:

$$Z_A = -\frac{V(x_A)\Big|_{finite}}{I(x_A)\Big|_{finite}};\ Z_B = -\frac{V(x_B)\Big|_{finite}}{I(x_B)\Big|_{finite}} \qquad [4.30]$$

Where Z_A and Z_B are the earthing impedance in the end points of the conductors, x_A and x_B respectively.

For complex distributed earth potentials, the curve of the potential distribution may be approximated by segments in which the potential is described by linear, exponential or hyperbolic functions [5]. The resultant distributed potential in the buried metallic conductor can be determined from the summation of all contributions from the segments, as follows:

$$V(x) = \frac{\gamma}{2}\sum_{k=1}^{n}\left[e^{-\gamma x}\int_{-\infty}^{x} V_{E_k}(v)e^{\gamma v}dv + e^{\gamma x}\int_{x}^{\infty} V_{E_k}(v)e^{-\gamma v}dv\right] \qquad [4.31]$$

4.4.2 Inductive Coupling

As with the conductive coupling analysis of the previous section, Figure 4.7 provides a convenient starting point for the analysis of inductive coupling from a railway line to a nearby buried metallic conductor. For this case, the electric field component is simplified to $j\omega A$. For analysis purposes, the source and victim circuit are considered infinitely long and parallel, and the source circuit is assumed constant.

$$Edx = -j\omega A\,dx \qquad [4.32]$$

The induced electric field in the buried metallic conductor from a source conductor may be obtained from

$$E(x) = Z_m(x)I_s(x) \qquad [4.33]$$

Where Z_m is the mutual impedance between the conductors per unit length and $I_s(x)$ is the current in the source conductor. For infinitely long parallel conductors and constant source current, $Z_m(x)$ and $I_s(x)$ will be constant. Thus, the induced current in the buried metallic conductor can be obtained from:

$$I(x) = -I_s\frac{Z_m}{Z_v} = -kI_s \qquad [4.34]$$

There will be zero cable potential with respect to earth due to the absence of leakage current from the earth return circuit to earth. For the case of the

earth return circuit having a finite length, the current and potential are determined from [4.27] to [4.30]. In the situation where the source circuit is of finite length, carrying constant current and the earth return circuit is of infinite length, Figure 4.9 provides a convenient starting for analysis assuming the source current is constant.

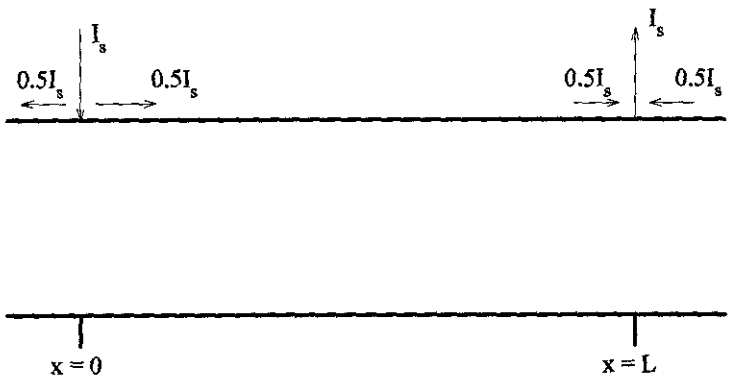

Figure 4.9: Infinitely long conductor subjected to inductive coupling from a conductor of finite length

The currents in the earth return circuit can be determined from [4.24]

$$I(x) = -\frac{1}{2} I_s k \left[2 - e^{-\gamma x} - e^{-\gamma(L-x)} \right] \qquad [4.35]$$

$$V(x) = \frac{Z'}{2} I_s k \left[e^{-\gamma x} - e^{-\gamma(L-x)} \right] \qquad [4.36]$$

For infinitely long lines (i.e. $x = \infty$), [4.35] reduces to $-I_s k$, furthermore for a source conductor of finite length [4.35] tends to $-I_s k$ as γ the propagation constant increases. For a variable source current, potentials with respect to earth will be present on the earth return circuit due to variable induced

current. The current in infinitely long earth return circuit with variable source current can be determined from an expression given in [8].

$$I(x) = \frac{1}{2Z'}\left[e^{-\gamma x}\int_{-\infty}^{x} Z_m I_s(v)e^{\gamma v}dv + e^{\gamma x}\int_{x}^{\infty} Z_m I_s(v)e^{-\gamma v}dv\right] \quad [4.37]$$

$$V(x) = \frac{1}{2}\left[e^{-\gamma x}\int_{-\infty}^{x} Z_m I_s(v)e^{\gamma v}dv - e^{\gamma x}\int_{x}^{\infty} Z_m I_s(v)e^{-\gamma v}dv\right] \quad [4.38]$$

4.5 Impedance Parameters

4.5.1 Single Conductor over a Lossy Earth

A solution for the electromagnetic field and current density in the earth for an infinitely long conductor over a homogenous non-ideal earth was presented by Carson [6]. Carson's solution is based on Maxwell's equation and circuit theory, however due to the use of the circuit theory the validity of the solution is limited to low frequencies.

There are four necessary conditions that must be fulfilled for the application of Carson's equation to be valid, these are:

1) The magnitude of the wave number of the earth must be far greater than that of free space;
2) The length of the observation point to the conductor (or its image) should be far less than the wavelength at free space;
3) The radius of the conductor (rail, catenary, signalling cable etc) must be far less than the height of the conductor above ground;
4) The propagation constant of the conductor must be far less than the wave number of the earth.

For railway installations, conditions (1) and (2) are easily fulfilled due to the frequency of operations, 50Hz (or 16 2/3 Hz as used in some European countries). The issue regarding the application of Carson's equation to railway applications lays in the fulfilment of condition (3) and (4). Condition (3) can not be fulfilled as both rails and signalling/communications cables are in continuous contact with the ground. Similarly, the condition (4) is partially fulfilled as the propagation constant of the rail is of the same order as the wave number of the earth.

Olsen and Pankaskie [9] provided an exact solution of Carson's equation in terms of the approximations that must be made to derive Carson's equation from the exact theory. In [9], two approximate expressions for the propagation constant of wire is given; these expressions apply to a case of a conductor above or at the earth surface. The results obtained from these approximate expressions suggest that the violation (or otherwise) of the Condition (4) depends on the quality of the contact between the conductors and earth. Chang and Wall in [10] also came to the same conclusion.

In the UK railway installation, the insulation between rails and earth is relatively good due to the ballast and the insulating pads used between the rails and the ties on railway lines with concretes slabs. Furthermore, the use of booster transformers (BTs), as discussed in Section 2.3.2, contributes to keeping the current in the rails. These features ensure that the level of leakage current is very low; and thus the rail can be viewed as being slightly above the ground. Condition (4) can thus be regarded as fulfilled and as an approximation Carson's equations can be applied to railway applications.

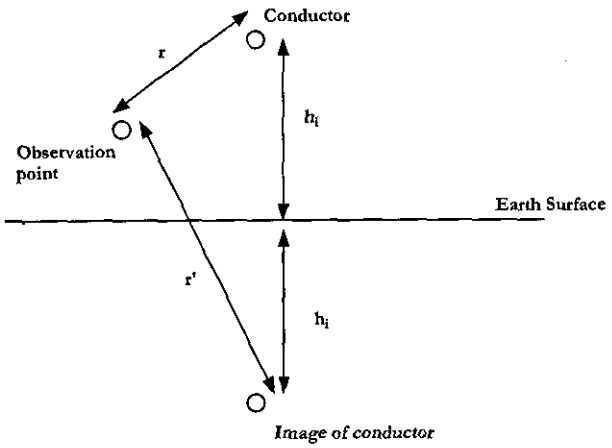

Figure 4.10: Single Conductor over lossy earth

The series impedance for a conductor over a *lossy earth* (as shown in Figure 4.10) can be expressed by the sum of the impedance over a perfectly conducting earth and a contribution that is due to the non-ideal characteristic of the earth. The later is given by an infinite integral; the solution to the infinite integral can be expressed in terms of two functions P and Q. The function P accounts for the dissipated energy in the earth path, while Q accounts for the magnetic effects of the earth current. The following expression can be written for the self impedance of the conductor:

$$Z_{ii} = R_{int} + jX_{int} + j\frac{\omega\mu_0}{2\pi} Ln\frac{2h_i}{r_i} + \frac{2\omega\mu_0}{2\pi}\left(P_{ii} + Q_{ii}\right) \qquad [4.39]$$

Both P and Q can be expressed as infinite series, which are rapidly convergent. For cases where $r = 2h_i\sqrt{\omega\mu\sigma_e} \leq 1/4$, the series can be written as:

$$P_{ii} = \frac{\pi}{8} - \frac{r}{3\sqrt{2}} + \frac{r^2}{16}\left[0.6728 + Ln\frac{2}{r}\right] + \frac{r^3}{45\sqrt{2}} - \frac{\pi r^4}{1536} + \ldots \qquad [4.40]$$

$$Q_{ii} = -0.0386 + \frac{1}{2}Ln\frac{2}{r} + \frac{r}{3\sqrt{2}} - \frac{\pi r^2}{64} + \frac{r^3}{45\sqrt{2}} - \frac{r^4}{384} - \frac{r^4}{384}\left[Ln\frac{2}{r} + 1.0895\right] + \ldots \quad [4.41]$$

The leading terms of [4.40] and [4.41] is dependent on the frequency and on the accuracy required. For low frequency problems, an equivalent depth approximation deduced from Carson's equation can be used. The approximation obtained for cases where $r \leq 1$ and only the leading terms are retained with the earth path viewed as an equivalent conductor at a given depth. The depth is dependent on earth resistivity and frequency and is given by:

$$D_e = 660\sqrt{\frac{\rho}{f}} = 1.31\sqrt{\frac{2\rho}{\mu\omega}} \quad [4.42]$$

The imaginary return conductor has an internal resistance that can be determined from the dissipated energy in the earth. A simplified expression for the series impedance of a conductor over a lossy earth is given as:

$$Z_{ii} = R_{\text{int}} + R_e + jX_{\text{int}} + j\mu_0 fLn\frac{D_e}{r_i} \quad [4.43]$$

Where $R_e = \frac{\mu\pi f}{4}$, a closer look at [4.43] reveals an independence of the conductor's height above the ground. However, the assumption that the conductor height above ground is much larger than the conductor radius be fulfilled.

The analysis presented above assumes that the earth is a homogeneous conducting half space, in reality railway installations span several kilometres and variations in soil characteristics is to be expected. This variation can result in difficulties in defining a multilayer soil model which adequately describes

the whole installation. [4.43] can be extended to deal with horizontally stratified earth with multiple layers. Nakagawa *et al* detailed and provided expressions for a 3 layer case in [11] and a multiplayer case in [12].

For buried conductors, if propagation effects are neglected, an expression for the impedance of a conductor at the earth's surface for cases where $|k_e r_i| \leq 1/4$ is given by Sunde [4] as:

$$Z_{ii} = Z_{\text{int}} + \frac{j\omega\mu}{2\pi}\left[\frac{-j\pi}{4} + Ln\left(\frac{1.85}{|r_i k_e|}\right)\right] \qquad [4.44]$$

where $k_e = j\omega\mu\sigma_e$ and r_i is the radius of the conductor. According to Sunde, the self inductance of an insulated conductor buried at normal depth will be essentially the same as the self inductance of a conductor at the earth's surface. Consequently, Carson's equations can be used for buried conductors as long as the leakage currents are small. For situations where the propagation effects are non-negligible, i.e. large leakage currents, the expressions for the impedance will be dependent on the propagation constant, γ, of the buried conductor and is given as:

$$Z_{ii}(\gamma) = Z_{\text{int}} + \frac{j\omega\mu}{2\pi} Ln\left(\frac{1.85}{r_i\sqrt{k_e^2 + \gamma^2}}\right) \qquad [4.45]$$

4.5.2 Mutual Impedance between Two Conductors with Earth Return

An expression for the mutual impedance for two conductors over a perfectly conducting earth (as shown in Figure 4.11) and a term representing the non-ideal characteristic of the earth was provided by Carson [6].

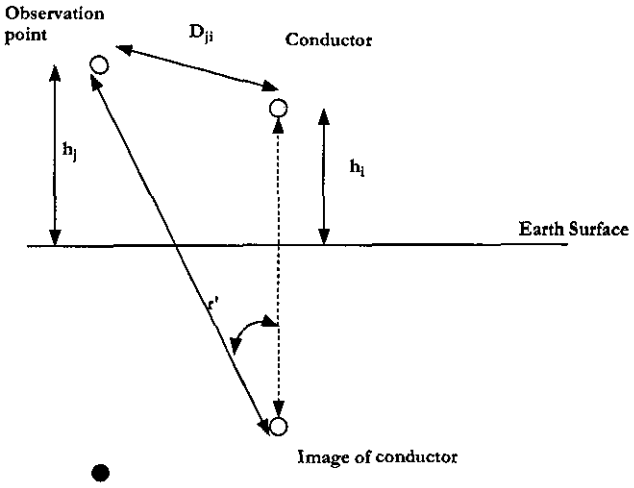

Figure 4.11: Single Conductor over lossy earth

$$Z_{ik} = \frac{j\omega\mu_0}{2\pi} Ln\left(\frac{D'_{ik}}{D_{ik}}\right) + \frac{2\omega\mu_0}{2\pi}\left(P_{ik} + Q_{ik}\right) \qquad [4.46]$$

For $r \leq 1/4$, the infinite series P_{ik} and Q_{ik} are given by:

$$P_{ik} = \frac{\pi}{8} - \frac{rCos\theta}{3\sqrt{2}} + \frac{r^2}{16} Cos2\theta\left(0.6728 + Log\frac{2}{r}\right) + \frac{r^2\theta Sin2\theta}{16} \qquad [4.47]$$

$$Q_{ik} = -0.0386 + \frac{1}{2} Log\frac{2}{r} + \frac{rCos\theta}{3\sqrt{2}} \qquad [4.48]$$

Where $r = kD'_{12} = \sqrt{\omega\mu_e\sigma_e} D_{12}$ and $\theta = \sin^{-1}\left|\frac{D_{12}}{D'_{12}}\right|$

Using the concept of equivalent depth of return for this system leads to the following expression for the mutual impedance between the two conductors:

$$Z_{ik} = R_e + j\mu_0 fLn\left|\frac{D_e}{D_{ik}}\right| \qquad [4.49]$$

This equation applies to cases where the earth is supposed to be homogenous. A simplified expression based on Carson and Pollaczek [13] for mutual coupling of multiple conductors referenced in [14] is given as:

$$M_{ij} = \frac{\mu_0}{2\pi}\left|-j\alpha\frac{\pi}{4} + Ln\left(\frac{D_e}{D_{ij}}\right)\right| \qquad [4.50]$$

4.5.3 Internal Impedance and Inductance of Rail

The internal impedance of a conductor is defined in [15] as the ratio of the surface voltage drop V_s and the total current in the conductor I. The internal impedance is due to the electromagnetic fields within the conductor under investigation.

$$\begin{aligned} Z_{\text{int}} &= \frac{V_s}{I} \\ R_{\text{int}} &= \text{Re}\{Z_{\text{int}}\} \\ L_{\text{int}} &= \frac{\text{Im}\{Z_{\text{int}}\}}{2\pi f} \end{aligned} \qquad [4.51]$$

The real part, R_{int}, of [4.43], reflects the dissipated energy within the conductor, while the imaginary part, X_{int}, reflects the stored magnetic energy within the said conductor. For circular conductors, where cylindrical symmetry in the fields exists, a unique definition of the internal and external impedance can be given. The border between them will be situated at the outer surface of the conductor. For non-cylindrical conductors the concept of internal impedance is more obscure since the fields do not exhibit any

cylindrical symmetry. The impedance can be linked to the electromagnetic fields physically inside the conductor but this approach would be difficult in linking with any calculation of the external field to determine the total impedance for the conductor. A common approach to determining the internal impedance of non-cylindrical conductors is to define a border between the internal and external impedance as a circle with a given radius outside of the conductor. The radius is chosen in such a way that the magnetic flux lines are approximately circular at this distance from the centre of the conductor. This concept is shown schematically in Figure 4.12.

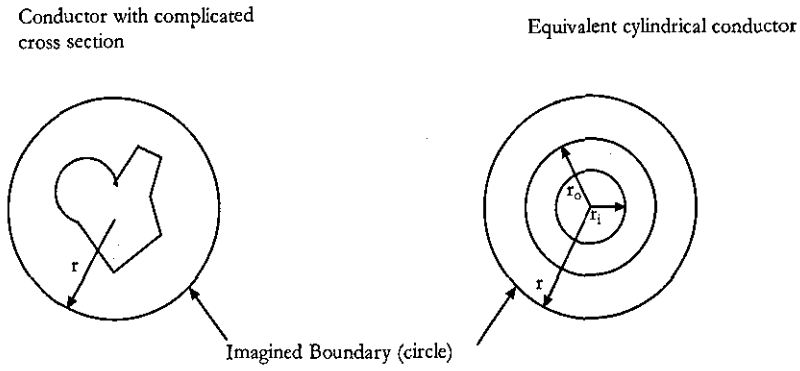

Figure 4.12: Treatment of non-cylindrical conductors as cylindrical.

For low frequencies and non magnetic conductors, the current in such a conductor will be evenly distributed over the cross section. For such conditions the concept of geometric mean radius can be used to give a compact description of the total reactance of the conductor with earth return, as given below in [4.49]. Referred [16] dwells extensively on geometric mean radius.

$$Z_{ii} = R_{int} + R_e + j\mu_0 f \ln \frac{D_e}{g_{ii}} \qquad [4.52]$$

For magnetic material the skin depth effects will be noticeable at relatively low frequencies due to the high permeability of the material. In addition, the material properties are often non-linear varying with both current and frequency. The current will no longer be evenly distributed over the cross section, and the concept of geometric mean radius cannot be used. The internal impedance of conductors of non-linear magnetic materials is better achieved through measurement for this reason.

The internal impedance of a circular conductor whose base material is magnetic can be calculated if the magnetic properties of the conductor are considerable constant. The internal impedance can be determined by considering the eddy currents in an isolated conductor of circular cross section. A general expression for the internal impedance of a hollow cylindrical conductor with outer radius r_o and a inner radius r_i is given by [1]:

$$Z_{int} = \frac{1}{2\pi r_o}\sqrt{\frac{j\omega\mu_c}{\sigma_c}}\left(\frac{I_0(\gamma r_o)K_1(\gamma r_i)+K_0(\gamma r_o)I_1(\gamma r_i)}{I_1(\gamma r_o)K_1(\gamma r_i)-I_1(\gamma r_i)K_1(\gamma r_o)}\right) \qquad [4.53]$$

Where I_o and K_o designate Bessel functions of the first and second kind for imaginary arguments, and $dI_o/r_o = I_1$ and $dK_o/r_o = -K_1$. For a solid conductor $(r_i = 0)$, [4.52] simplifies to:

$$Z_{int} = \frac{1}{2\pi r_o}\sqrt{\frac{j\omega\mu_c}{\rho_c}}\frac{I_0(\gamma r_i)}{I_1(\gamma r_i)} \qquad [4.54]$$

The skin effect must also be taken into account in any analysis of the internal resistance and inductance behaviour of the conductor with respect to

frequency [20], [6]. Two simplified expressions may be derived from [4.50] by using the assumption of very low frequency (large skin depth) and very high frequency (small skin depth) as follows:

$$R(f) = \begin{cases} \dfrac{1}{\sigma \pi r_o^2} & r_o < 2\delta \\ \dfrac{1}{2\pi} \sqrt{\dfrac{\mu}{\pi \sigma f}} & r_o > 2\delta \end{cases} \qquad [4.55]$$

$$L(f) = \begin{cases} \dfrac{\mu}{8\pi} & r_o < 2\delta \\ \dfrac{1}{4\pi r_o} \sqrt{\dfrac{\mu}{\pi \sigma f}} & r_o > 2\delta \end{cases} \qquad [4.56]$$

4.5.4 Determination of the Equivalent Radius of the Rail

Given the complex shape of the running and power rails (See Figure 4.13) and the strong skin effect, there are two additional issues that need resolving: determination of the equivalent radius of the rails and the determination of the magnetic permeability. The running rails are ferromagnetic and have non-linear properties; in addition the rail has a large cross section and a peculiar shape (as discussed in Section 2). The rails can be analysed as an equivalent solid cylinder with constant material properties [17] - [19] and the internal impedance of the rail can be determined from [4.53].

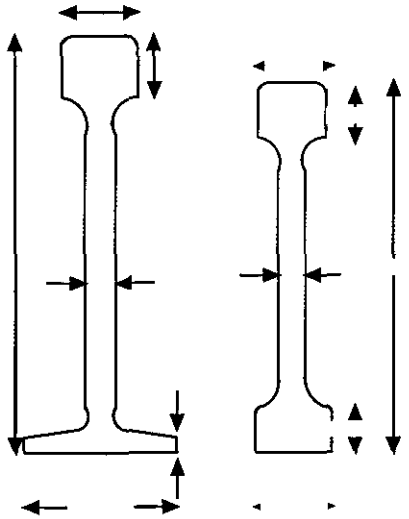

Figure 4.13: Schematic of typical rail profile

At high frequency, where the current is distributed almost along the rail perimeter, p_{rail} , the equivalent rail radius may be determined from:

$$2\pi r_{eq} = p_{rail} \qquad [4.57]$$

At low frequency, where the current is distributed almost uniformly across the rail section A_{rail} , the equivalent rail radius may be determined from:

$$\pi r_{eq}^2 = A_{rail} \qquad [4.58]$$

The equivalent radius can also be determined from the inductance of the rail. The inductance comprises of two components: the internal inductance and external inductance. The internal inductance is due to the magnetic fields inside the rail whereas the external inductance is due to the magnetic field

outside the rail. As the frequency increases, the internal inductance decreases since the fields concentrate toward the surface (the skin depth effect). This re-distribution of the fields and current changes the internal inductance and resistance. Thus, the internal inductance is a function of frequency. The external inductance is not affected by frequency since only the fields within the rail are affected by skin effect.

With reference to Figure 4.10, the inner radius r_i only influences the frequency response at low frequency since at high frequency the current concentrates at the surface of the rail. Thus, for $r_i = 0$ and at high frequencies (such that the skin depth is much less than the equivalent rail radius and the internal inductance is negligible), the inductance of the rail may be described by [21]:

$$L \cong L_{ext} \cong \frac{\mu_o}{2\pi} \ln\left(\frac{r}{r_o}\right) \qquad [4.59]$$

The equivalent rail radius is thus determined from [4.56] as:

$$r_o \cong r.e^{\left(-\frac{2\pi L}{\mu_o}\right)} \qquad [4.60]$$

The internal inductance at dc and frequencies such that the skin depth is greater than the equivalent rail radius is:

$$L_{int(dc)} \cong \frac{\mu_c}{8\pi}\left(\frac{1-3R^2}{1-R^2} - \frac{4R^4 \ln(R)}{\left(1-R^2\right)^2}\right) = \frac{\mu_c}{8\pi} g(R) \qquad [4.61]$$

Where $R = r_i / r_o$ is the ratio of the inner radius to the outer radius and $g(R)$ is a correction factor. For a solid round conductor $(r_i = 0)$, $g(R)$ is equal to unity. The permeability of the equivalent conductor can be determined from:

$$\mu_c = L_{int(dc)} \left(\frac{8\pi}{g(R)} \right) \qquad [4.62]$$

The dc resistance and conductivity of the equivalent rail can then be expressed by the following:

$$R_d = \frac{1}{\left(\sigma_c \pi \left\{ r_o^2 - r_i^2 \right\}\right)} = \frac{1}{\left(\sigma_c \pi r_o \left\{ 1 - R^2 \right\}\right)}$$

$$\sigma_c = \frac{1}{R_d \pi r_o^2 \left(1 - R^2\right)} \qquad [4.63]$$

Equation [4.59] – [4.63] can then be used to determine the impedance of the equivalent rail.

4.6 Summary

An understanding of the current distribution between different conductors of the return path of an electrified railway is an important element in the evaluation of the electromagnetic coupling from a railway line to nearby buried metallic conductors or structures.

There are no analytical techniques developed specifically for the study of railway electromagnetic coupling problems, as a result use is made of the theories and analytical techniques developed for the power and telecommunication sectors. This requires modifications to the basic theory,

taking into account the physics of the installation , electromagnetic interaction and the uniqueness of a railway installation.

The analysis developed herein highlights the usefulness and effectiveness of the transmission line theory, as applied to the railway systems. It is demonstrated that the analytical models works for simple railway configurations but becomes difficult to implement as the complexity of the railway model increases.

4.7 References

[1] Sunde, E. D. "*Earth conduction effects in transmission systems*", Van Nostrand., New York, 1946

[2] Riordan, J. "*Current propagation in electric railway propulsion systems*", Transactions of the American Institute of the Electrical Engineers, December 1932, Pg. 1011 – 1019.

[3] Machczynski, W. "*Currents and potentials in earth return circuits exposed to alternating current electric railways*", IEE Proceedings, Volume 129, Part B, No 5, September 1982, Pg. 279 – 288.

[4] Sunde, E. D. "*Currents and potentials along leaky ground return conductors*", Transactions of the American Institute of Electrical Engineer, December 1936, Pg. 1338 - 1346

[5] Machczynski, W, "*Evaluation of conductive effects on earth return circuits*", EMC Zurich 1993, Pg. 117 – 120.

[6] Carson, J. R. "*Wave propagation in overhead wires with ground return*", Bell System Technical Journal, Volume 5, 1926, Pg. 539 – 554.

[7] Vance, E. F. "*Coupling to Shielded Cable*", Wiley, New York

[8] Krakowski, M. "*Currents and potentials along extensive underground conductors*", IEE Proceedings, Volume 115, No. 9, September 1968, Pg. 1299 – 1304.

[9] Olsen, R. G., Panaskie, T. A., "*On the exact Carson and image theories for wire at or above the earth's interface*", IEEE Transactions on Power Apparatus and Systems, Vol. PAS-102, No. 4, April 1983, pg 769 – 778.

[10] Chang, D. C., Wait, J. R., "*Extremely low frequency (ELF) propagation along a horizontal wire located above or buried in the earth*", IEEE

Transactions on Communications, Vol. COM-22, No. 4, April 174, pg. 421 – 427.

[11] Nakagawa, M et al, "*Further studies on wave propagation in overhead lines wit earth return: impedance of stratified earth*", Proceedings of the IEE, Vol 120, No. 12, December 193, Pg. 1521 - 1528

[12] Nakagawa, M and Iwamoto, K, "*Earth return impedance for the multilayer case*", IEEE Transaction on Power Apparatus and System, Vol PAS-95, No 2, march/April 1976, Pg. 671 - 676

[13] Pollaczek, F, "*Uber das Feld einer unendlich langen wechselstromdurchflossenen Einfachleitung*', Electrishe Nactrichten Technik, Vol 3, No 9, 19926, Pg. 339 – 39.

[14] RT/E/C/500018, "*Methodology for the determination of interaction with neighbouring railways*", Railtrack Company, 2001

[15] Ramo, S., Winnery, J. R., and Van Duzer, T., "*Fields and Waves in Communications Electronics*", John Wiley and Sons, 1965.

[16] Tesche, F. M *et al*, "*EMC Analysis Methods and Computational Models*", John Wiley and Sons, New York, 1997.

[17] Hill, R. J and Carpenter, D.C, "*Determination of rail internal impedance for electric railway traction system simulation*", Proc. Inst. Elect.. Eng. Part B, Vol. 138, No. 6, pg. 311 – 321, 1991.

[18] Ametani, A. and Fuse, I., "*Approximate method for calculating the impedance of multi-conductors with cross sections of arbitrary shapes*", Elec. Eng. Japan, Vol. 111, No. 2, Pg 117 -129, 1992.

[19] Ametani et al, "*Wave propagation characteristics of iron conductors in a intelligent buildings*", Trans. Inst. Elec. Eng. Japan, Vol. 120-B, No. 1, Pg. 31 – 39, 2000.

[20] *Directives concerning the protection of telecommunication lines against harmful effects from electric power and electrified railway lines. Vol. 2: Calculating induced voltages and currents in practical cases.* CCITT, 1989.

[21] Wang, Y. and Tsai, Y. "*Calculation of the frequency dependent impedance of rail tracks using a four parameter equivalent tubular conductor model*", IEEE Trans. on Power Delivery, Vol. 19, No. 3, July 2004.

[22] Hill, R. J. "*Electric railway traction – Part 7 Electromagnetic interference in traction systems*", Power Engineering Journal, December 1997, Pg. 259 – 266.

[23] Hill, R. J, Carpenter, D. C and Tasar. T, "*Railway track admittance, earth leakage effects and track circuit operation*", IEEE/ ASSME Joint Railroad Conference, Philadelphia, April 1989, Pg. 55 - 62

[24] Haubrich, J. H, Flechner, B. A and Machczynski, W. "*Universal model for the computation of the electromagnetic interference on earth return circuits*", IEEE Transactions on Power Delivery, Volume 9,

No. 3, July 1994, Pg. 1593 – 1598.

[25] Pleym, A. "*EMC in railway systems: conductive coupling from track to nearby metallic structure*", EMC Zurich 1999, Pg. 425 – 430.

[26] *Directives concerning the protection of telecommunication lines against harmful effects from electric power and electrified railway lines. Vol. 1: Design, construction and operational principles of telecommunication, power and electrified railway facilities.* CCITT, 1989.

[27] *Directives concerning the protection of telecommunication lines against harmful effects from electric power and electrified railway lines. Vol. 3: Capacitive, inductive and conductive coupling: physical theory and calculation methods.* CCITT, 1989.

[28] *Directives concerning the protection of telecommunication lines against harmful effects from electric power and electrified railway lines. Vol. 4: Inducing currents and voltages in electrified railways systems.* CCITT, 1989.

[29] *Directives concerning the protection of telecommunication lines against harmful effects from electric power and electrified railway lines. Vol. 6: Dangers and disturbance.* CCITT, 1989.

Chapter 5

LOW FREQUENCY COUPLING ANALYSIS USING NUMERICAL MODELLING

There are numerous calculation methods that can be employed to compute the electromagnetic problems described in the previous chapter, however the degree of accuracy will depend on the method employed, the assumptions made and the accuracy of the model employed. The benefit of using numerical modelling in railway signalling applications is the ability to compute the inductive and conductive coupling to nearby buried metallic conductors. This is of particular importance during the design phases of new or re-signalling works and/or the locations of other services wayside to the track.

Numerical modelling is concerned with the representation of physical systems by specific quantities, which are obtained by numerical methods. For electromagnetic systems, it is generally required to obtain the electric and magnetic field within a volume of space, subject to appropriate boundary conditions. The increase of computer power over the last 20 years has made the tools for numerical modelling widely accessible but although computation is well understood, the application of numerical modelling in the railway industry, is still in its infancy [1]. This is because the view has prevailed that phenomena are governed by equations; once the relevant equations are known, it is a simple matter of computation to find the solution. It is now becoming more accepted that the equations are themselves models of the real system and they may be the most appropriate way of expressing a problem, which then has to be solved numerically because the analytical solution is

intractable. Thus use of computer graphics allows electromagnetic field behaviour to be observed directly and the speed of computation makes it possible to use numerical methods as experimental tools both for visualizing fields, in a way, which cannot be achieved via measurements, and to undertake sensitivity studies, which would otherwise be unacceptably expensive.

Most electromagnetic field problems involve either partial differential equations or integral equations. For complex geometries and inhomogeneous materials these equations are not solved analytically. The partial differential equations can be solved using, among other methods, the Finite Element Method, while Method of Moments (MOM) can be used to solve integral equations. In such numerical approximations, the continuous partial differential equations or integral equation is replaced by an approximate numerical description characterized by discrete points.

This section reviews the application of numerical modelling to solve electromagnetic interference issues in railway applications.

5.1 Finite Elements Method

The Finite Element Method is a procedure for solving field problems by dividing the region of interest into small elements and by solving differential equations in each of those elements. The method is usually employed in the frequency domain but can also be used for time domain problems. The finite elements analysis of any problem involves the following basic steps:

- Discretising the region under consideration into a finite number of sub-regions;

- Approximate the field in each sub-region as a series of known functions with unknown coefficients;
- Express the energy in each sub-region as a function of the unknown coefficients;
- Introduce constraints on the coefficients in order to satisfy boundary conditions;
- Obtain the unique solution by minimizing the energy.

The procedure outlined above is partly based on physical reasoning in that the physical principles of minimizing energy can be used. However, the procedure is general in its application and can be used for any functional equation i.e. for equations not associated with energies.

5.1.1 Solution to a Lossy DC Transmission Line

In Figure 4.6, an equivalent circuit that can be used for the analysis of inductive and conductive coupling to buried metallic conductors was introduced. In this section FEM is applied to determine the line voltage of a two conductor DC transmission line.

Referring to Figure 4.6, the line parameters are the Resistance, R and the Conductance, G per unit length. Applying Kirchoff's voltage and current laws to the infinitesimal sections dx, gives:

$$\frac{dV}{dx} = -RI(x) \qquad [5.1]$$

$$\frac{dI}{dx} = -GV(x) \qquad [5.2]$$

Equation [5.1] and [5.2] can be transformed to Helmholtz equation[6] by taking the derivative of [5.1] with respect to x and applying the solution to Helmholtz equation. Using FEM however, requires the transmission line to be divided into N equally sub regions as shown in the figure below:

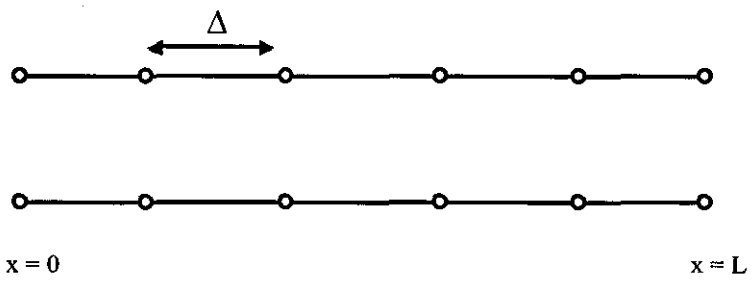

Figure 5.1: Line divided into N sections

Where $\Delta = \frac{L}{N}$

From [5.1], it is clear that the voltage is differentiable and thus the voltage is approximated by a piece wise linear function:

$$V_n(x) = V_n^- \left[\frac{X_n^+ - x}{X_n^+ - X_n^-}\right] + V_n^+ \left[\frac{x - X_n^-}{X_n^+ - X_n^-}\right] = \frac{1}{\Delta}\left[V_n^- \ X_n^+ - x \ + V_n^+ \ x - X_n^- \ \right] \qquad [5.3]$$

The power loss in an infinitesimal section, as shown in Figure 5.1, can be obtained as the sum of the power loss in the resistance and the conductance.

---

[6] The scalar homogenous Helmholtz equation is $\nabla^2 f + k^2 f = g$ where f is the wanted scalar potential function and g is a known driving or excitation function

$$\begin{aligned} P_{dx} &= \left[Rdx|I(x)|^2 + Gdx|V + dV|^2 \right] \\ &\approx \left[Rdx|I(x)|^2 + Gdx|V(x)|^2 \right] \end{aligned} \quad [5.4]$$

Combining [5.1], [5.2] and [5.4], and dividing with dx leads to the power loss per unit length:

$$\begin{aligned} P &= \left[R|I(x)|^2 + G|V(x)|^2 \right] \\ &= \frac{1}{R}\left[\frac{dV}{dx} \right]^2 + G|V|^2 \end{aligned} \quad [5.5]$$

Thus, the total power loss in section n is given as:

$$P_n = \int_{X_n^-}^{X_n^+} \left\{ \frac{1}{R}\left[\frac{dV_n}{dx} \right]^2 + GV_n^2 \right\} dx \quad [5.6]$$

Inserting [5.3] into [5.6] leads to:

$$P_n = \frac{1}{\Delta R}\left| V_n^+ - V_n^- \right|^2 + \Delta G\left\{ V_n^- V_n^+ + \frac{1}{3}\left| V_n^+ - V_n^- \right|^2 \right\} \quad [5.7]$$

Since the voltage is continuous along the transmission line, the voltage at the right end of section n is equal to the voltage at the left end of section $n+1$. Thus we can apply the following boundary conditions:

$$\begin{aligned} V_{n=1}^- &= V_{gen} \\ V_n^+ &= V_{n+1}^- \end{aligned} \quad [5.8]$$

The constraints on the voltages imply that it is not necessary to keep the voltages at an intersection apart, thus rewriting [5.7] gives:

$$P_n = \frac{1}{\Delta R}\left| V_{n+1} - V_n \right|^2 + \Delta G\left[V_n V_{n+1} + \frac{1}{3}\left| V_{n+1} - V_n \right|^2 \right];\ n = 1...N \qquad [5.9]$$

And the total power loss in the line is given as:

$$P_{total} = \sum_{n=1}^{N} P_n \qquad [5.10]$$

The nest step in the process is the minimisation of the overall power loss with respect to the node voltages. This is achieved by applying the relation below:

$$\frac{dP_{total}}{dV_m} = 0;\ m = 2...N+1 \qquad [5.11]$$

Assuming $N = 6$, [5.11] can be written in matrix form as:

$$\begin{bmatrix} B & A & 0 & 0 & 0 & 0 \\ A & B & A & 0 & 0 & 0 \\ 0 & A & B & A & 0 & 0 \\ 0 & 0 & A & B & A & 0 \\ 0 & 0 & 0 & A & B & A \\ 0 & 0 & 0 & 0 & A & B/2 \end{bmatrix} \begin{bmatrix} V_2 \\ V_3 \\ V_4 \\ V_5 \\ V_6 \\ V_7 \end{bmatrix} = \begin{bmatrix} -V_1 A \\ 0 \\ 0 \\ 0 \\ 0 \\ 0 \end{bmatrix} \qquad [5.12]$$

Where $A = \frac{\Delta G}{3} - \frac{2}{\Delta R}$ and $B = \frac{4\Delta G}{3} + \frac{4}{\Delta R}$

5.1.2 Elements

Elements are the small regions in which the wanted function is approximated as a series of known functions with undetermined coefficients. Depending on the geometrical shape, an element can be one-, two- or three- dimensional. Elements are also classified by the type of approximation functions used,

these are referred to as shape functions and are very often polynomial. The degree of the polynomial is called the order of the element. The element can be described by mathematically by:

$$f = \sum_{i=1}^{n} \alpha_i f_i \qquad [5.13]$$

5.1.1.1 One – dimensional, first order

This element was used in the analysis performed in section 5.1.1. It is the simplest element as shown in Figure 5.2.

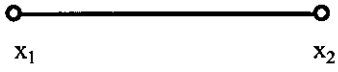

Figure 5.2: A one – dimensional finite element of the first order

For a first order element the function value along the element is assumed to vary linearly, thus $V = a + bx$. The element is fully described by the function values at the nodes and the co-ordinates of the nodes. Boundary conditions, of the Dirchlet type[7], can be fulfilled by forcing the function values at the nodes. If the function values at $x = x_1$ and $x = x_2$ are V_1 and V_2 respectively, the following matrix relation must be valid:

---

[7] The simplest form of the Dirichlet boundary condition is one where the value of the dependent variable is specified on the boundary. In a two-dimensional problem where ϕ is the dependent variable, the relation $\phi = g(x, y)$ (x, y) on S specifies a Dirichlet condition, where $g(x, y)$ is a known function of position.

$$\begin{bmatrix} V_1 \\ V_2 \end{bmatrix} = \begin{bmatrix} 1 & x_1 \\ 1 & x_2 \end{bmatrix} \begin{bmatrix} a \\ b \end{bmatrix} \qquad [5.14]$$

Solving for the coefficients a and b gives:

$$\begin{bmatrix} a \\ b \end{bmatrix} = \begin{bmatrix} 1 & x_1 \\ 1 & x_2 \end{bmatrix}^{-1} \begin{bmatrix} V_1 \\ V_2 \end{bmatrix} \qquad [5.15]$$

Thus the function $V = a + bx$ can be written as:

$$V = \begin{bmatrix} 1 & x \end{bmatrix} \begin{bmatrix} a \\ b \end{bmatrix} = \begin{bmatrix} 1 & x \end{bmatrix} \begin{bmatrix} 1 & x_1 \\ 1 & x_2 \end{bmatrix}^{-1} \begin{bmatrix} V_1 \\ V_2 \end{bmatrix} \qquad [5.16]$$

Equation [5.16] can be written as:

$$V = \sum_{i=1}^{2} V_i h_i(x); \text{ where } h(x) = \begin{bmatrix} 1 & x \end{bmatrix} \begin{bmatrix} 1 & x_1 \\ 1 & x_2 \end{bmatrix}^{-1} \qquad [5.17]$$

5.1.1.2 Two – dimensional, first order

There are many different shapes of two dimensional finite elements, however the most commonly used shape is the triangle element. The triangular element is often used because it is easy to approximate an arbitrary surface with several triangular elements.

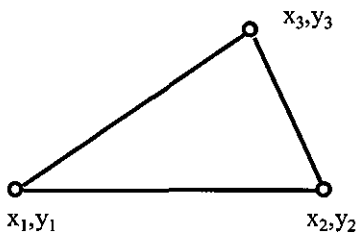

Figure 5.3: Two dimensional triangle finite element of the first order.

The function value for the first order triangle surface is assumed to vary linearly in both co-ordinates, thus $V = a + bx + cy$ and [5.14] becomes:

$$V = 1 \quad x \quad v \begin{bmatrix} 1 & x_1 & y_1 \\ 1 & x_2 & y_2 \\ 1 & x_3 & y_3 \end{bmatrix}^{-1} \begin{bmatrix} V_1 \\ V_2 \\ V_3 \end{bmatrix} \qquad [5.18]$$

5.1.1.3 Three – dimensional, first order

The simplest three-dimensional element is the tetrahedron. The function value for the first order tetrahedron volume element is assumed to vary linearly in all three co-ordinates, thus $V = a + bx + cy + dz$ and [5.14] becomes:

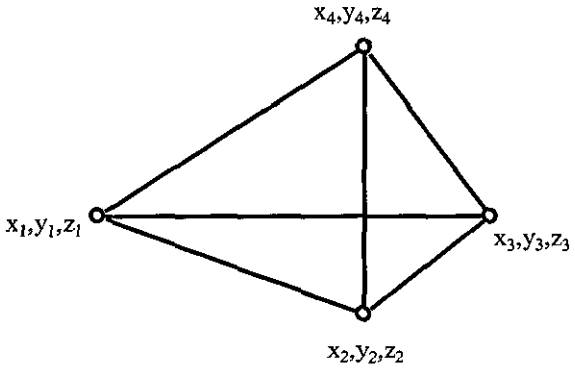

Figure 5.4: Three dimensional tetrahedral finite element of the first order

$$V = 1 \quad x \quad y \quad z \begin{bmatrix} 1 & x_1 & y_1 & z_1 \\ 1 & x_2 & y_2 & z_2 \\ 1 & x_3 & y_3 & z_3 \\ 1 & x_4 & y_4 & z_4 \end{bmatrix}^{-1} \begin{bmatrix} V_1 \\ V_2 \\ V_3 \\ V_4 \end{bmatrix} \qquad [5.19]$$

5.1.2 FEM and Railway Modelling

Finite element method has been applied to compute the resistance and internal inductance of a rail [2] - [5]. In both applications two dimensional finite elements methods was employed; for an overhead line electrified single track finite element model, large elements were used for long distances from the track where the fields are low and smaller meshes were used near and within the rails where the field gradients change rapidly. Triangular elements are used near the tail surface to provide more flexibility when modelling complex shapes. The difficulties associated with finite element modelling of railway traction network are [5]:

- The electromagnetic fields extend far from the track, which conflict with the need to use a bounded FEM mesh;

- The electric and magnetic properties of the rails, catenary, track sub-structure and ground must be accurately defined, including any non-linearities with current, frequency and temperature;
- The optimum number and size of mesh element is unknown and must be found by experience.

Satsios *et al* [6] employed finite element modelling to compute the inductive interference caused by AC electric traction to nearby telecommunications cables. In this application, end effects were ignored enabling the use of two-dimensional FEM. If current transfer zones are long, the rail current will never reach the stationary values of kI_c used in this FEM calculation. As an indication two-dimensional FEM cannot be used to compute the inductive and conductive interference from a railway system to nearby buried conductor.

The desire to compute the inductive and conductive coupling starting from the catenary current will require the use of three-dimensional finite element method. However, this will place a greater demand of computational resources since FEM requires the entire problem region to be modelled with elements. Since an infinite number of elements is not possible, problems with boundaries at infinity have to be treated in a special way using techniques such as infinite elements, artificial boundaries or a combination of FEM and other methods. The combination of FEM with other method is implemented in such a way that FEM is used for the interior region, which is bounded, and the other method is used for the exterior region. The other method used for the exterior region could be an analytical method or a numerical method such as the method of moments. Finally, the two solutions are combined since the fields at the common boundary have to be continuous.

Nekhoul *et al* [7], [8] have shown that a three-dimensional finite element method with an efficient model for open boundaries of the semi-infinite regions (air and earth) is capable of predicting the electromagnetic fields produced by an earthing system. In their work, air and earth are discretised into volume elements, while the conductors are discretised into line elements. Employing line elements in this application is possible if one assumes that the current is distributed evenly over the cross section of the conductors. This assumption is valid for non-magnetic conductors that are thin compared to their length and at low frequencies.

Various formulation of the problem was used, depending on the material properties, in the different regions of the model. For conducting volumes an AV formulation was used, where A is the magnetic vector potential and V is the scalar electric potential. For non-conducting volumes with source currents a vector potential formulation is generally used, however a total magnetic scalar potential can be used to save computational time. Starting from the work undertaken by Nekhoul *et al* it is possible to apply three dimensional FEM to railway applications without booster transformers. The pre-processing part of 3D FEM models can be cumbersome, and will generally take quite some time. A possible problem is also the limitation in boundary conditions that can be applied. Also there currently lacks a simple method of incorporating the effects of booster transformers in FEM.

5.2 Transmission Line Matrix

The Transmission Line Matrix method is a numerical technique for solving field problems using circuit equivalents. The technique is based on the fact that the equations obtained from the transmission line theory have certain similarities with the equations obtained directly from Maxwell's equations. The main feature of this method is the simplicity of formulation and

programming for a wide range of application [9], [10]. Like FEM, TLM is a descretisation process, however unlike FEM; TLM is a physical discretisation approach [11]. The technique seeks to describe problems directly in terms of the time response of the telegraphers' equation, which in general form can be described by:

$$\nabla^2\phi = A\frac{\partial^2\phi}{\partial t^2} + B\frac{\partial\phi}{\partial t} \qquad [5.20]$$

The region under consideration is modelled by a large number of short transmission line sections connected together in a mesh. The next step is to solve the resulting set of transmission line equations for the voltages and currents at all nodes in the mesh. This is done in the time domain with an iterative method.

5.2.1 The Transmission Line Section

A transmission line is an entity, which has electrical capacitance, inductance and resistance distributed along its length. The inductance, capacitance and resistance will depend on the length of the transmission line, thus the distributed components are defined as, L_d, R_d and C_d. It is often convenient to collect these distributed parameters over a unit length and display them as if they were lumped into a series of discrete components. Figure 5.5a shows an equivalent circuit model for a short transmission line section, Figure 5.5b shows a lumped parameter representation of a lossless $R_d = G_d = 0$ transmission line.

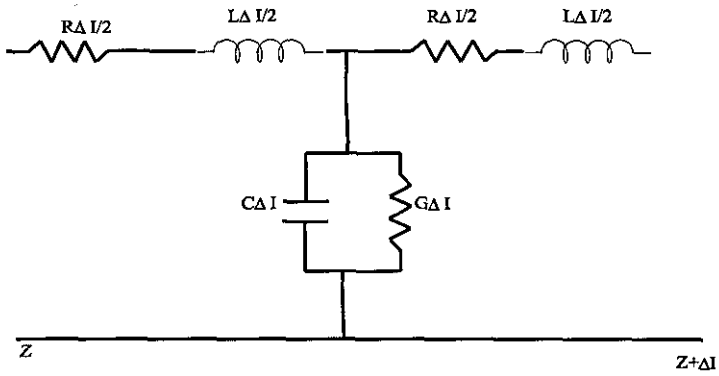

Figure 5.5a: Equivalent circuit model for a section of a two conductor transmission line

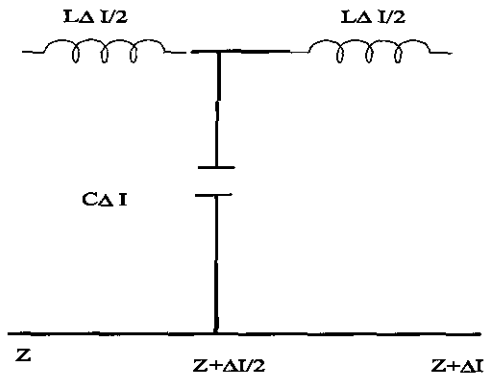

Figure 5.5b: A section of a lumped circuit parameter representation of a lossless transmission line

The distributed capacitance and inductance in a lossless transmission line can be used to deduce two important parameters, namely the impedance z and the velocity v of an impulse on the line:

$$z = \sqrt{\frac{L_d}{C_d}} \qquad [5.21]$$

$$v = \sqrt{\frac{1}{L_d C_d}} \qquad [5.22]$$

The time taken for an electrical signal impressed on the line to traverse it will be determined by the total velocity of light, which depends on the permittivity of the material, which makes up the line.

5.2.2 Basic Algorithm

In TLM, space is modelled by a network of transmission lines. The point at which the transmission lines, or link-lines, intersect is referred to as a node [12]. The structure of the node and the characteristic impedance of the link-lines are chosen so that the voltage and current give information on the electric and magnetic fields in each part of space. If a voltage impulse is launched into terminal 1 of the node in Figure 5.6, one fourth of the energy will be launched into terminals 2, 3, 4 and one fourth of the energy will be reflected back into terminal 1. If the incident voltage impulse is of unit magnitude, the transmitted and reflected impulses will all have a voltage magnitude of one half. For the more general case of four impulses being incident at time $t = k\frac{\Delta l}{c}$ on the four terminals of a node, the total voltage impulse reflected along the line, n, at time $t = k+1\ \frac{\Delta l}{c}$ will be:

$$_{k+1}V_n^r = \frac{1}{2}\sum_{m=1}^{4} {}_kV_m^i - {}_kV_n^i \qquad [5.23]$$

Where i and r denote the incident and reflected component respectively.

Since any impulse emerging from a node (reflected impulse) at position (x, z) automatically becomes an incident impulse on the neighbouring node, the following relationships can be determined:

$$
\begin{aligned}
{}_{k+1}V_1^i(x,z) &= {}_{k+1}V_3^r(x-\Delta x,z)\\
{}_{k+1}V_2^i(x,z) &= {}_{k+1}V_4^r(x,z-\Delta z)\\
{}_{k+1}V_3^i(x,z) &= {}_{k+1}V_1^r(x+\Delta x,z)\\
{}_{k+1}V_4^i(x,z) &= {}_{k+1}V_2^r(x,z+\Delta z)
\end{aligned}
\qquad [5.24]
$$

Equation [5.23] and [5.24] states that if magnitude, position and direction of all impulse are known at time $t = k\,\Delta l/c$ the corresponding values at time $t = k+1\ \Delta l/c$ can be obtained. Thus, the impulse response of the network can be found by initially fixing the state of the network at time $t = 0$ and then calculating the state of the network at successive time intervals.

The impulse response can be used for calculation of the network for any input waveform. In the time domain this is accomplished by convolution of the impulse response with the input waveform; Fourier transform can be used to obtain the response to a sinusoidal excitation however the answer is valid for frequencies well below the cut-frequency.

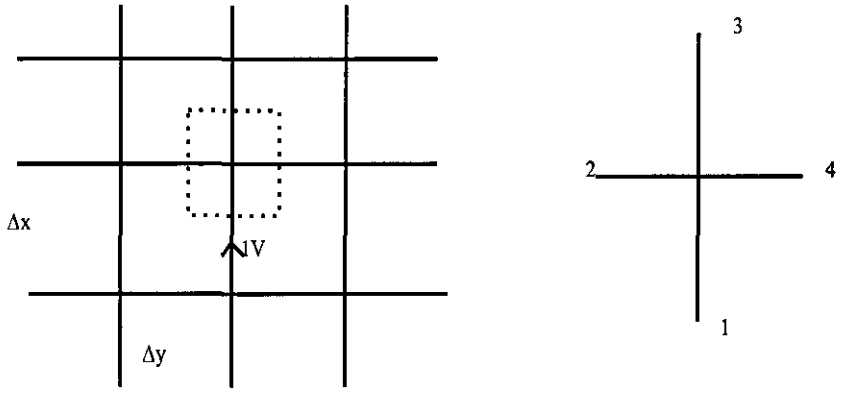

Figure 5.6: Excitation of Node

The most commonly used node in three dimensional TLM is the Symmetrical Condensed Node (SCN). The SCN is a development of earlier expanded [13] and asymmetrical nodes. The incident and reflected pulses in an SCN appear on the terminals of the transmission lines at ports which are numbered and directed as shown in Figure 5.7. In its basic form, termed the 12-port node, the node is the intersection of twelve transmission lines, each of total length Δl and characteristic impedance Z_0. If the discretisations in $x, y,$ and z are equal, designated as, h, and if the impedances in the three directions are also equal, then the field quantities can be determined as:

$$\begin{aligned}
E_x &= \frac{2}{h}\ V_1^i + V_2^i + V_9^i + V_{12}^i \\
E_y &= \frac{2}{h}\ V_3^i + V_4^i + V_8^i + V_{11}^i \\
E_z &= \frac{2}{h}\ V_5^i + V_6^i + V_7^i + V_{10}^i \\
H_x &= \frac{2}{h}\ V_4^i - V_5^i + V_7^i - V_8^i \\
H_y &= \frac{2}{h}\ -V_2^i + V_6^i + V_9^i - V_{10}^i \\
H_z &= \frac{2}{h}\ -V_3^i + V_1^i + V_{11}^i - V_{12}^i
\end{aligned} \qquad [5.25]$$

This scattering equation gives the output from all of the 12 ports in terms of the incident potentials at these ports:

$$^sV = S^iV \qquad [5.26]$$

Where the scattering matrix is given by:

$$S = \frac{1}{2}\begin{bmatrix} 0 & 1 & 1 & 0 & 0 & 0 & 0 & 0 & 1 & 0 & -1 & 0 \\ 1 & 0 & 0 & 0 & 0 & 1 & 0 & 0 & 0 & -1 & 0 & 1 \\ 1 & 0 & 0 & 1 & 0 & 0 & 0 & 1 & 0 & 0 & 0 & -1 \\ 0 & 0 & 1 & 0 & 1 & 0 & -1 & 0 & 0 & 0 & 1 & 0 \\ 0 & 0 & 0 & 1 & 0 & 1 & 0 & -1 & 0 & 1 & 0 & 0 \\ 0 & 0 & 0 & 0 & 1 & 0 & 1 & 0 & -1 & 0 & 0 & 0 \\ 0 & 0 & 0 & -1 & 0 & 1 & 0 & 1 & 0 & 1 & 0 & 0 \\ 0 & 0 & 1 & 0 & -1 & 0 & 1 & 0 & 0 & 0 & 1 & 0 \\ 1 & 0 & 0 & 0 & 0 & -1 & 0 & 0 & 0 & 1 & 0 & 1 \\ 0 & -1 & 0 & 0 & 1 & 0 & 1 & 0 & 1 & 0 & 0 & 0 \\ -1 & 0 & 0 & 1 & 0 & 0 & 0 & 1 & 0 & 0 & 0 & 1 \\ 0 & 1 & -1 & 0 & 0 & 0 & 0 & 0 & 1 & 0 & 1 & 0 \end{bmatrix} \quad [5.27]$$

5.2.3 Boundary Representation

Boundaries are represented by defining the reflection coefficient at the appropriate position in the network. To ensure synchronism the boundaries are placed halfway between nodes. This is achieved by making the distance between two nodes, Δl, equal to an integer fraction of the structure dimensions.

The reflection coefficient for a wave travelling along a transmission line section can be written as:

$$\rho = \frac{Z - \sqrt{2}}{Z + \sqrt{2}} \quad [5.28]$$

Where Z is normalized to the impedance of the simulated medium. The reflection coefficient for a few different types of boundaries is presented in Table 5.1:

Boundary Type	Reflection Coefficient
Electric Wall (Short Circuit)	-1
Magnetic Wall (Open Circuit)	1
Free Space (Matched)	-0.1716

Table 5.1: Reflection coefficient for different boundaries

The values given in Table 5.1 are valid if the voltage in the transmission line mesh is representing the electric field; if the voltage is representing the magnetic field then the values for the electric and magnetic walls in the table above will have to be interchanged.

5.2.4 TLM and Railway Modelling

The common form of coupling in a signalling environment is inductive and conductive coupling. Capacitive coupling is deemed to be negligible. It is typical to analyse this coupling (inductive and conductive) mechanism using discrete lumped circuit components, which are estimated by means of practical EMC measurements [14]. The structure of TLM models with its emphasis on field description in terms of lumped currents and transmission lines is a natural choice for incorporating models of circuits and cables, and thus is ideal for studying, in a unified manner, coupled fields and circuit problems within a railway environment. Calculating the inductively and conductively coupled currents and potentials in buried metallic structures in the vicinity of a railway line can be viewed as an electromagnetic field problem.

The electric and magnetic fields in the ground originating from the currents in the railway installation are the source of these coupled currents and potentials. The magnetic field will be present along the whole length of the railway line, while the electric field caused by leakage currents from the rails is connected

to the current transfer zones described in Chapter 4. The distribution of current in the traction current return path is an AC problem of quasi-stationary nature. The currents and potential vary with time according to $e^{j\omega t}$. This is a three dimensional problem since the electric field and scalar potential will vary in all three dimensions. The railway interference problem can be described as a multi-conductor coupled transmission line; such a model must include the running rails, the OLE and signalling / telecommunication cables (and parallel electric power rails and cables for DC traction system).

In [14], the authors proposed a methodology for modelling wideband electromagnetic coupling with possible applications to the railway environment. The methodology uses the equivalences between the electric lumped components and transmission lines modelled in terms of shunts and links. In their model, a Generic Series Electric Load (GSL) in a 3 dimensional TLM mesh is proposed. The GSL is suitable for modelling non-linear resistors, inductors, capacitors or a series combination of these elements and is connected to the SCN.

TLM has been used to study the coupling between incident electromagnetic fields and single conductor transmission system [15], [16]. The basic approach, known as the two stage system, involves modelling the incident field and then solving a one dimensional model of the transmission line to obtain the voltage and current in the conductor. This method has been extended to multi-conductor transmission line system [17].

5.3 Computer Code

Of the two methods described above, TLM is the most recent and the least applied to railway electromagnetic problems. The advantage of the TLM

method is the ease with which complicated structures can be analysed. The great flexibility and versatility of the method reside in the fact that the TLM mesh incorporates the properties of the electromagnetic fields and their interactions with the boundaries and material media. The main limitation of the method is the computational resource required, which depends on the complexity of the TLM mesh.

In the next two chapters, TLM is applied to two railway case studies: the study of inductive coupling from an ac electrified line to a nearby buried metallic conductor, and the analysis of concrete slabs/structures as used in the railway environment. The case studies highlight the suitability of computational analysis, in particular TLM, in railway applications.

In both cases a commercially available TLM code is used; the computer code Microstripes™ supplied by Flomerics Limited, is based on a general three-dimensional formulation of the TLM. The code computes the time domain impulse response of the analysed system. The code also has a Fourier transformation capability that makes it possible to determine the frequency response. Certain post calculation can be performed, such as convolution in the time domain, which gives the possibility to determine the system response for, in principle, any wave form.

5.4 Summary

In this chapter, a brief description of two different numerical computation techniques that can be used to calculate the electromagnetic field in a railway environment is given. The techniques can be used from low frequencies up to and just above the resonance frequency of the analysed structure. Of the two techniques described, Finite Element Method (FEM) has been applied to solve a variety of railway electromagnetic coupling problems, however these

have been limited to evaluating the catenary and rail impedance as well as the analysis of inductive coupling from an AC railway to nearby telecommunication lines using a two dimensional FEM code. A complete analysis of the electromagnetic coupled interference from a railway system to nearby buried metallic structures will necessitate the need for a three dimensional FEM code. While three-dimensional FEM codes exist, it is viewed that the computational resource and time required to evaluate the electromagnetic coupling from a railway would be enormous.. Transmission Line Matrix (TLM) modelling is based on the fact that there are certain similarities between the equations obtained from transmission line theory and those obtained directly from Maxwell's equations. By solving the set of transmission line equations for voltages and currents in the mesh and using the analogies with Maxwell's equations, the wave propagation can be studied. While TLM offers some advantage over FEM, it has not be used to evaluate the electromagnetic interference from a railway system to nearby buried metallic structures.

There are other numerical techniques that can be used to evaluate the railway electromagnetic coupling problem described in chapter 4, however the focus of this thesis is the application of TLM in railway system.

5.5 References

[1] De Cogan, D and De Cogan A, "*Applied Numerical Modelling for Engineers*", Oxford University Press, 1997.

[2] Hill, R. J and Carpenter, D.C, "*Electromagnetic field modelling of rail track using the Finite Element Method*", Rail Engineering International Edition, Number 4, 1991, Pg. 17 - 20

[3] Hill, R. J, "*Simulation of AC and DC rail traction network using parallel computers*", Rail Engineering International, Number 2, 1990, Pg. 7 – 9.

[4] Hill, R. J, "*Rail track modelling for signalling and electrification system simulations studies*", *ibid*, Pg. 16 – 20.

[5] Hill, R. J and Carpenter, D. C, *"Determination of rail impedance for electric railway traction system simulation*", IEE Proceedings B, Vol. 138, No. 6, November 1991, Pg. 311 – 321.

[6] Satsios, K. J, Labridis, D. P and Dokopoulos, P. S, "*Inductive interference caused to telecommunication cables by nearby AC electric traction lines. Measurements and FEM Calculations*", IEEE Transactions on Power Delivery, Vol. 14, No. 2, April 1999, Pg. 588 – 594.

[7] Nekhoul, B, Labie, P, Zgainski, F. X and Meunier, G, "*Calculating the impedance of a grounding system*", IEEE Transactions on Magnetics, Vol. 32, No. 3, May 1996, Pg. 1509 – 1512.

[8] Nekhoul, B, Guerin, C, Labie, P, Meunier, G and Feuillet, R, "*A finite element method for calculating the electromagnetic fields generated by substation grounding systems*", IEEE Transactions on Magnetics, Vol. 31, No. 3, May 1995, Pg. 2150 – 2153.

[9] Hoefer, W. J. R, "The *transmission line matrix method – theory and applications*", IEEE Transactions of Microwave Theory and Technique, Vol. MTT 33, No. 10, Oct. 1985, pg. 882 – 893.

[10] Christopoulus, C. "*The Transmission Line Modelling Method (TLM)*", New York, IEEE Press, 1995.

[11] Sadiku, M. N. O., "*Numerical Techniques in Electromagnetic*", 2nd Edition, CRC Press, USA.

[12] Herring, J. L, "*Developments in the Transmission Line Modelling Methods for Electromagnetic Compatibility Studies*", PhD Thesis, University of Nottingham, 1993

[13] Akhtarzad, S and Johns, P. B, "*Solution of Maxwell's equations in three space dimensions and time by the TLM method of analysis*", Proceedings of the IEE, Vol. 122, No 12, 1975, Pg 1344 – 1348.

[14] Christopoulos, C; Galdi, V; Ippolito, L. and Piccolo, A, "*A TLM approach for the modeling of high and low frequency EMC problems in power systems*", Computers in Railways VII

[15] Naylor, P., Christopoulos, C and Johns, P. B., "*Analysis of the coupling of electromagnetic radiation into wires using transmission line modelling*", 5th Int. Conf. EMC. York, England, IERE Publ. 71, 1986, Pg 129 – 135.

[16] Naylor, P., Christopoulos, C and Johns, P. B., "*Coupling between electromagnetic fields and wires using transmission line modelling*", Proceeding of the IEE, Part A, 134(8), 1987, Pg. 679 – 686.

[17] Christopoulos, C and Naylor, P, "*Coupling between electromagnetic fields and multiconductor transmission systems using TLM*", Int. Journal of Numerical Modelling: Electronic Networks, Devices and Fields, Vol. 1, 1989, Pg. 31 – 43.

[18] Balanis, C. A, "*Advanced Engineering Electromagnetic*", John Wiley & Sons, 1991.

[19] Zoltan, J. C, "*Unlocking the magic of Maxwell's equations*", IEEE Spectrum, April 1989, Pg 29 – 33.

[20] Silvester, P. P and Ferrari, R. L, "*Finite elements for electrical engineers*", Second Edition, Cambridge University Press, 1990.

[21] Johns, P. B and Beurle, R. l, "*Numerical solutions of 2 dimensional scattering problems using a Transmission Line Matrix*", Proceedings of the IEE, Vol. 118, 1971, Pg 1203 – 1208.

[22] Hook, M, "*The use of large electromagnetic computer models in EMC applications*", IEE Colloquium: Does electromagnetic modelling have a role in EMC design, London, February 1993.

[23] Hoefer, W. J. R, *Editorial, International Journal of Numerical Modelling*, Vol. 2(4), 1989, Pg 189 – 190.

[24] Johns, P. B, "*A new mathematical model to describe the physics of propagation*", The Radio and Electronics Engineer, 1974, Vol. 44(12), Pg 657 – 665.

[25] Johns, P.B, "*The art of modelling*", Electronics and Power, Vol. 25(8), 1979, Pg 565 – 569.

Chapter 6

NUMERICAL SIMULATION OF LOW FREQUENCY COUPLING IN RAILWAY

In previous chapters, the analytical approximations to inductive coupling in railway installations were explored. It was concluded that the configuration complexities in railway installations suggest the need for numerical techniques. A review of some numerical methods and the applicability to resolve railway electromagnetic interference problems was discussed in Chapter 5. It was observed that TLM has not been extensively applied to railway electromagnetic interference problems, despite its advantage over other numerical methods.

In the next two chapters, the possibilities and usefulness of TLM to resolve railway electromagnetic interference problems is explored.

6.1 Railway Model

A 10 km railway line was chosen as the test case. The railway line was modelled as a simple railway configuration as discussed in Section 2.3, in which the current return path is the running rails. The load (train) is modelled as a current source located arbitrarily along the line. The actual load condition is achieved by controlling the catenary current, which was set to 300 A for normal operation, a representative value for mainline service in the UK.

TLM can be described as an electromagnetic field model, and thus only the dimensions and material properties of the railway are required. The physical dimensions and material properties of the conductors as used in TLM are shown in Table 6.1. The rails are modelled as two separate conductors

bonded together at each end of the track. In real railway installations, the tracks will be regularly bonded – by impedance bonds – to ensure the even distribution of traction current between the rails. In the model, impedance bonds are replaced with simple copper connections between the rails. For simplicity, the radius of other conductors is assumed identical to that of the radius of the equivalent rail. In the model, only the catenary is modelled. Booster transformers are not included even though in reality these would be installed every 3 – 5 km along the line.

The running rails and catenary are modelled as solid cylindrical conductors having an equivalent radius determined from Equation 4.57. For ease of modelling, the radius of the catenary was made equal to that of the rail. The feeder station is modelled as 25 kV voltage source with appropriate line impedance to provide the desired catenary current of 300 A at 50 Hz.

Property	Components			
	Catenary	Rail	Bond between rails	Axle
Conductor outer radius (mm)	48	48	48	48
Conductor inner radius (mm)	0	0	0	0
Conductor conductivity (S/m)	5.61798×10^{7}	4.4444	4.4444	4.4444
Permeability	1	20	20	20

Table 6.1: Material parameters used

Figure 6.1, depict a simple railway configuration without a load (train), one of the running rails is modelled as a signal rail with a section gap representing the

presence of a track circuit. This model represents the basic railway configuration.

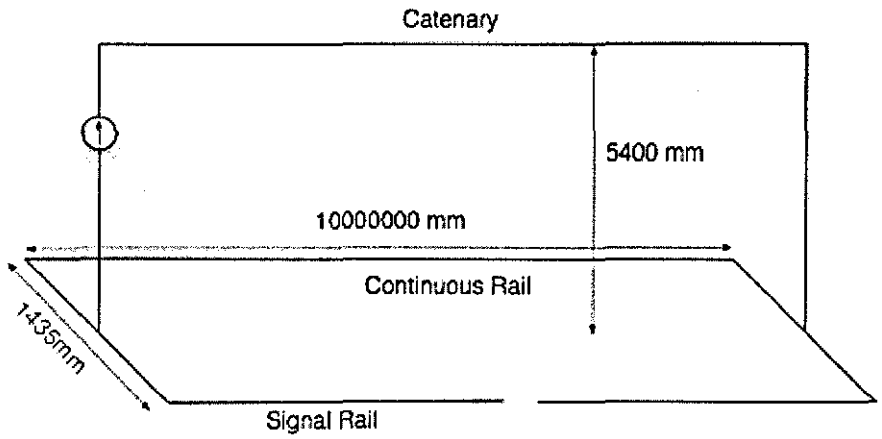

Figure 6.1: Schematic of Basic Railway Model

Figure 6.2, shows a modified basic railway model with a load (train) located just at the rail section.

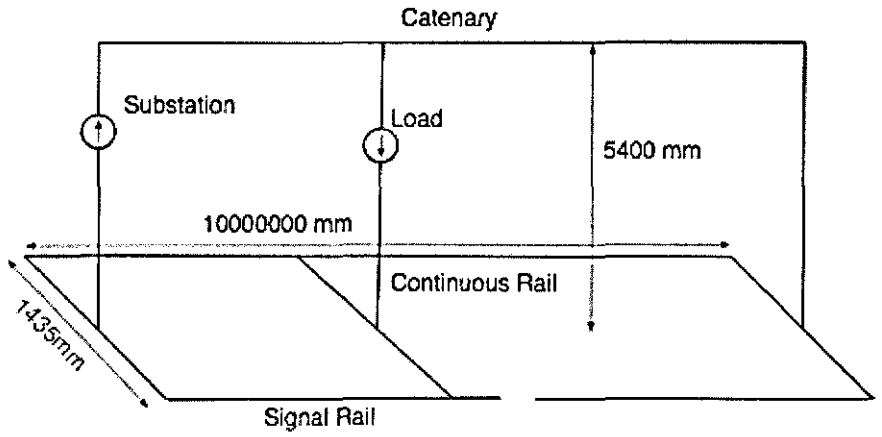

Figure 6.2: Schematic of a Basic Railway Model with a Train (Train Modelled as 1 A Current Source)

6.1.1 TLM Model Parameters

The numerical accuracy obtained from TLM is determined by the model parameters and simulation time. Increased accuracy is achievable but at the expense of increased computational time. Initial computational time took 50 days for a very simple model with fine meshing.

Boundary Condition: Absorbing boundary condition was used for all sides except Y_{min} for which an electric wall boundary condition was applied. An electric wall was applied to model the behaviour of Ground at the frequency of interest.

Cell Size: The maximum and minimum cell size is 10,000 mm and 48 mm respectively. In addition, the maximum cell width was fixed at 300,000 mm.

Number of Cells: The total number of cells for the basic model was 2612688

Number of Timesteps: The total number of timesteps was 27.439 million

The simulation was performed on a 4 GB RAM, dual AMD K6 process computer running 64 bit Windows OS. The CPU run time was 38 hours for a maximum frequency of 1 kHz, although the CPU run time increased to over 80 hours with increasing model complexity.

6.2 Results and Discussions

The basic model parameters were adjusted until the line current at the fundamental was as close to 300 A as reasonably possible. An impulse excitation from d.c to 1 kHz is used to introduce energy into the model; Convolution is then used to obtain the response of the model to a sinusoidal wave having the waveform characteristic of $ASin(2\pi f t)$, with the

A(amplitude) = 2.25 Amps and $f = 50Hz$. The amplitude of the convoluted sinusoidal waveform is chosen to obtain the desired catenary current.

Figure 6.3, show the line current characteristics of the model in the frequency domain, while Figure 6.4 is the convoluted output of the time domain output. As shown in Figure 6.5, the catenary current and the continuous rail current are both equal (i.e. the amplitude of the current is approximately 300A).

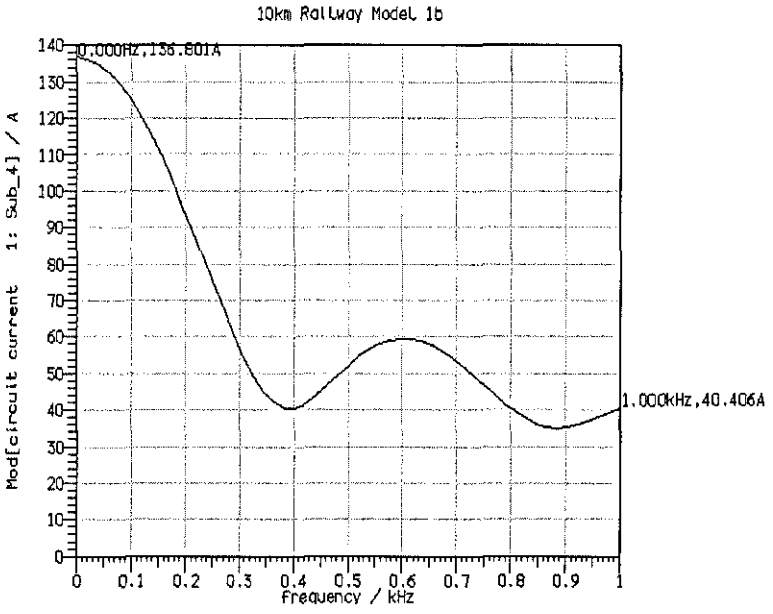

Figure 6.3: Current magnitude as a function of frequency

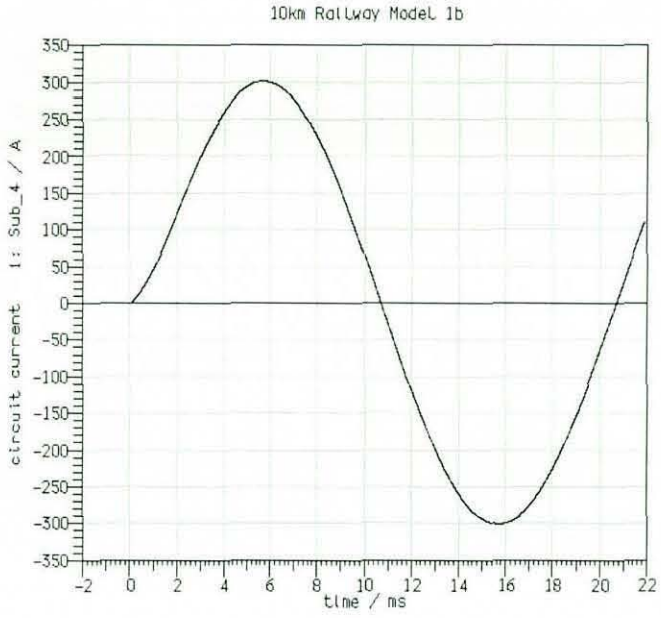

Figure 6.4: Catenary current at 50 Hz

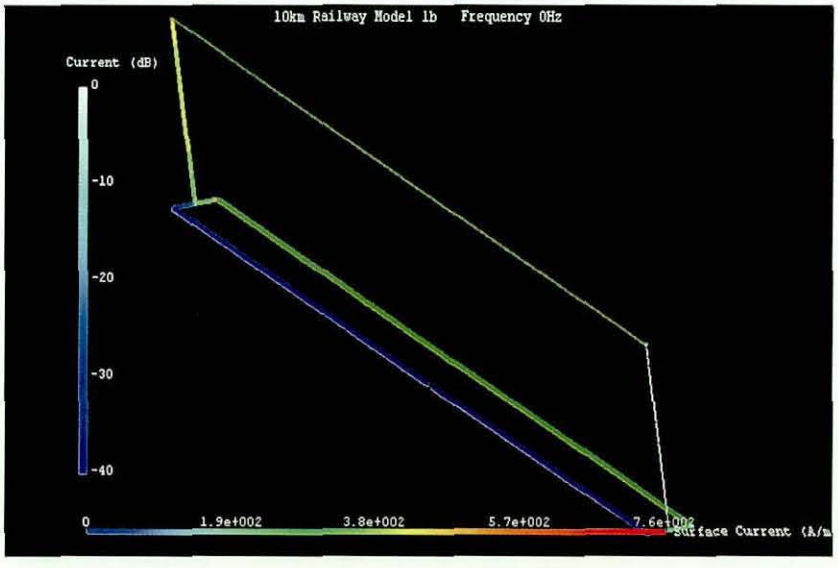

Figure 6.5: Current distribution (at 50 Hz) of basic railway model

Figure 6.5, shows the surface rail current distribution obtained for the basic railway model (as shown in Figure 6.1). As can be seen, the continuous rail current is approximately 300A as is the catenary current. The signal rail current is low as a result of the section gap included in the basic model. The basic railway model with a train modelled, as a 1A current source, located 0.1 km from the section gap was simulated. In this case, the rail current distributed equally, flowing through both running rails from the train location back to the substation. The model predicts that the magnetic field propagating in the z-axis could be as high as 230 A/m at a distance of approximately 1.8 m from the signal rail.

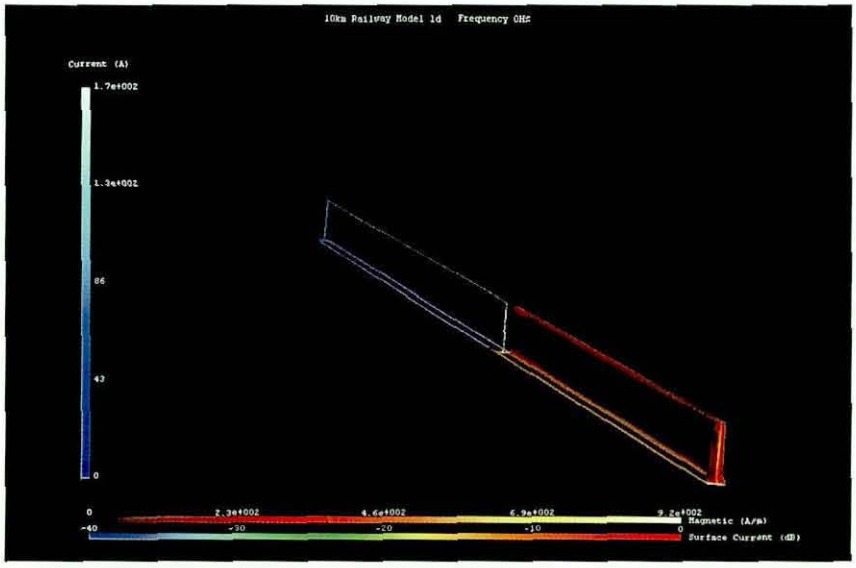

Figure 6.6: Current distribution (at 50 Hz) of basic railway model with a train in section

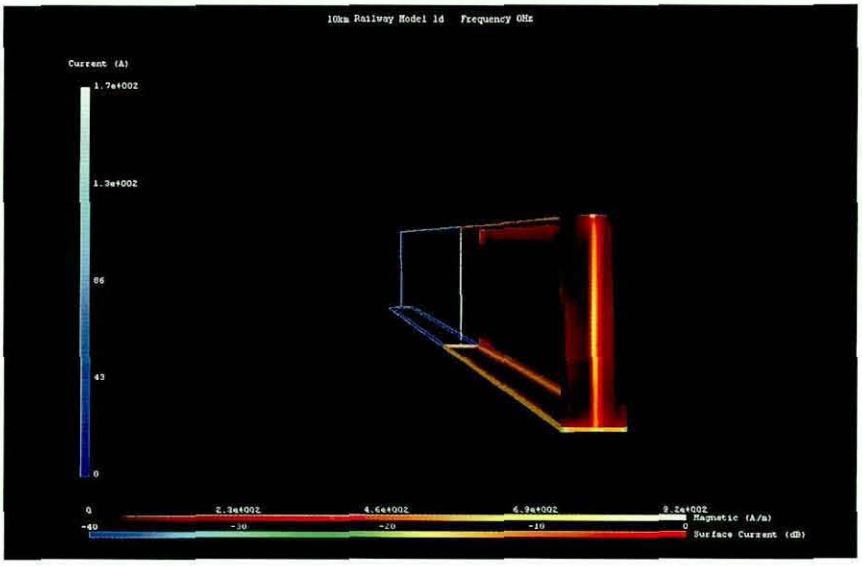

Figure 6.7: Current distribution and magnetic field distribution at 50 Hz - Basic railway model with load

It is desirable to predict the electromagnetic fields along a railway line with respect to a moving train. There is no way of implementing this within Microstripes ™, the commercial software used, however it is possible to provide a quasi-static response by manually changing the load position within the model and re-running the simulation. Figure 6.8 shows the current distribution and magnetic field with the load moved 0.6 km forward.

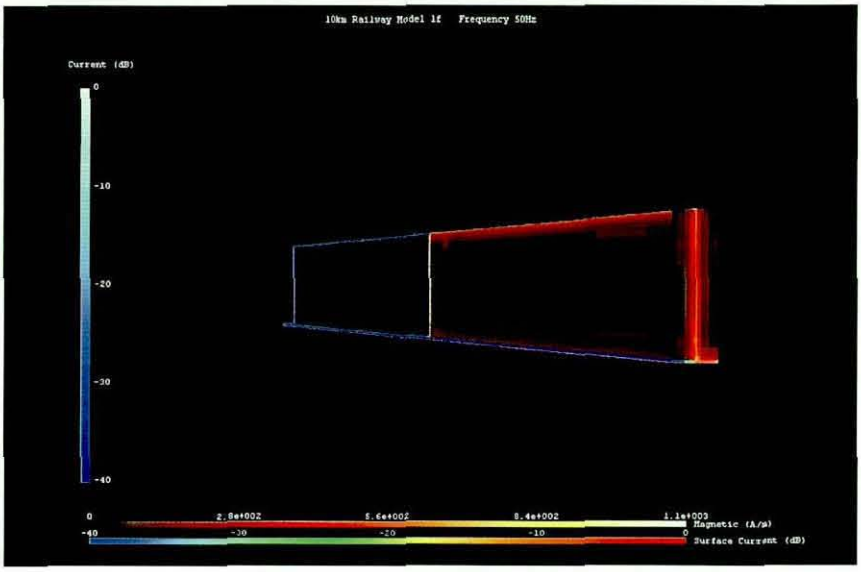

Figure 6.8: Same as Figure 6.7 but with the Train located 0.6 km forward.

In Figure 6.8, the load was positioned at a location slightly ahead of the rail gap, as obtained from the simulation the current return path to the substation is via the continuous rail. In this scenario, the magnetic field is generated via the substation- catenary wire – load - section of the continuous rail.

Electromagnetic interference coupling between the railway system to nearby buried metallic conductors was treated in detail in Chapter 4. As discussed in Chapter 4, the determination of interference effects in a typical railway right-of-way is a complex mathematical problem requiring knowledge of the physical and electrical parameters of the system space including a good representation of the soil structure. Potential impact of inductive interference to buried metallic conductor is one of potential damage/mal-operation of equipment, and injury or loss of life. It is desirable to use numerical tools such as TLM to assess the impact of right of way, the robustness of a cable

layout (and cable management system) and the impact of induced fields on nearby buried metallic services including signalling and communication cables. This is particularly important as signalling and communication cables tend to be installed very close to the track.

In Figure 6.9, a conductor having a radius of 0.605 mm and a line impedance of 50 Ω is positioned 1 m from the continuous running rail of the basic model (Figure 6.1). The victim cable length was 10 km, equivalent to the length of the railway model. Figure 6.10, shows the magnetic field due to the railway at the location of the wire. From the figure, it is predicted that the wire is likely to be exposed to field strengths between 20 A/m – 26 A/m. Care must be taken in the interpretation of this result since the model is an over simplification of the problem. However, the model does give an indication of the severity of the magnetic field as a function of separation distance between the railway and the victim wire; for example at a distance of about 2m from the rail, the wire is likely to be exposed to field strengths of 6.5 A/m – 13 A/m.

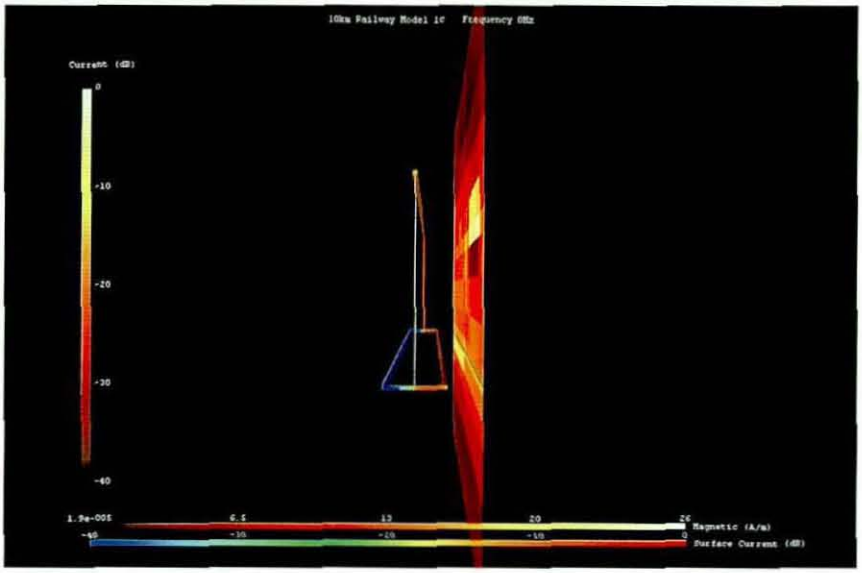

Figure 6.9: Predicted magnetic field at separation distance of 1m from the nearest rail

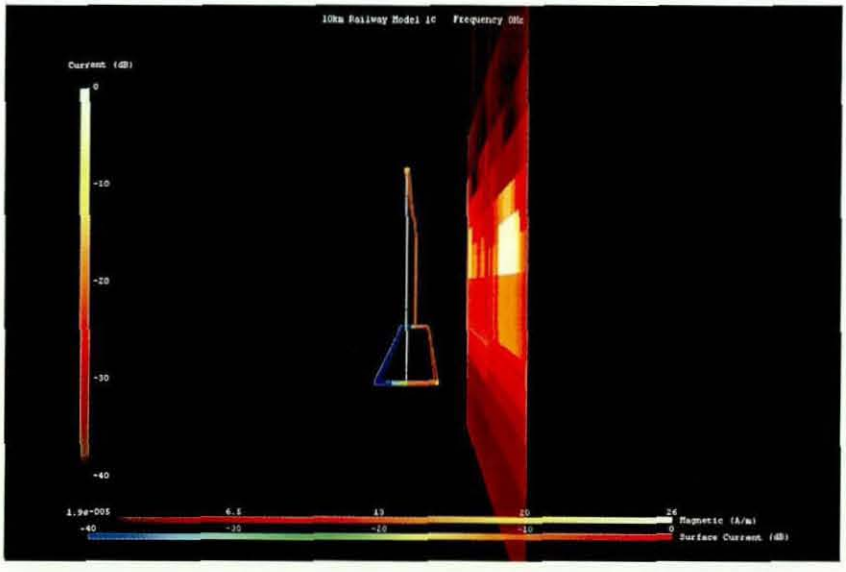

Figure 6.10: Predicted magnetic field at a separation distance of 2m from the nearest rail

In Figure 6.11, the magnetic field distribution at a separation distance of 1m from the nearest rail with a train in section was examined; in this case, the train was positioned in the same location as that shown in Figure 6.6 and Figure 6.7. The length of exposure of the victim cable is equivalent to the distance between the substation and train. The predicted magnetic field strength is between 23 A/m and 34 A/m, a significant increase from that obtained from the same basic railway without a train in section (i.e. Figure 6.6).

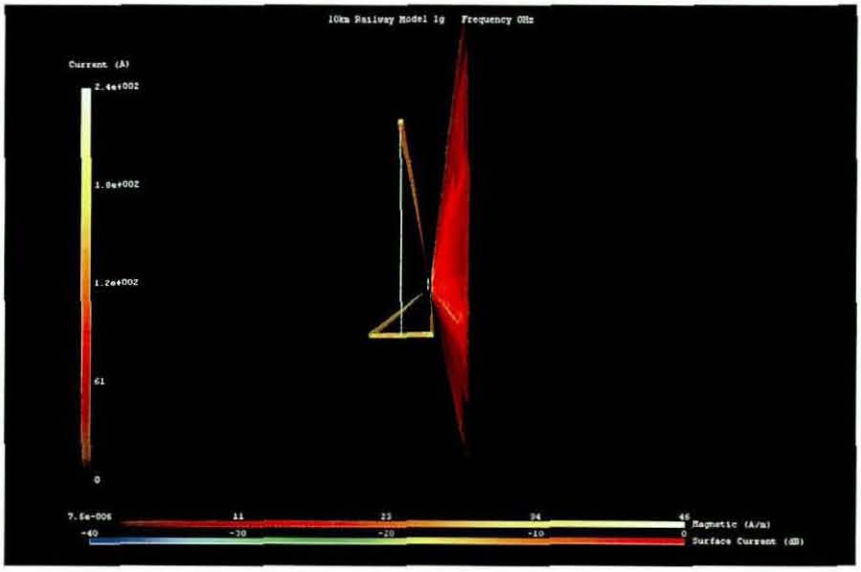

Figure 6.11: Predicted magnetic field at a separation distance of 2m from the nearest rail with a train in section

It is of importance to comment on the plausibility of applying TLM to the numerical modelling of a railway system. It has already been mentioned that that a major disadvantage is the computation time required, and that this increases with increased accuracy and complexity of the model. A moderate amount of work is required to translate the current distribution model of a

railway into an electromagnetic field model suitable for TLM. However, it is fairly easy to modify the baseline model (Figure 6.1) once prepared. Certain key parameters such as leakage resistance are not so easily implemented in TLM and depending on the desired output some post processing of the TLM data might be required.

One major setback with the TLM commercial package used, is its ability to model transformers. However using the physical and material approach of TLM, it is possible to develop a TLM transformer model, represented by as a restriction on current. Such a model could be achieved by inserting an artificial section of unit length containing an extra conductor playing the role of the transformer secondary. The extra conductor is placed physically close to the catenary, approximately 0.5 m from the catenary wire. The current in the conductor representing the transformer secondary is forced to be opposite to the current flowing in the catenary.

The simple railway model assumes that certain aspect of the infrastructure are non-metallic and thus do not contribute to the leakage of current from the rails to the ground. The leakage is consequently continuous. However, in every railway installation there will always be some metallic structures that are in contact with earth and are at the same time are bonded to the rails – track side installations and well as tunnel linings are bonded to the continuous rails. As can be seen from the simulated results of Figures 6.1 to 6.11, constant rail current is obtained throughout the return path, indicating that the rails are not grounded.

6.3 Summary

The electromagnetic field from a simple railway model has been evaluated in a three dimensional TLM code. The simplicity of the model implies that detail

evaluation of the electromagnetic coupling is not possible, however the simple model is useful as a first approximation of the electromagnetic field in the vicinity of the railway and thus can be used to assist in the design of wayside installations.

There are two main limiting factors impacting the use of TLM in the application of concern. One is the time it takes for the computation of fields; the computation time is dependent on the number of unknown variables which in turn in dependent on the complexity of the railway model. The other is the inability to incorporate the effects of transformers (Boosters or Autotransformers) in the model.

Chapter 7

ANALYTICAL AND NUMERICAL SIMULATION OF CONCRETE SLABS/STRUCTURES

Concrete structures are abundant in the railway where they perform a variety of functions. They form the main structural element of train stations but are also used for functional purposes such as sleepers and equipment rooms. The use of concrete in numerous applications in this environment demands a detailed understanding of its properties, most especially its electrical properties. For example, the electrical resistivity of concrete plays a vital role when analysing stray currents in an electrified railway environment. In other applications, the impedance of the concrete structure may form part of the tuning circuit of the train detection circuit. For modern control centre buildings or signalling equipment rooms, the design requirements need to include provisions for EMC and the protection against intentional electromagnetic disturbance.

With respect to EMC, the parameter of interest is the ability of the concrete structure to inhibit the propagation of electromagnetic waves external to the structure, thus providing an electromagnetic environment in which sensitive railway signalling and communication equipment can operate. The electrical properties of concrete are important as they affect a variety of applications, the real part of the complex permittivity and effective conductivity of concrete have a fundamental role in assessing the ability of concrete to inhibit the propagation of electromagnetic wave. This has direct relevance to such applications as the protection of sensitive circuits that are housed in concrete

or reinforced concrete structures, where the concrete structure is designed to provide additional shielding against electromagnetic disturbance. The shielding ability of a concrete structure is directly related to the cement chemistry, water/cement ratio and the use of additives [1] - [4].

Concrete slabs and structures in use in the railway are either reinforced or simple concrete structures. Reinforcement is typically provided by steel bars placed as an array or set up in the form of a grid, embedded in the slab of concrete. The geometrical design of the reinforced structure varies from structure to structure and depends on the structural and architectural requirement. As a secondary function, the reinforcement matrix also forms part of the system earthing topology and lightning protection system. More than often the design of such structures has not taken advantage of the inherent shielding ability of the reinforcement, and thus any attenuation provided by the structure is incidental. The structure's attenuation of electromagnetic disturbance is a combination of the attenuation due to concrete and that provided by the reinforcement. The ability to model the behaviour of concrete over a wide frequency range in numerical simulators used for EMC and structural design applications is particularly important for a variety of railway signalling design applications.

In this chapter, the ability to accurately model concrete in numerical simulators, in particular TLM is explored. The electrical properties of concrete are investigated including its ability to attenuated electromagnetic wave.

7.1 A Concrete Electrical Model for Numerical Simulators

Concrete is a porous, heterogeneous material with pores partially filled with ionic solutions. It is possible to decompose concrete into three phases: the

solid phase consisting of all solid components, a liquid phase and a gaseous phase [6]. The electrical properties of concrete thus relates to the phases, for instance the relative permittivity of the solid phase is real and thus presents negligible losses, whereas the inevitable mixture of the solid and gaseous phase results in a non-dispersive medium whose permittivity is not frequency dependent. Dispersion in concrete is feasible due to the presence of free water in pores and the degree of dispersion is dependent on the water content within the structure. Since the complex permittivity of water varies with frequency it follows that the complex permittivity of concrete is dependent on its water content.

Concrete is a non-magnetic material and thus its magnetic permeability is deemed equal to that of free space. This frequency dependent complex permittivity of concrete can be modelled as a Debye material, obeying the following equations:

$$\hat{\varepsilon}(\omega) = \varepsilon'(\omega) - j\varepsilon''(\omega) \qquad [7.1]$$

$$= \varepsilon_{\infty} + \frac{\Delta\varepsilon}{(1 + j\omega\tau)} \qquad [7.2]$$

$$= \varepsilon_{\infty} + \frac{\Delta\varepsilon}{(1 + \omega^2\tau^2)} - j\frac{\omega\tau\Delta\varepsilon}{(1 + \omega^2\tau^2)} \qquad [7.3]$$

where $\Delta\varepsilon = \varepsilon_{static} - \varepsilon_{\infty}$ is the difference between the values of the dielectric constant at very low and very high frequency, respectively. σ_{dc} is the dc conductivity, ε is the vacuum dielectric constant, and τ is the relaxation time and $\omega_r = 1/\tau$ is the relation frequency. We can re-write [7.2] as:

$$\hat{\varepsilon}(\omega) = \varepsilon_{\infty} + \frac{\Delta\varepsilon}{1 + \left(j\frac{\omega}{\omega_r}\right)} \qquad [7.4]$$

From [7.3], the real part of the complex relative permittivity, which represents the capacity of concrete to store electromagnetic energy, can be written as:

$$\varepsilon'(\omega) = \varepsilon_{\infty} + \frac{\Delta\varepsilon}{1 + \left(\frac{\omega}{\omega_r}\right)^2} \qquad [7.5]$$

Similarly, the imaginary part of the relative permittivity expresses the electromagnetic energy losses and is given as:

$$\varepsilon''(\omega) = \frac{(\omega/\omega_r)\Delta\varepsilon}{1 + (\omega/\omega_r)^2} + \frac{\sigma_{dc}}{\omega\varepsilon_0} \qquad [7.6]$$

The real part represents the capacity of concrete to store electromagnetic energy, while the imaginary part represents the losses of energy due to absorption. The attenuation of electromagnetic waves in concrete through absorption is due to the ionic conduction and dielectric relaxation. The imaginary part has a minimum at which the ionic conductive loss and dielectric loss are equal to each other. This frequency is given as:

$$\omega = \left(\frac{\sigma_{dc} \omega_r^2}{\Delta \varepsilon \varepsilon_0 \omega_r + \sigma_{dc}} \right)^{1/2} \qquad [7.7]$$

The impact of free water pores in concrete is more pronounced on the loss factor than on the permittivity of the concrete sample [7]. This statement is evident through analysis of published measurement data such as those presented by Soutos *et al* [8]. Soutos experimental data refer to concrete specimens made of Ordinary Portland cement, 10 mm gravel aggregate and sand. Permittivity and permeability data were obtained by means of a co-axial transmission line in the frequency range of 10 MHz – 1 GHz.

The moisture content in each specimen was calculated from the ratio of the water volume to concrete weight (i.e. the difference in weight of the specimen immediately after measurement and after it had been oven dried). Soutos data is particularly relevant to the analysis presented herein and the concrete mix is significantly similar to those used in the construction of the new Northern Line Control Centre building on London Underground. Figure 7.1, show the extrapolated data for a concrete specimen having a moisture content of 0.2% and 12% respectively, the data has been extrapolated from [8]. The two extreme moisture content data represents two concrete states: *dry* concrete (where the moisture content is 0.2% or less) and *wet* concrete (where the moisture content is 12% or higher). This distinction of dry and wet concrete is made only for ease of analysis.

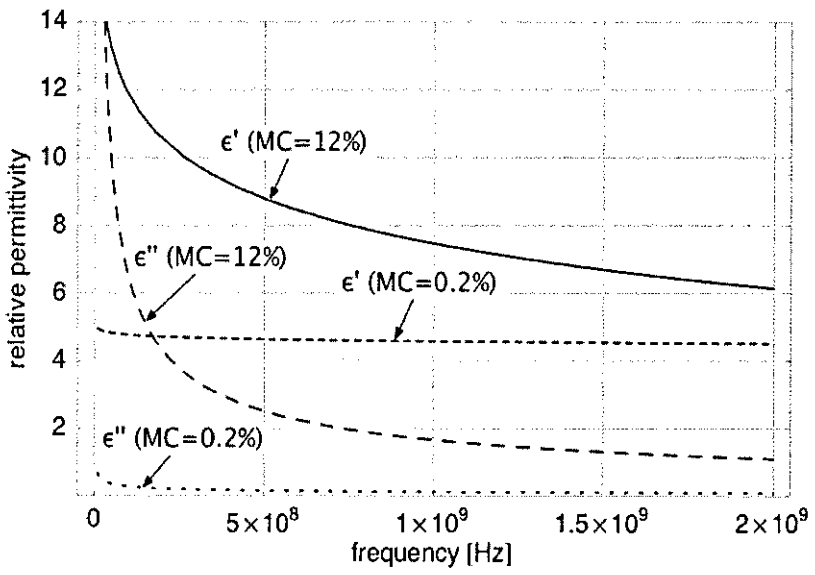

Figure 7.1: Relative Permittivity of Concrete as a Function of Moisture Content (Extrapolated from data presented in [8])

In TLM, concrete can be modelled as a simple dielectric material characterised by the real part of the complex permittivity and an effective conductivity, which is deemed constant over the frequency range of interest. Alternatively, concrete can be modelled as a dispersive material, in which the variation of its electrical parameters with frequency can be accurately described. The appropriateness of both approaches is discussed and analysed below.

7.2 Shielding Effectiveness of Concrete Slabs and Structures

The attenuation offered by a concrete slab is the combination of the natural shielding of the concrete materials and that provided by the metal reinforcement, if any. The reinforcement is typically reinforcing rods but could equally be metal foils, conductive paints, conductive fibres and wire

meshes [9] - [17]. The natural shielding provided by the concrete is a function of the amount of moisture within the concrete structure.

The shielding effectiveness of a concrete slab/structure can be estimated analytically by applying the transmission line principle. To simplify the analysis, discontinuities in concrete structures such as doors, windows and ventilation holes are not considered, furthermore the impinging electromagnetic wave is considered a uniform plane wave to an infinite plane and the concrete structure is assumed isotropic and homogenous. The shielding effectiveness can then be obtained as the sum of three contributions: absorption loss, reflection loss and an additional corrective term to account for multiple reflections within the concrete slab.

$$SE_{dB} = A_{dB} + R_{dB} + B_{dB} \qquad [7.8]$$

where the absorption loss term A_{dB} is given as:

$$A_{dB} = 20\log_{10} e^{\alpha t} \qquad [7.9]$$

and R_{dB} and B_{dB} are the reflection loss and multiple reflection correction term, given respectively by:

$$R_{dB} = 20\log_{10}\left(\frac{\left\{Z_0 + \hat{Z}\right\}^2}{4Z_0\hat{Z}}\right) \qquad [7.10]$$

and

$$B_{dB} = 20\log_{10}\left|1 - \left(\frac{Z_0 - \hat{Z}}{Z_0 + \hat{Z}}\right)^2 e^{-2\hat{\gamma}t}\right| \qquad [7.11]$$

In [7.9] - [7.11], t is the thickness of the concrete wall, $Z_0 = \sqrt{\mu_0/\varepsilon_0}$ and $\hat{Z} = j\omega\mu/\hat{\gamma}$ are the intrinsic impedances of free space and concrete, respectively, with $\mu_0 = 4\pi\ 10^{-7}$ H m^{-1} magnetic permeability and $\varepsilon_0 = 8.854\ 10^{-12}$ F m^{-1} permittivity of free space, μ is the magnetic permeability of the concrete slab, ω is the angular frequency and

$$\gamma = \alpha + j\beta = \sqrt{j\omega\mu\left(\sigma_{eff} + j\omega\varepsilon^{'}\right)} \qquad [7.12]$$

is the complex propagation constant of the concrete, where α and β are its attenuation and phase constants. [7.12] has been written taking into account the inherently lossy nature of concrete through a complex permittivity

$$\hat{\varepsilon} = \varepsilon^{'} - j\varepsilon^{''} \qquad [7.13]$$

where $\varepsilon^{'}$ is the real part of the concrete complex permittivity and $\sigma_{eff} = \omega\varepsilon^{''}_{eff}$ is the effective conductivity for concrete, which is often determined by measurement. Simple calculations yield the following expressions for α and β:

$$\alpha = \omega\sqrt{\frac{\mu\varepsilon^{'}}{2}}\left[\sqrt{1+\left(\frac{\sigma_{eff}}{\omega\varepsilon^{'}}\right)^2} - 1\right]^{1/2} \qquad [7.14]$$

$$\beta = \omega\sqrt{\frac{\mu\varepsilon^{'}}{2}}\left[\sqrt{1+\left(\frac{\sigma_{eff}}{\omega\varepsilon^{'}}\right)^2} + 1\right]^{1/2} \qquad [7.15]$$

7.2.1 *Modification to account for Reinforcing Rods*

As discussed above, the attenuation of the concrete structure needs to account for any reinforcement embedded in the structure. More often than not, concrete slabs/structures in use in the railway are reinforced with reinforcing rods (rebars). The effectiveness of the reinforcing rods to attenuate electromagnetic waves depends largely on the grid spacing but is comparatively insensitive to the reinforcing rod diameter [9]. The geometry may be described as an array of small dipoles, with partial cancellation at their adjacent edges. The attenuation provided by this type of structure is predominantly caused by reflection loss with essentially no loss due to absorption. The attenuation provided by the reinforcing structure is ineffective at high frequencies, particularly above 100 MHz.

The problem of plane wave incidence on a plane boundary is well known and solved in literature. In particular, expressions describing the plane wave shielding effectiveness of reinforcing rods were presented by Casey [18]. Casey expressed the shielding effectiveness of reinforcing rods in terms of transmission coefficient:

$$SE(\theta) = -20\log_{10}\left|T_{1,2}(\theta)\right| \qquad [7.16]$$

where θ and $T_{1,2}$ are the angle of incidence with respect to the direction normal to the mesh, and the transmission coefficient, respectively. For a perfectly conducting mesh, [7.16] resolves to the following expressions:

$$SE_{\parallel}(\theta) = -20\log_{10}\left(\frac{\left\{\frac{2\omega L_s}{Z_0}\right\}\cos\theta}{\sqrt{1+\left\{\frac{2\omega L_s}{Z_0}\right\}^2\cos^2\theta}}\right) \qquad [7.17]$$

and

$$SE_2(\theta) = -20\log_{10}\left(\frac{\left\{\frac{2\omega L_s}{Z_0}\right\}\left\{-\frac{1}{2}\sin^2\theta\right\}}{\sqrt{\left\{\frac{2\omega L_s}{Z_0}\right\}^2\left\{-\frac{1}{2}\sin^2\theta\right\}+\cos^2\theta}}\right) \quad [7.18]$$

where L_s is the sheet inductance given by:

$$L_s = \frac{\mu_0 d}{2\pi} In\left(1 - e^{\frac{2\pi r}{d}}\right)^{-1} \quad [7.19]$$

In [7.19], r is the radius of the rebar and d is the width (or length) of the mesh (assuming a square mesh). To consider randomly polarised waves, a polarisation independent shielding effectiveness formula can be expressed as:

$$SE_0(\theta) = \log_{10}\left[\frac{1}{2}\left(|T_1(\theta)|^2 + |T_2(\theta)|^2\right)\right] \quad [7.20]$$

Thus, taking account of [7.20], the shielding effectiveness expression for a reinforced concrete slab/structure is obtained by modifying [7.8] as given below:

$$SE_{dB} = A_{dB} + R'_{db} + B_{dB} \quad [7.21]$$

where the reflection loss term is given as:

$$R'_{dB} = 20\log_{10}\left(\frac{\left\{Z_0 + \hat{Z}\right\}^2}{4Z_0\hat{Z}}\right) + \log_{10}\left(\frac{1}{2}\left\{|T_1(\theta)|^2 + |T_2(\theta)|^2\right\}\right) \quad [7.22]$$

The validity of [7.20] was demonstrated analytically using a mathematical software (mathematica) and two numerical simulation software codes (TLM and Finite Integration Technique, FIT[8]). The analytical code was developed to assist in the design of a dedicated signalling equipment room as part of a new railway control centre (Northern Line Control Centre) at Highgate in North London.

For this application, the rebar is modelled as an array of square meshes, as shown in Figure 7.2, of thickness 5 mm with a width of 50 mm. The individual meshes are electrically small in comparison to the free space wavelength. The spacing between each mesh is 5 mm equating roughly to a radius of 2.5 mm. The rebar is modelled as comprised of iron having a conductivity of 10^7 S m^{-1} and a relative magnetic permeability of 200. The junctions of the mesh are bonded.

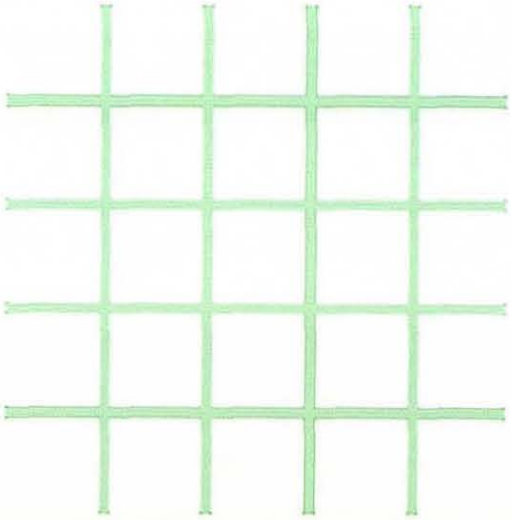

Figure 7.2: Schematic of the reinforcement rods arrangement

[8] The FIT solver used is the commercially available CST Studio

To validate the analytical approach, the shielding effectiveness of the rebar is obtained with the analytical method and then compared with numerical results obtained from TLM and Finite Integral Technique (FIT). The frequency range of interest is from 30 MHz to 2 GHz. As can be shown in Figure 7.3, the analytical and numerical results are in good agreement.

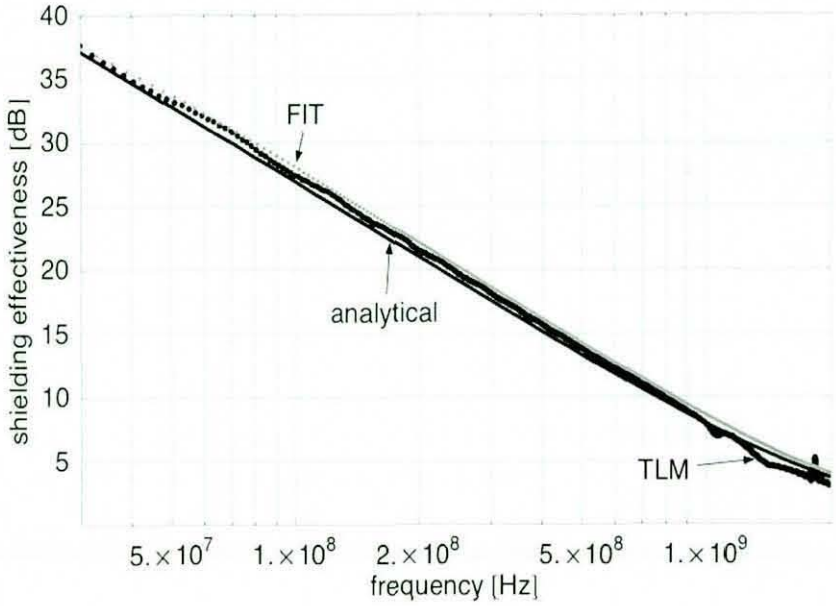

Figure 7.3: Numerical and Computational Determined Shielding Effectiveness of Rebar Mesh

7.2.2 *Concrete Modelled as a Simple Dielectric*

Two concrete slabs of thickness 30 mm and 300 mm with moisture content of 0.2% and 12% are considered for this analysis. The shielding effectiveness of the concrete slab is determined analytically using the transmission line approach presented above; in addition concrete is modelled in TLM and FIT. In this implementation, concrete is modelled in TLM and FIT, as a simple

dielectric with electrical parameters constant throughout the frequency range of interest. The implication of this simple model is an underestimation of ε' and an overestimation of ε'' with respect to frequency.

The shielding effectiveness of concrete slabs having a thickness of 30 mm and a moisture content of 0.2% and 12% is shown respectively in Figures 7.4 and 7.5. As can be seen the shielding effectiveness predicted by TLM and FIT is much higher than that determined analytically via the transmission line approach, this increase is due to the overestimation of the loss factor. Furthermore the impact of moisture content resulting in an increase in the predicted shielding effectiveness is clearly observable in Figure 7.5.

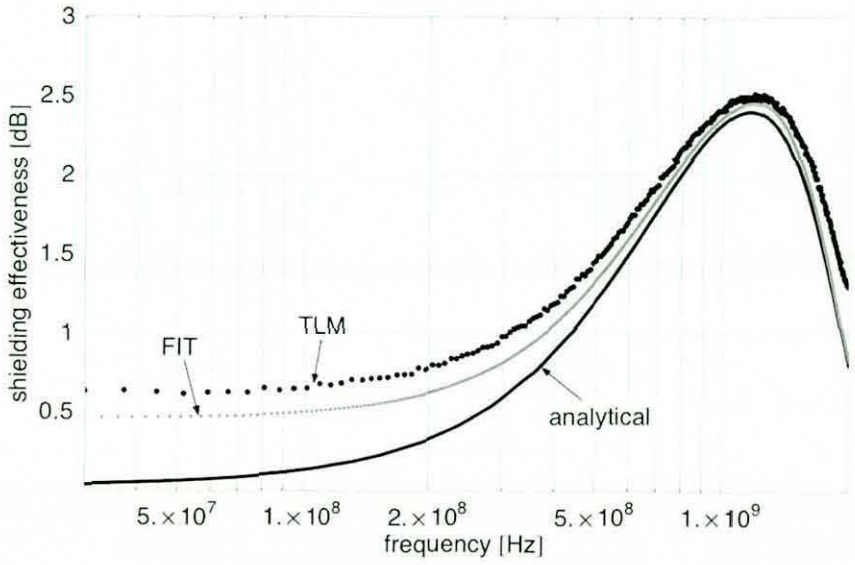

Figure 7.4: Predicted Shielding Effectiveness of 30mm Thick *Dry* Concrete Slab (Moisture Content of 0.2%)

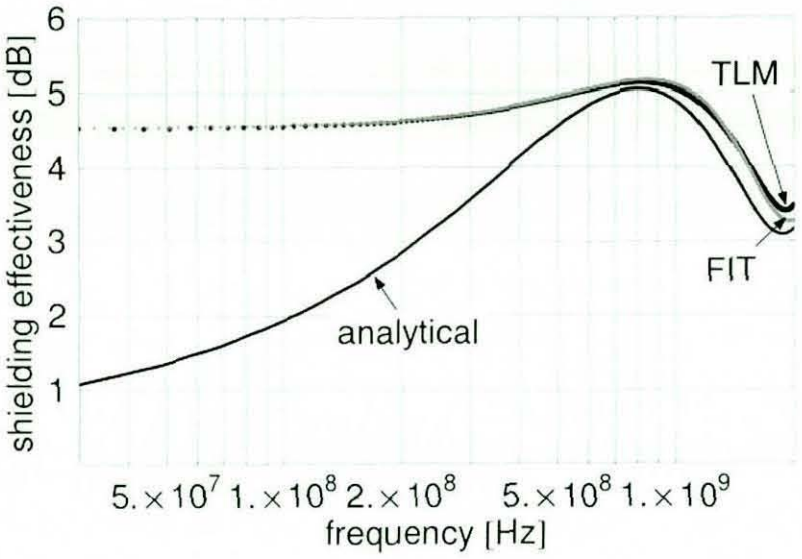

Figure 7.5: Predicted Shielding Effectiveness of a 30 mm Thick *Wet* Concrete Slab (Moisture Content of 12%)

In Figures 7.6 and 7.7, the predicted shielding effectiveness of a concrete slab having a thickness of 300 mm and a moisture content of 0.2% and 12% are respectively shown.

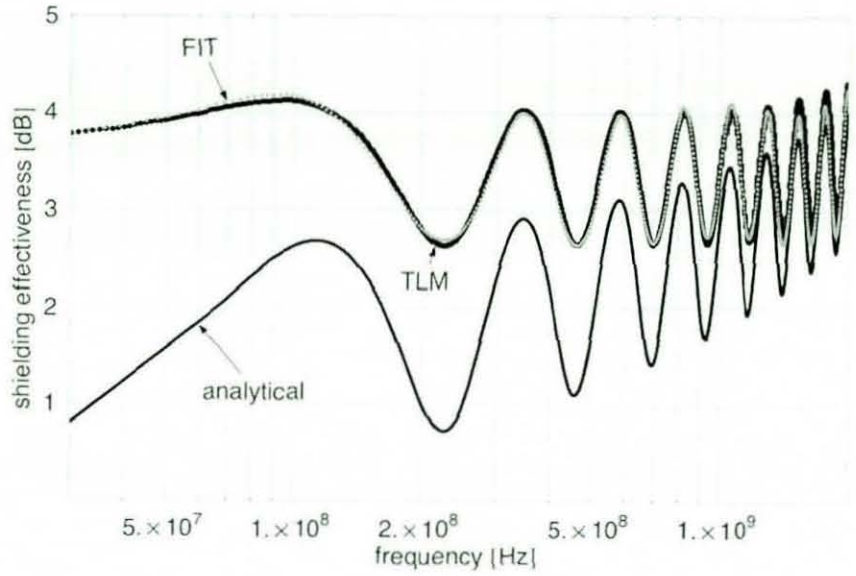

Figure 7.6: Predicted Shielding Effectiveness of a 30 mm Thick Dry Concrete Slab (Moisture Content of 0.2%)

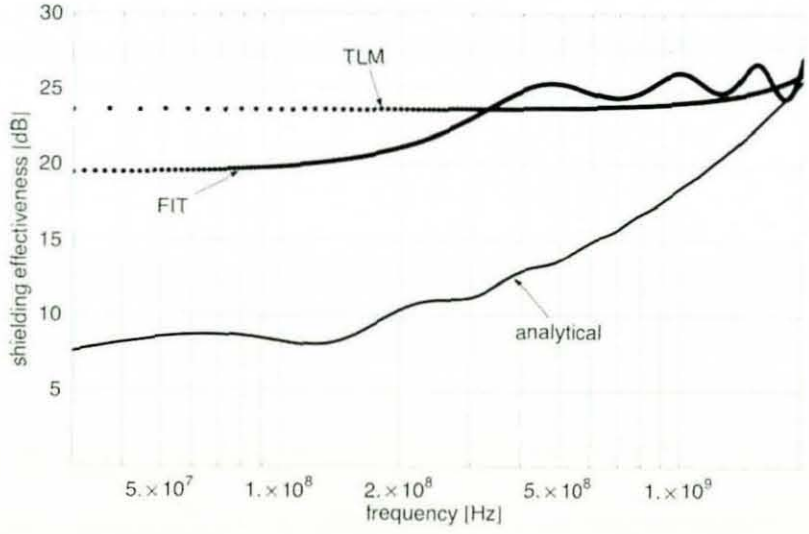

Figure 7.7: Predicted Shielding Effectiveness of a 30 mm Thick Wet Concrete Slab (Moisture Content of 12%)

The discrepancy in Figure 7.7 is due to the overestimation of ε^*. There is an observable oscillatory pattern in Figure 7.7; this is best explained by studying the contributing factors of each term (absorption loss, reflection loss and the re-reflection correction term) of the global shielding effectiveness expression given in [7.8]. Figures 7.8 and 7.9, shows the contributory factor due to each term of the global shielding effectiveness expression for a 300 mm thick *dry* and *wet* concrete slab. These figures highlight the dominant terms of the shielding effectiveness as a function of moisture content, for example for dry concrete the reflection is the dominant factor and absorption losses becomes considerable at high frequencies whereas for wet concrete the absorption loss term is the dominate factor.

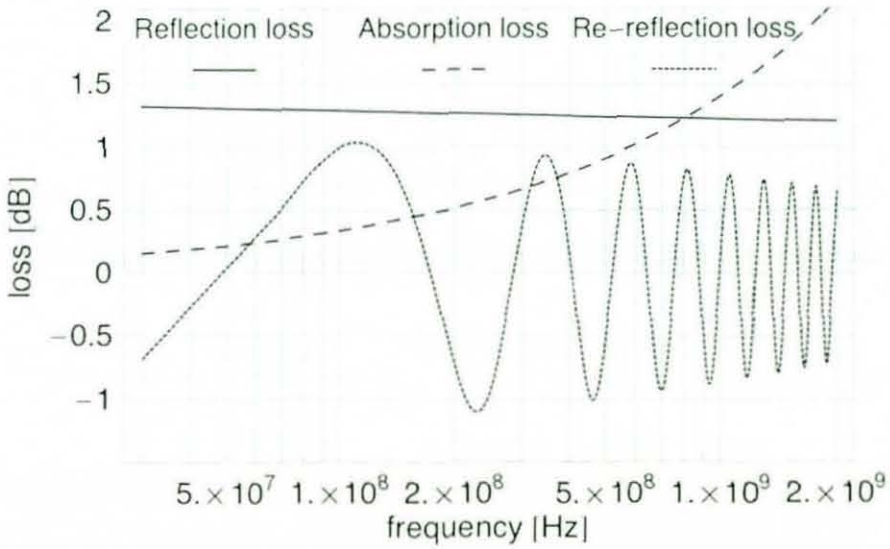

Figure 7.8: Contributory Factor due to Reflection Loss, Absorption Loss and Re-reflection Correction Term on a Dry Concrete

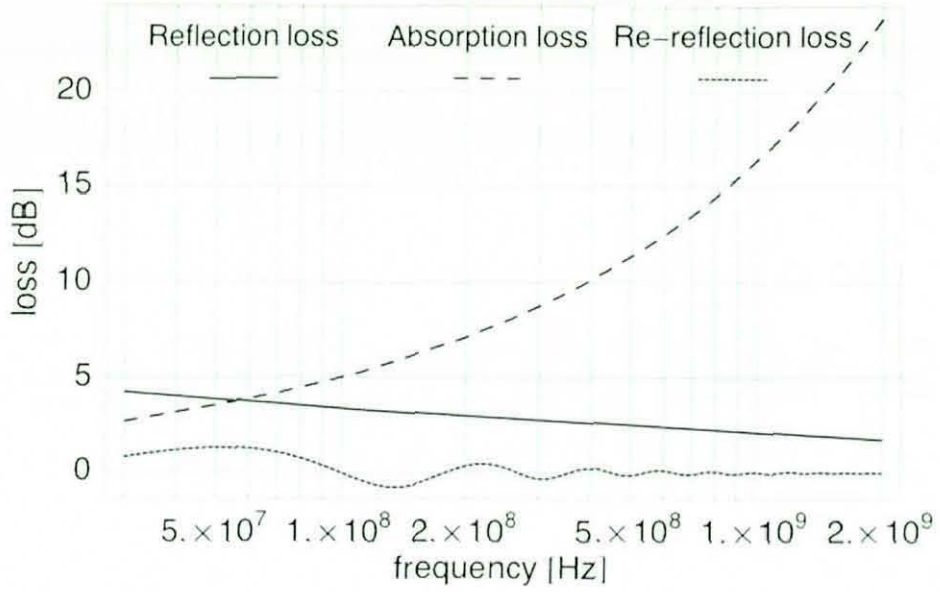

Figure 7.9: Contributory Factor due to Reflection Loss, Absorption Loss and Re-reflection Correction Term on a Wet Concrete

7.2.3 *Concrete Modelled as a Dispersive Material*

In the previous section, concrete was modelled as a simple dielectric material. This simplification did not hold for all conditions analysed, particularly when trying to estimate the shielding effectiveness of a wet concrete. Analysis of the results, suggest that the simplification results in an over estimation of the loss factor and thus an incorrect assessment of the reflection, absorption and re-reflection losses. It is equally clear from the results given in Section 7.2.2 that the simple dielectric model did not account for the energy loss due to the concrete electrical conductivity. The simple dielectric model accurately describes the imaginary part of the complex relative permittivity; it fails to describe the behaviour of the concrete structure at low frequencies.

In [19], dielectric properties of 5 sample of concrete were measured using a co-axial transmission line. The measurements were performed from 50 MHz to 1 GHz. The maximum aggregate size used was 30 mm. Roberts provided plots describing the influence of moisture content, in particular the effects of chloride on the permittivity of the concrete. Roberts also presented 5 materials models with frequency dependent permittivity, three for homogenous and two heterogeneous materials, which were compared with experimental data through numerical fitting. Of the material models presented, the Cole-Cole model provided better agreement with measurement data. The Cole-Cole model is a model for homogeneous materials.

TLM has the ability to model complex dielectric materials but these are limited to materials that obey either a Debye or Lorentz characteristics. For the purpose of this analysis, the behaviour of concrete's complex permittivity is modelled as a Debye material by curve fitting the [7.5] and [7.6] to the measurement data published by [8]. A non-linear least square Marquardt-Levenberg algorithm [20] was used for the fitting. The algorithm was used to obtain the values for $\varepsilon_{statics}$, ε_{∞}, τ and σ_{dc} which are summarised in Table 7.1 below for six different moisture contents.

Moisture Content	ε_{static}	ε_{∞}	$\tau[ns]$	$\sigma_{dc}\ [\Omega^{-1}m^{-1}]$
0.2%	4.814 ± 0.002	4.507 ± 0.002	0.82 ± 0.01	$6.06\times10^{-4} \pm 0.06\times10^{-4}$
2.8%	6.75 ± 0.03	5.503 ± 0.005	2.28 ± 0.08	$2.03\times10^{-3} \pm 0.04\times10^{-3}$
5.5%	8.63 ± 0.02	6.023 ± 0.009	1.00 ± 0.02	$5.15\times10^{-3} \pm 0.06\times10^{-3}$
6.2%	9.14 ± 0.06	5.93 ± 0.02	0.80 ± 0.03	$6.7\times10^{-3} \pm 0.3\times10^{-3}$
9.3%	11.19 ± 0.05	7.2 ± 0.02	0.73 ± 0.02	$23\times10^{-3} \pm 2\times10^{-3}$
12%	12.84 ± 0.03	7.42 ± 0.02	0.611 ± 0.006	$20.6\times10^{-3} \pm 0.2\times10^{-3}$

Table 7.1: Fitted parameter for concrete samples

Figures 7.10 – 7.17, show $\varepsilon_r^{'}$ and $\varepsilon_{r,eff}^{''}$ versus frequency for four concrete samples of different moisture content (i.e. 0.2%, 5.5%, 6.2% and 12%), using parameters presented in Table 7.1. As it can be observed, a good agreement is obtained between the experimental data and fitted curves, however the following observations can be made:

1. The Debye model tends to yield lower values for $\varepsilon_r^{'}$ at low and intermediate frequencies, and higher values at other frequencies when compared to the experimental data
2. The Debye model tends to yield higher values for $\varepsilon_{r,eff}^{''}$ at intermediate frequencies when compared to the experimental data.

These differences are more pronounced for concrete with higher moisture content. To assess the suitability of the proposed dispersive material model in predicting the shielding effectiveness of concrete, a concrete wall having a thickness of 300 mm with varying moisture content values of 0.2%, 5.5%, 6.2% and 12% was analysed. The frequency range of the analysis was 30

MHz to 1 GHz and extended to 2 GHz for a moisture content of 6.2%. The results of the comparative analysis of the shielding effectiveness determined numerical using [7.8] and TLM, using the relevant parameters from Table 7.1, are shown in Figures 7. 18 – 7.21.

A close look at these figures, highlight the similarity between the results, however in all cases, the shielding effectiveness determined using [7.8] is greater than that obtained with TLM at higher frequencies, and at the lower frequencies for concrete with moisture content of 12%.

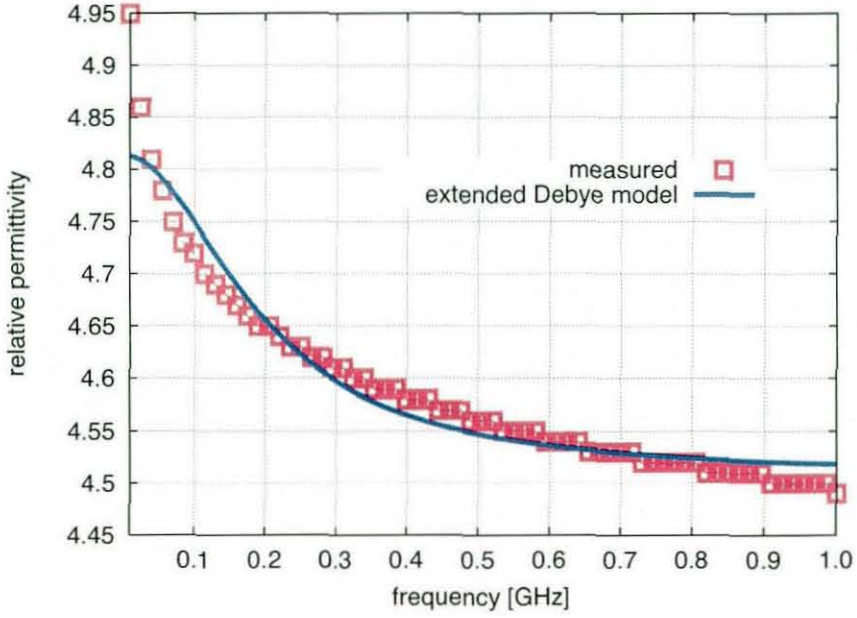

Figure 7.10: Measured and fitted $\varepsilon_r^{'}$ versus frequency for a moisture content of 0.2%

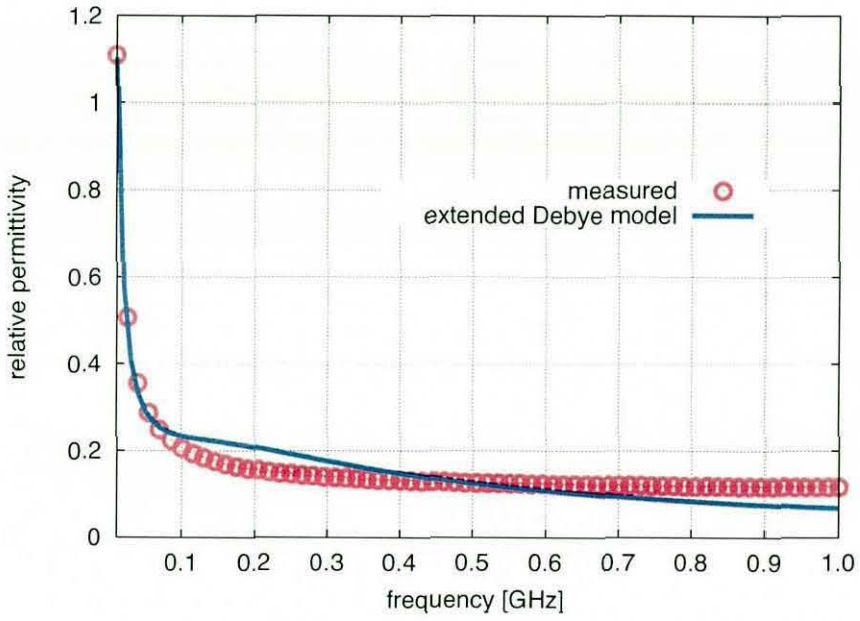

Figure 7.11: Measured and fitted $\varepsilon_{r,eff}^{''}$ versus frequency for a moisture content of 0.2%

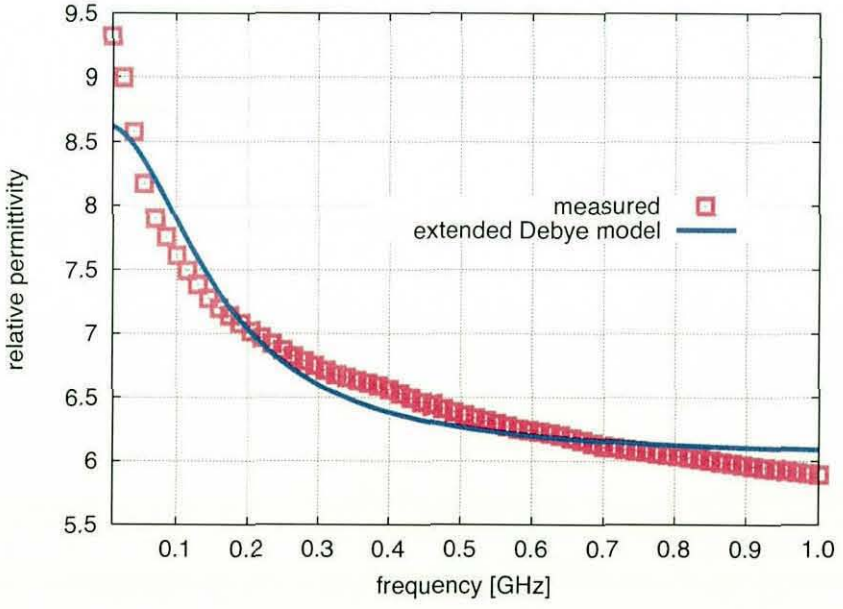

Figure 7.12: Measured and fitted $\varepsilon_{r}^{'}$ versus frequency for a moisture content of 5.5%

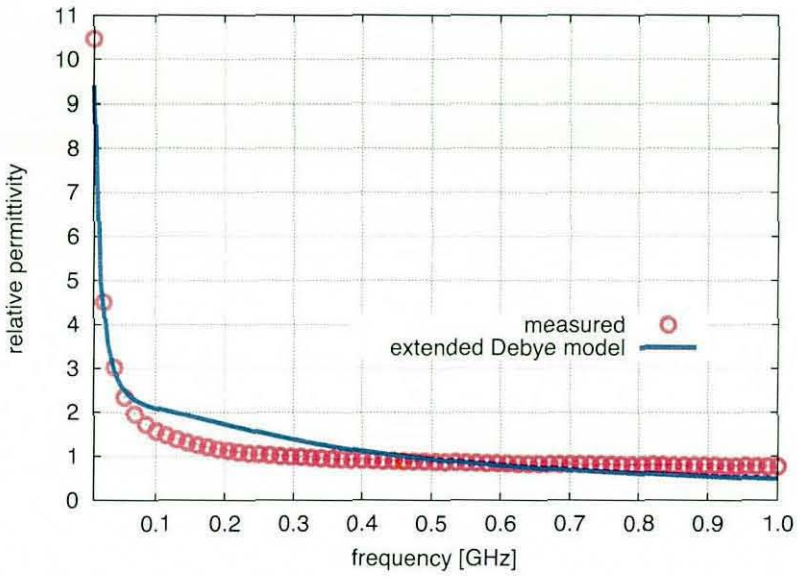

Figure 7.13: Measured and fitted $\varepsilon'_{r,eff}$ versus frequency for a moisture content of 5.5%

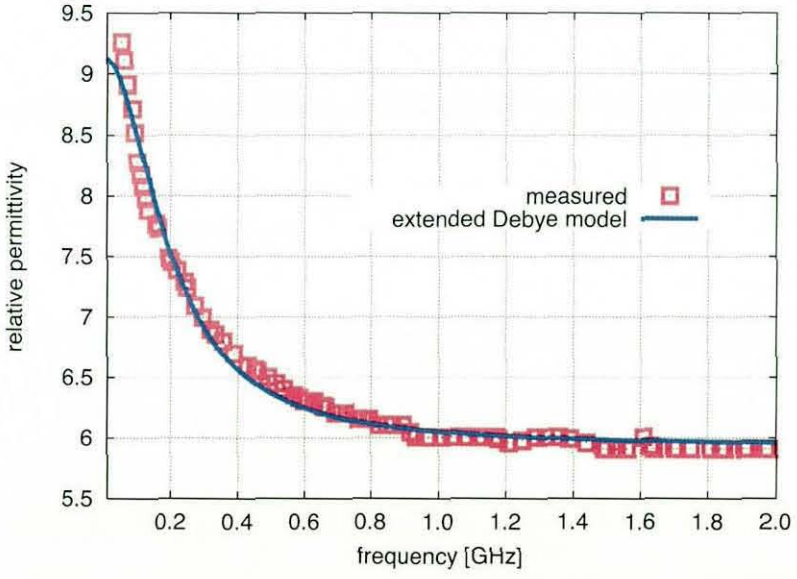

Figure 7.14: Measured and fitted ε'_r versus frequency for a moisture content of 6.2%

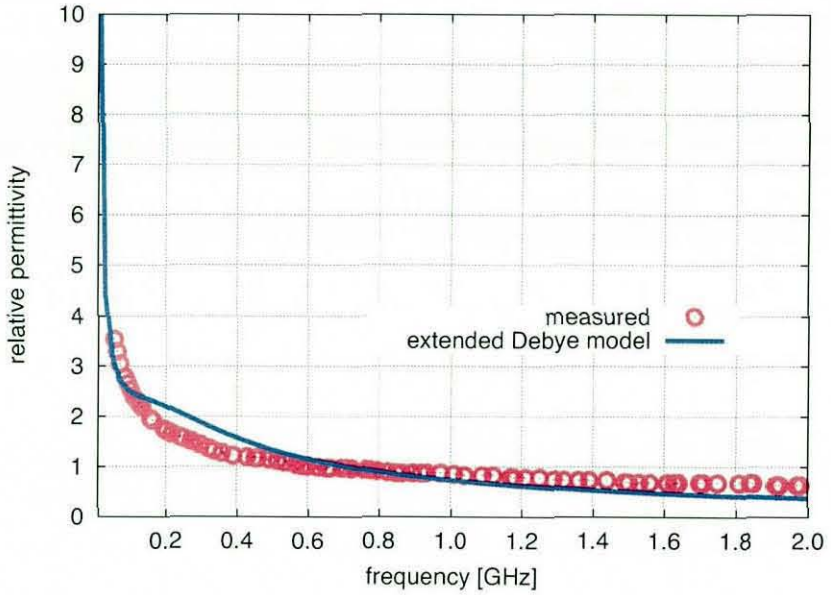

Figure 7.15: Measured and fitted $\varepsilon^{*}_{r,eff}$ versus frequency for a moisture content of 6.2%

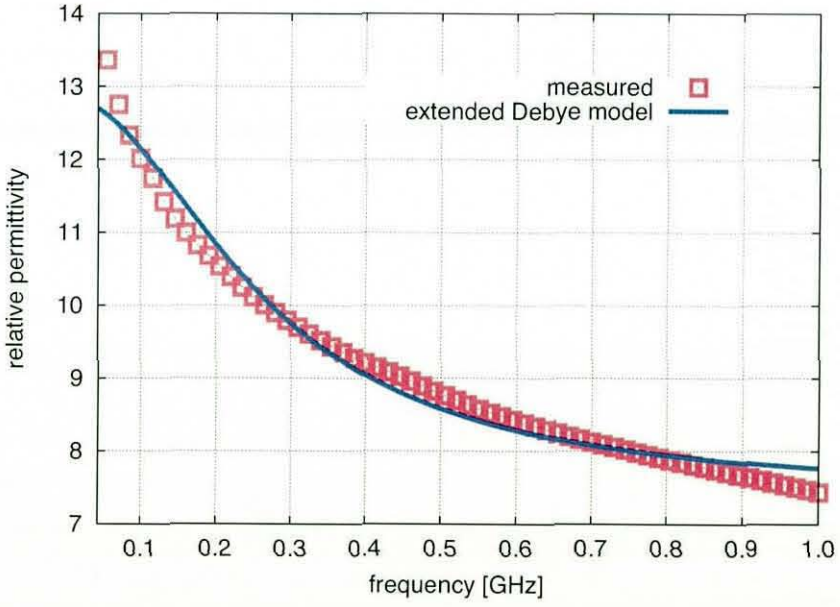

Figure 7.16: Measured and fitted $\varepsilon_r^{'}$ $\varepsilon_r^{'}$ versus frequency for a moisture content of 12%

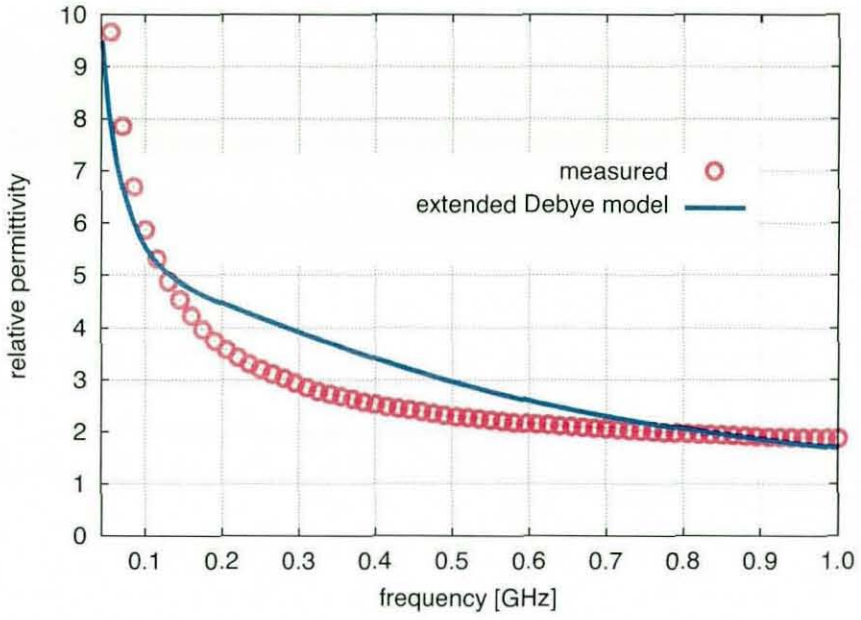

Figure 7.17: Measured and fitted $\varepsilon^{"}_{r,eff}$ versus frequency for a moisture content of 12%

This may be explained by the differences between the measured electrical parameters used in the analytical approach and those obtained by fitting the dispersive model and employed in TLM. In particular, the shielding effectiveness appears to be affected by $\varepsilon^{"}_{r,eff}$ more than $\varepsilon^{'}_{r}$. A detail review of Figure 7.18 indicates that the shielding effectiveness predicted by TLM is higher for frequencies between about 70 MHz and 500 MHz, the exact frequency range where the dispersive model gives higher values of $\varepsilon^{"}_{r,eff}$. This trend applies in all cases analysed. Similarly, it can be observed that where the value of $\varepsilon^{"}_{r,eff}$ is lower than that obtained experimentally, the resultant shielding effectiveness predicted by TLM is lower.

To further explore the influence of the fitted parameters on the shielding effectiveness calculation as well as the limits of the dispersive model, a further comparison between the results obtained with TLM and that obtained through the analytical approach is necessary. Figures 7.19 and 7.20 were chosen for this comparative analysis, as they are the ones that showed the most pronounced differences between both methods. In particular, differences of up to 5 dB at high frequencies are observable. Using the fitted parameters for concrete in both cases, good agreement is obtained between the analytical calculation and the numerical simulation as shown in Figures 7.22 and 7.23. This result highlights the fact that the simple dispersive model is not appropriate in all cases and suggests the implementation of other material models such as Cole-Cole's.

The proposed concrete model is a large-scale model that defines concrete as a homogeneous material and thus leaves the size of the heterogeneities present in concrete out of the consideration, provided that the aggregate size is considered electrically small in the frequency range of interest. Thus the validity and limitations of the proposed modelling approach would need to be assessed for the situation where the aggregate size is electrical large. Furthermore, the use of such dispersive model requires greater computational power (more computer memory and longer run time) than the simple dielectric model.

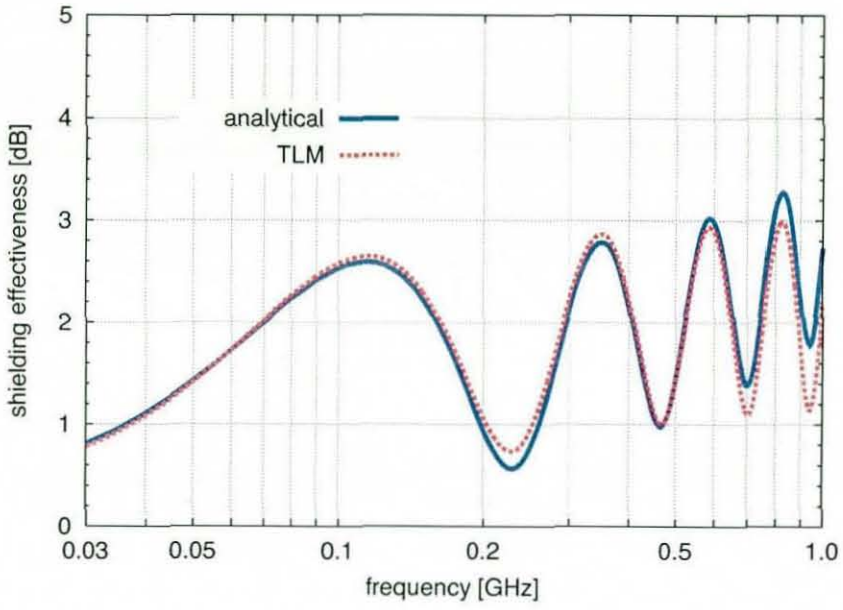

Figure 7.18: Comparison of shielding effectiveness for a concrete wall of thickness 300 mm and moisture content of 0.2%

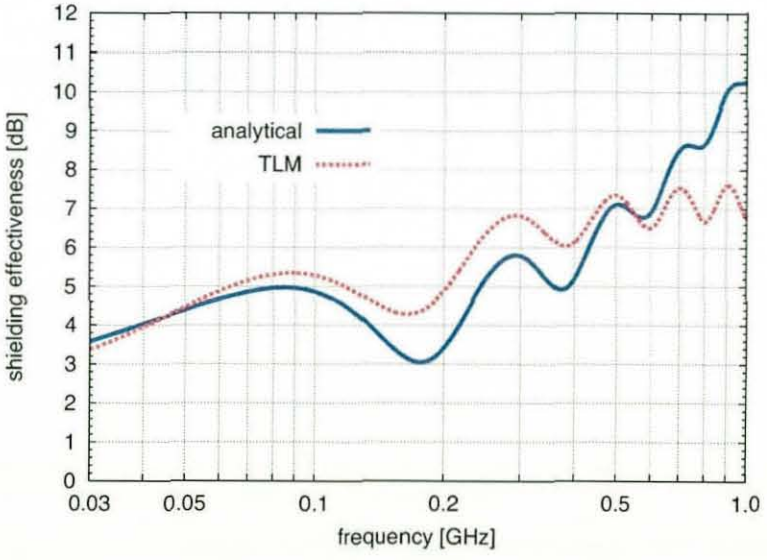

Figure 7.19: Comparison of shielding effectiveness for a concrete wall of thickness 300 mm and moisture content of 5.5%

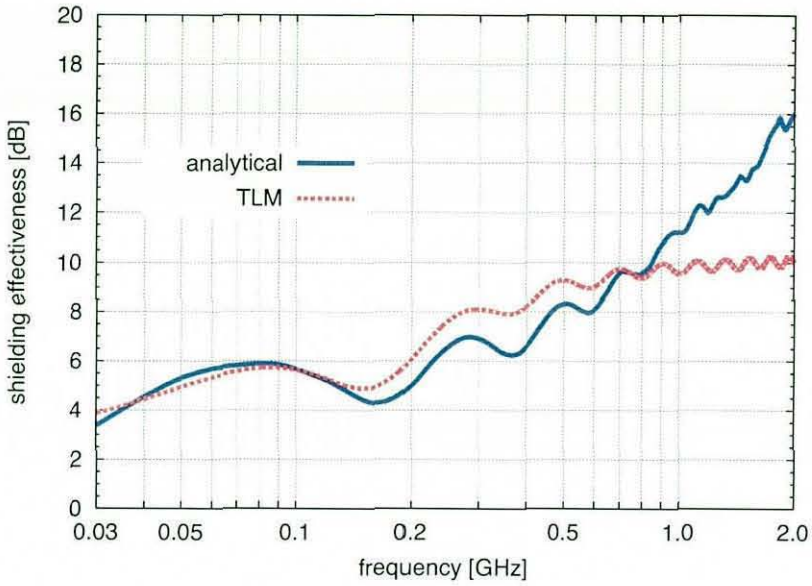

Figure 7.20: Comparison of shielding effectiveness for a concrete wall of thickness 300 mm and moisture content of 6.2%

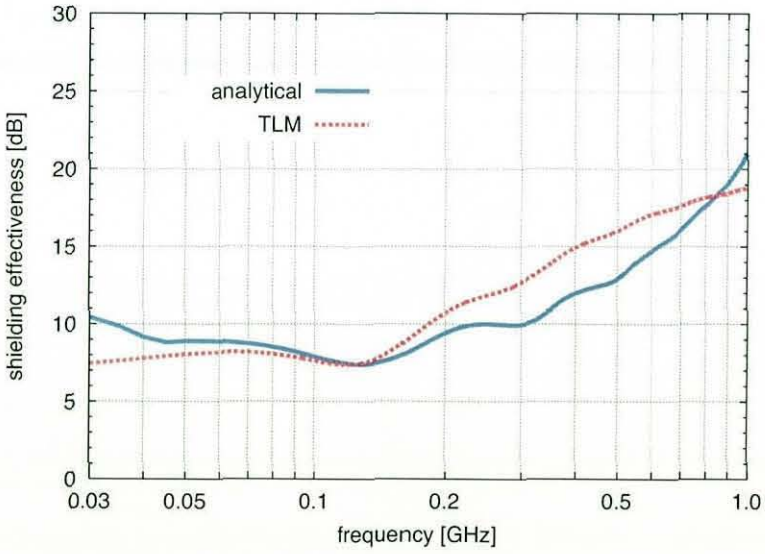

Figure 7.21: Comparison of shielding effectiveness for a concrete wall of thickness 300 mm and moisture content of 12%

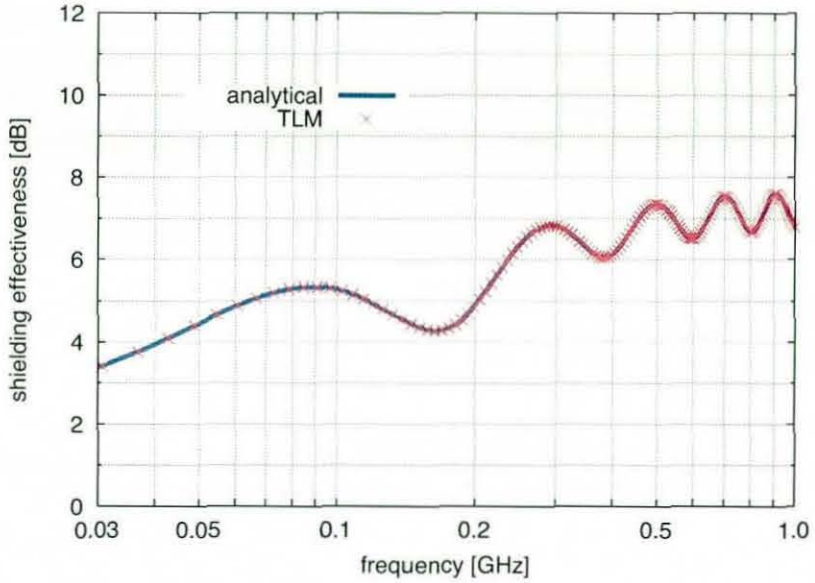

Figure 7.22: Comparison of shielding effectiveness for a concrete wall of 300 mm and moisture content of 5.5 % with parameters defined by the Debye model

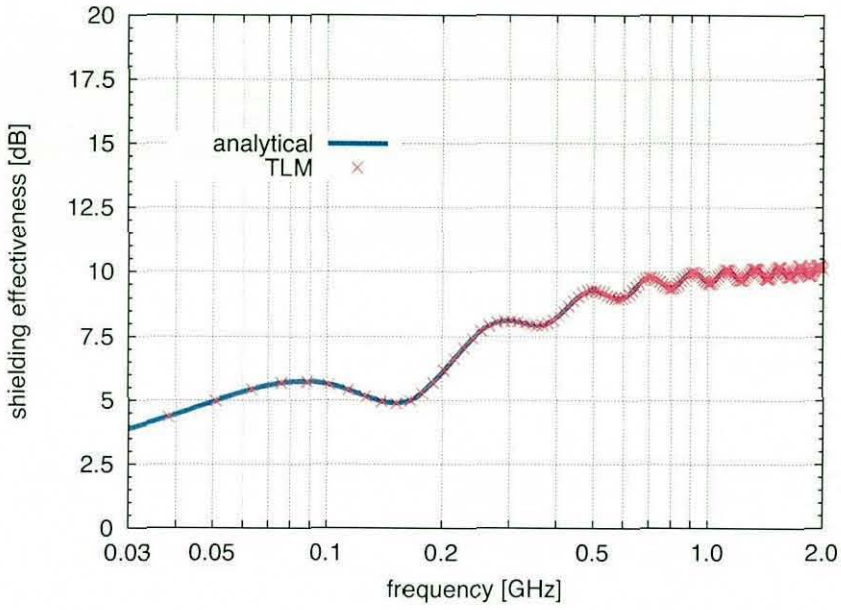

Figure 7.23: Comparison of shielding effectiveness for a concrete wall of 300 mm thick and moisture content of 6.2% with parameters defined by the Debye Model

7.3 Shielding Effectiveness of Conductive Concrete

In previous sections the ability of concrete structures to attenuate electromagnetic waves was analysed, it is clear from the analysis that concrete provides very low attenuation to electromagnetic disturbance. The inclusion of reinforcing rods in concrete slab/structure improves the ability of the structure to attenuate electromagnetic waves, particularly below 300 MHz. The effectiveness of the reinforcement depends largely on the mesh size and may not be feasible in all structures.

It is possible to dope concrete to increase its conductivity and thus its ability to attenuation electromagnetic waves. Conductive fillers can be added to the concrete mix resulting in what is referred to as conductive concrete. In doing so, care must be exercised to ensure the mechanical strength of the resultant

structure is not compromised. This is similar in principle to polymer matrix composites containing electrically conductive fillers [21] - [26], which are widely used in the industry as enclosure for the high shielding efficiency they can offer. In contrast to polymer matrix, which is electrically insulating, plain concrete matrix is slightly conductive (mainly due to moisture content which results in ionic conduction). Therefore the use of a cement matrix allows some degree of electrical conductivity among the conductive filler units, even when the filler volume fraction is below the percolation threshold.

To use these materials for shielding applications, it is necessary to understand and quantitatively predict the complex permittivity of the conductive concrete as a function of conductive filler concentration. Numerous studies have been undertaken on the study of polymer matrix composites, however it is outside the scope of this thesis to provide a detailed literature review. With respect to conductive concrete, limited studies have been performed and majority of these relate to measurement of electrical properties of the composite [12],[13] [27] - [29]. Matsumoto et al [30] presented simple models for estimating the complex permittivity of polymer/metal composite. In Karr *et al* [31], a numerical approach is developed to estimate the complex permittivity of conductive concrete, however no verification of the approach was provided due to lack of measurement data. In this section, an extension of the numerical approach presented by Karr *et al* is given, this extension includes the ability to estimate the shielding effectiveness of conductive concrete.

Two scenarios can be described: (1) low conductive filler concentration, in which the number of fillers per unit concrete volume is low and the inclusions are separated by the concrete composition. In this scenario, it is assumed that the average distance between two arbitrarily selected fillers within the concrete is fairly long such that conductive particles do not touch; (2) high conductive filler concentration, in which the number of fillers per unit

concrete volume is high, such that the conductive particles within the concrete composite directly touch each other. In this analysis, concrete is assumed to be doped with low concentration of short thin steel fibres, which are homogenously but randomly dispersed. The analysis presented involves solving the induced current problem for a thin wire with appropriate boundary conditions applied. An estimate of the polarization due to currents in the conductive fibres is then obtained, and this current is then used in conjunction with the polarization of the concrete structure (without fibres) to determine the complex permittivity of the conductive concrete. The attenuation provided by the structure is then estimated via the simple approximations detailed in [32].

7.3.1 *A Conductive Concrete Model*

For this analysis, an infinite slab of concrete characterised as a dispersive material with a frequency-dependent complex permittivity, obeying [7.4] is considered. The dielectric response of this material will exhibit a different dispersive behaviour when doped with conductive fibres, which behaves as electric dipoles scatterers. The amount of steel fibre added to the concrete depends on the type of fibre and on the required mechanical strength, and is typically in the range of $20 - 80\,kg/m^3$. Conductive concrete is a heterogeneous mixture of cement, sand, aggregates, water, air and steel fibres. Having already assumed the concrete as a homogeneous material, when the largest particle dimension, in this case the length of the steel fibre, is much smaller than a wavelength at the frequency of interest, the resultant mixture can still be regarded as homogeneous. For arbitrarily oriented and randomly dispersed inclusions the composite can be considered isotropic with an effective complex relative permittivity $\hat{\varepsilon}_{eff}$, such that

$$\langle \hat{D} \rangle = \varepsilon_0 \varepsilon_{eff} \langle \hat{E} \rangle \qquad [7.23]$$

where $\langle\ \rangle$ denotes the spatial averaging of the macroscopic electric field $\hat{E}$ and electric induction $\hat{D}$ complex vectors over a volume that is large with respect to the scale of the heterogeneities in the mixture. Considering steel fibre reinforced concrete to be a two phase mixture of randomly oriented conducting fibres in an isotropic homogeneous concrete host with effective complex relative permittivity $\hat{\varepsilon}_{con}$, [7.23] can be re-written as:

$$\langle \hat{D} \rangle = \varepsilon_0 \langle \hat{E} \rangle + \langle \hat{P} \rangle \qquad [7.24]$$

where

$$\langle \hat{P} \rangle = \varepsilon_0 (\hat{\varepsilon}_{eff} - 1) \langle \hat{E} \rangle \qquad [7.25]$$

is the polarisation relative to the composite. The effective permittivity of the composite can then be calculated. From [7.25], the effective complex relative permittivity of the composite can be obtained as:

$$\hat{\varepsilon}_{eff} = 1 + \frac{\langle \hat{P} \rangle}{\varepsilon_0 \langle \hat{E} \rangle} \qquad [7.26]$$

7.3.2 *Thin Wire Approximation*

It is assumed that the conductive fibres are cylindrical and of the same length and diameter, as illustrated in Figure 7.23. An incident wave $\hat{E}_z^i$ impinging on the surface of the conductive fibre will induce current on the surface of the conductive fibre. The current distribution on the fibre can be obtained by solving the Pocklington's Integrodifferential Equation [33]:

$$\int_{-l/2}^{l/2} \hat{I}_z\left(z'\right)\left[\left(\frac{\partial^2}{\partial z^2}+\hat{\gamma}^2\right)\hat{G}\left(z,z'\right)\right]dz' == j\omega\hat{\varepsilon}_{conc}\hat{E}_z^i \qquad [7.27]$$

where l is the length of the steel fibre, $\hat{\gamma}$ is the propagation constant of concrete, ω is the angular frequency and

$$\hat{G}\left(z,z'\right)=\frac{1}{2\pi}\int_0^{2\pi}\frac{e^{-j\hat{\gamma}R}}{4\pi R}d\phi' \qquad [7.28]$$

where $R=\sqrt{r^2+\left(z-z'\right)^2}$, with z' a running length co-ordinate along the steel fibre, r the radius of the steel fibre, and z the co-ordinate on the steel fibre. For thin wires $\left(r \ll \lambda\right)$, where λ is the wavelength in the concrete at the frequency of interest, [7.28] reduces to:

$$\hat{G}\left(z,z'\right)=\hat{G}\left(R\right)=\frac{e^{-j\hat{\gamma}R}}{4\pi R} \qquad [7.29]$$

[7.27] can be expressed in a more convenient form as:

$$\int_{-l/2}^{l/2}\hat{I}_z\left(z'\right)\frac{e^{-j\hat{\gamma}R}}{4\pi R}\left\{\left(1+j\hat{\gamma}R\right)\left(2R^2-3r^2\right)+\left(\hat{\gamma}rR^2\right)\right\}dz' = j\omega\hat{\varepsilon}_{conc}\hat{E}_z^i \qquad [7.30]$$

[7.30] can be easily solved numerically in the frequency domain by means of the Method of Moments, in order to obtain the induced current distribution on the surface of the steel fibre (refer to the Appendix for the MoM code). In doing so, we employ the boundary conditions that the current at the ends of the wire is zero (the conductivity of steel is much higher than that of concrete), and assume a unit electric field incident onto the steel fibre.

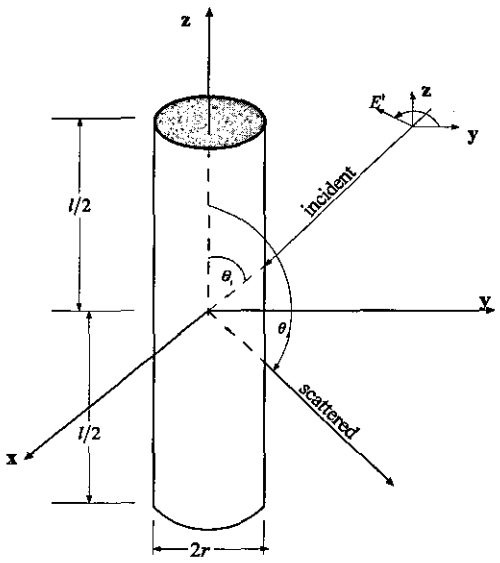

Figure 7.23: Uniform plane wave obliquely incident on a steel fibre.

7.3.3 *The polarization of the composite due to the conductive filler*

The incident electric field induces a current with a linear density distributed along the length of the steel fibre. The electric dipole moment per unit volume $\langle \hat{\mathbf{p}}_{10} \rangle = \langle \hat{p}_{10} \rangle \mathbf{a}_z$ of the composite due to the steel fibres, averaged over the inclusions orientations, can be calculated using the continuity equation $\partial J_z(z)/\partial z + j\omega\rho(z) = 0$

$$\langle \hat{p}_{10} \rangle = -\frac{2N}{3j\omega}\int_0^{l/2} \frac{d\hat{I}(z)}{dz} z\,dz \qquad [7.31]$$

where N is the number of steel fibres per unit volume. A refinement of [7.31] can be obtained by incorporating Onsager's correction [34] that yields:

$$\langle \hat{P}_1 \rangle = \frac{3}{4}\left\{ \left(\langle \hat{P}_{10} \rangle - \hat{\varepsilon}_{conc}\varepsilon_0 \right) + \sqrt{\left(\langle \hat{P}_{10} \rangle - \hat{\varepsilon}_{conc}\varepsilon_0 \right)^2 + \frac{8}{3}\hat{\varepsilon}_{conc}\varepsilon_0 \langle \hat{P}_{10} \rangle} \right\} \quad [7.32]$$

The effective complex relative permittivity of the conductive concrete can then be calculated as:

$$\hat{\varepsilon}_{eff} = \varepsilon'_{eff} - j\varepsilon''_{eff} = 1 + \frac{\langle \hat{P}_1 \rangle}{\varepsilon_0 \langle \hat{E} \rangle} + \hat{\varepsilon}_{con} \quad [7.33]$$

In [7.33], the incident electric field $\langle E \rangle$ can be set to unity for ease of calculation. The effective conductivity of the conductive concrete is:

$$\sigma_{eff} = \omega\varepsilon_0\varepsilon''_{eff} \quad [7.34]$$

7.3.4 *Validation of Numerical Approach*

The validity of the numerical approach was verified against published measurement data for steel fibres reinforced conductive concrete. In [8], measurements of the relative permittivity and conductivity of steel fibre reinforced concrete specimens were performed for different moisture content at the frequency of 500 MHz. The steel fibres added to the concrete mix have a length of 30 mm and a diameter of 0.5 mm. Using the same parameters for the steel fibres, the number of steel fibres per unit volume, N, for 50 kg of fibres in 1 m^3 of concrete is determined as $N = 1.08 \times 10^6$. Implementing the numerical techniques described previously, the complex permittivity and conductivity of the steel fibre reinforced conductive concrete can then be determined.

In Figure 7.24, the real part of the effective complex relative permittivity is compared with actual measurement data. The real part of the complex

permittivity obtained as a first approximation from [7.31], as well as from the second approximation given in [7.32] is presented.

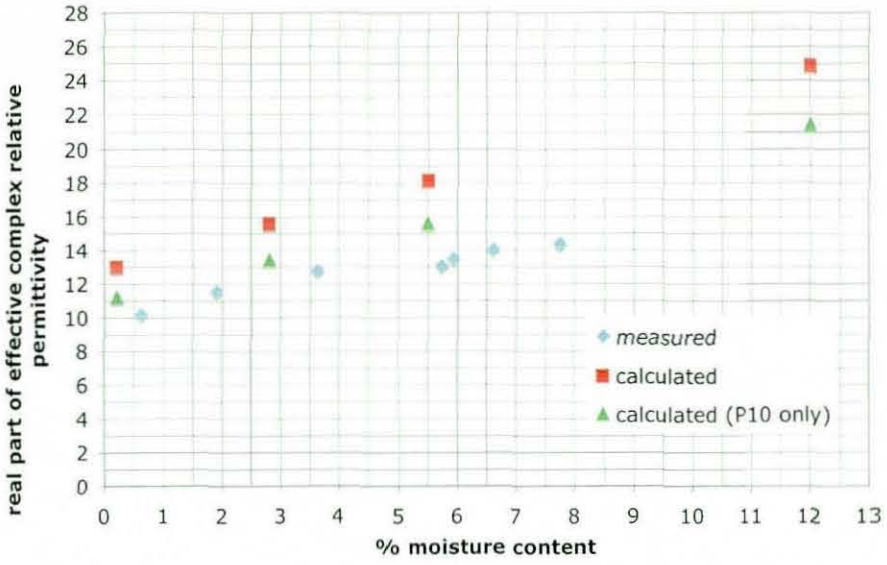

Figure 7.24: Real part of the effective complex relative permittivity of conductive concrete with $N = 1.08 \times 10^6$ steel fibre inclusions.

In Figure 7.25, a similar comparative analysis is presented for conductivity. Table 7.2 shows the estimated shielding effectiveness of a 300 mm thick concrete wall for four different values of moisture content. From the data presented in the Table, an improvement of approximately 5 dB can be obtained from dry concrete (0.2% moisture content) if it is doped with $1.08/cm^3$ steel fibres of the dimensions stated. This improvement increases to approximately 10 dB for wet concrete (12% moisture content). While the data presented is only valid at 500 MHz, the general trend can be expected throughout the frequency range of 30 MHz – 1 GHz.

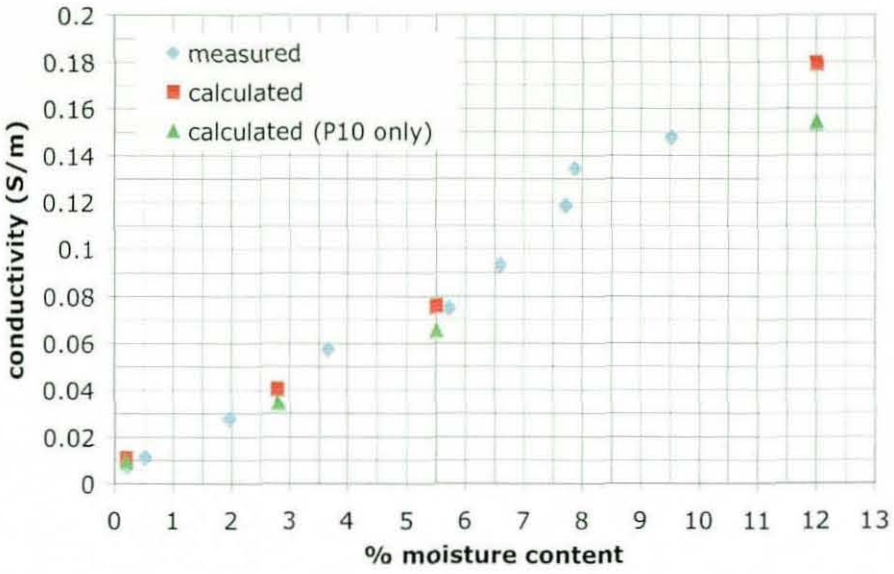

Figure 7.25: Real part of the conductivity of a conductive concrete with $N = 1.08 \times 10^6$ steel fibre inclusion.

Moisture Content %	Plain Concrete SE dB	Conductive Concrete SE dB
0.2	1.66	6.31
2.8	5.05	7.91
5.5	7.50	13.13
12.0	12.72	22.64

Table 7.2: Estimated shielding effectiveness of a conductive concrete with $N = 1.08 \times 10^6$ steel fibre inclusions.

7.4 Summary

In this chapter, the electrical properties of concrete have been analysed, including a detailed investigation into concrete's ability to attenuate electromagnetic waves. The analysis covered plain concrete (i.e. concrete without any conductive filler/additive), reinforced concrete and conductive concrete (i.e. the steel was used as the conductive filler).

It has been demonstrated analytically that plain concrete offers very low shielding efficiency but that the shielding effectiveness can be improved through the use of conductive reinforcement or conductive fillers. It was highlighted that moisture content is a very important parameter when analysing the shielding effectiveness of concrete, as it relates directly to the complex permittivity of concrete. The amount of moisture content within the concrete structure also relates the degree of dispersion possible within the concrete.

The ability to accurately model concrete within numerical simulators, in particular TLM, was explored. It was demonstrated that the simple dielectric

material model available within TLM (and FIT) was not adequate in providing a full description of the electrical behaviour of concrete. A major contribution of this analysis is the development of material model based on Debye Model, which accurately describes the electrical behaviour of concrete.

The material model proposed for concrete tends to yield lower values for the real part of the relative complex permittivity at low and intermediate frequencies, and higher values at other frequencies when compared to experimental data. The material model also tends to yield higher values of the imaginary part of the relative complex permittivity at intermediate frequencies when compared to measurement data. These differences tend to be more pronounced for concrete with higher moisture content.

An important note is that the electrical parameters of concrete (i.e. concrete's permittivity and permeability data) are parameters that are only determined via measurement. When the measured electrical properties are used in both the analytical and numerical approach developed to assess the shielding effectiveness of concrete the results obtained from both methods are in good agreement.

Finally the subject of conductive concrete is covered. An analytical method is proposed to assist in the design of conductive concrete and to predict the shielding effectiveness of the conductive concrete structure. It is predicted that by adding conductive fillers of appropriate quantity to a concrete mix, that the resultant product would provide a shielding effectiveness of appropriately 5 dB higher than plain concrete.

7.5 References

[1] Burchler, D.; Elsher, B. and Bohni, H. "*Electrical resistivity and dielectric properties of hardened cement and mortar*", Institute of

materials chemistry and corrosion, Swiss Federal Institute of Technology, ETH Honggerber, CH-8093 Zurich, Switzerland, 1996

[2] Hunkeler, F. "*The resistivity of pore water solution - a decisive parameter of rebar corrosion and repair methods*", Construction and Building materials, Vol. 10, No. 5 pages 381 - 389, 1996.

[3] Hammond, E and Robson, T. D. "*Comparison of electrical properties of various cements and concretes*", the Engineer, Vol.199, No 5156, Pg. 78 -80, Jan 21, 1955 and No 5166, pg 114 -115, Jan 28, 1955.

[4] Chung, D. D.L, " *Electrical conduction behaviour of cement-matrix composites*", Journal of Materials Engineering and Performance, Vol. 11, No. 2, April 2002, Pg. 194 – 204.

[5] Cristina, S and Orlandi, A, "*EMC effects of the lightning protection system: shielding properties of the roof grid*', in Proc. IEEE Int. Symp. Electromagnetic Compatibility, Aug. 1991, Pg. 78 – 83

[6] Laurens, S, Balayssac, J.P, Rhazi, J., Klysz, G. and Arliguie, G. "*Non destructive evaluation of concrete moisture by GPR technique: experimental study and direct modelling*', in Proc. Int. Symp. NDT in Civil Engineering, 2003

[7] Richalot, E, Bonilla, M, Man-Fai Wong, V. Fouad-Hanna, H Baudrand, and J Wiart, *"Electromagnetic Propagation into Reinforced Concrete Walls*', IEEE Trans. On Microwave Theory and Techniques, Vol. 48, Issue 3, Mar 2003, pp. 357 – 366.

[8] M. N. Soutsos, J. H. Bungey, S. G. Millard, M.R. Shaw, and A. Patterson, "*Dielectric properties of concrete and their influence on radar testing*," NDT&E International, Vol. 34, pp. 419-425, 2001

[9] Battilana, J. "*Electromagnetic Screening by Reinforced Concrete*', Magazine of Concrete Research, Vol. 41, September 1989, pp. 163 – 169.

[10] Cristina, S and Orlandi, A, "*EMC effects of the lightning protection system: shielding properties of the roof grid*', in Proc. IEEE Int. Symp. Electromagnetic Compatibility, Aug. 1991, pp. 78 – 83.

[11] R.A. Dalke, C. L Holloway, P. McKenna, M. Johansson, and A.S. Ali, "*Effects of Reinforced Concrete Structures on RF Communications*", IEEE Trans on Electromagnetic Compatibility, Vol 42, No 4, November 2000, pp. 486 – 496.

[12] Cao, J. and Chung, D., "*Use of fly ash as an admixture for electromagnetic interference shielding*', Cement and Concrete Research, Vol. 34, Pg. 1889 -1892, Oct. 2004.

[13] Wen, S. and Chung, D, "*Electromagnetic interference shielding reaching 70 dB in steel fiber cement*", Cement and Concrete Research, Vol. 34, Pg. 329 -332, Feb. 2004

[14] H. M. Elkamchouchi, A. T Abdelkader, *"Shielding Effectiveness of reinforced Concrete Structures in cellular Communication"*, Proceedings of the Nineteenth National Radio Science Conference, Alexandra, Egypt, March, 2002, pp. 192 -198.

[15] G. Antonini, A. Orlandi, S. D'elia, *"Shielding Effects of Reinforced Concrete Structures to Electromagnetic Fields due to GSM and UMTS Systems"*, IEEE Trans on Magnetics, Vol 39, No 3, May 2003, pp. 1582 – 1585

[16] Chen Bin; Yi Yun; Gao Cheng; Zhou Bihua; and Wang Wei, *"Analysis of shielding effectiveness of reinforced concrete in high power electromagnetic environment"*, in Proc. Asia Pacific Conf. on Environmental Electromagnetic, CEEM 2003, Nov. 2003, pp. 547 – 553.

[17] Ogunsola, A.; U. Reggiani and L. Sandrolini, *"Shielding effectiveness of reinforced concrete structures"*, in Proc. Int. Conf. on Electromag. Compatib., Phuket, Thailand, July 2005, pp. 1A-2-1–1A-2-4.

[18] Casey, K.F, *"Electromagnetic Shielding Behaviour of Wire Mesh Screens"*, IEEE Trans Electromagn. Compatibility, Vol 30, No 3, August 1998, pp. 298 - 306

[19] Robert, A. *"Dielectric permittivity of concrete between 50 MHz and 1 GHz and GPR measurements for building materials evaluation"*, Journal of Applied Geophysics, Vol. 40, 1998, pp. 89 – 94.

[20] Gill, P. E. and Murry, W. *"Algorithms for the solution of non-linear least square problem"*, SAIM Journal on Numerical Analysis, Vol. 15, Pg. 977 – 992, 1978.

[21] Naishadham, K, *"Shielding effectiveness of conductive polymer"*, IEEE Trans on Electromagnetic Compatibilità, Vol. 34. No. 1, Feb 1992

[22] Rosenow, M. W. K and Ogunsola, A, *"EMI Shielding Effectiveness of Long Fibre Nickel Concentrates"*, International Conference on Conductive Coatings and Compounds, Brussels, June 1999

[23] Yang, S., Lozano, K., Lomeli, A, Foltz, Jones, Robert, *"Electromagnetic interference shielding effectiveness of carbon nanofiber/LCP composites"*, Composites Part A: Applied Science and Manufacturing, Vol. 36, Pg, 691 – 697, 2005.

[24] Rupprecht, L. *"Conductive polymers and plastics in industrial applications"*, Plastic Design Library, 1999

[25] Kaynak, A. *"Electromagnetic shielding effectiveness of galvanostatically synthesized conducting polypyrrole films in the 300 – 2000 MHz frequency range"*, Material Research Bulletin, Vol. 31, No. 7, Pg. 845 – 860, 1996

[26] Versieck, J, "*Electromagnetic shielding and protection against ESD by using stainless steel fibres*", International Conference on Conductive Coatings and Compounds, Brussels, June 1999

[27] Guan, H., Liu, S., Duan, Y. and Cheng, J, " *Cement based electromagnetic shielding and absorbing building materials*", Cement and Concrete Composite, Vol. 28, Pg. 468 – 474, 2006

[28] Wu, S., Mo, L., Shu, Z., and Chen, Z., "*Investigation of the conductivity of asphalt concrete containing conductive fillers*", Carbon, Vol. 43, Pg. 1358 – 1363, 2005.

[29] Wen, S., Chung, D. D. L, "*Partial replacement of carbon fiber by carbon black in multifunction cement-matrix composites*", Carbon, Vol. 45, Pg. 505 – 513, 2007.

[30] Makhnovskiy, D. P. and Panina, L. V, "*Field Dependent Permittivity of Composite Materials Containing Ferromagnetic Wires*", Journal of Applied Physics, American Institute of Physics, Vol. 93, No: 7, April 2003, pp. 4120 – 4129.

[31] Karr, P. R. and Smith, R. A, "*Electrical Properties of a Lossy Dielectric Containing Short Randomly Disposed Metal Fibers*", International Symposium on Antenna and Propagation, Vol. 17, June 1979, pp. 612 – 615.

[32] Ogunsola, A.; U. Reggiani and L. Sandrolini, "*Shielding effectiveness of concrete buildings*", in Proc. VIth Int. Symp. on Electromag. Compatib. and Electromag. Ecology, St Petersburg, Russia, June 2005, pp. 65-68.

[33] Pocklington, H. C., "*Electrical Oscillations in Wires*", Cambridge Philos. Soc. Proc., Vol. 9, 1897, pp. 324 -332.

[34] Onsager, L, "*Electric moments of molecules in liquids*", Journal of America Chemical Society, Vol. 58, 1486 – 1493, 1936.

[35] Savov, S.V and Herben, M.H.A.J, "*Modal transmission line modeling of propagation of plane radiowaves through multilayer periodic building structures*", IEEE Trans on Antenna and Propagation, Vol. 51, No 9, September 2003, pp.2244 – 2251.

[36] D. Pena, R. Feick, H. Hristov, and W. Grote, "*Measurement and Modeling of Propagation Losses in Brick and Concrete Walls for 900MHz Band*", IEEE Trans on Antenna and Propagation, Vol. 51, No 1, January 2003, pp. 31 -39

[37] Metwally, I. A; Zischank, W. J, and Hieder, F.H, "*Measurement of magnetic fields inside single and double layer reinforced concrete buildings during simulated lightning currents*", IEEE Trans on Electromagnetic Compatibility, Vol. 46, No 2, May 2004, pp. 208 – 221.

[38] Balanis, C. A, "*Advanced Engineering Electromagnetic*", John Wiley & Sons, 1991.

[39] Inan, U. S and Inan, A. S., "*Electromagnetic waves*", Prentice Hall, Upper Saddle River, NJ, USA, 2000

[40] Sadiku, M. N. O., "*Numerical Techniques in Electromagnetic*", 2nd Edition, CRC Press, USA.

[41] Tesche, F. M., Ianoz, M. V. and Karlsson, T., "*EMC Analysis Methods and Computational Models*", John Wiley & Sons, Inc., New York, 1997.

Chapter 8

DISCUSSION AND CONCLUSIONS

Electromagnetic interference in an electrified railway is an important issue and one that continues to impact the introduction of electrical and electronics equipment into railway revenue service. The complexity of the railway – the close proximity of high power electronics to high sensitive equipment coupled with the dual use of the running rails for signalling and electrification – demands the need to fully understand the electromagnetic coupling that can occur within the railway infrastructure.

Numerous studies have been undertaken which analyse the sources of interference within a railway with a view of assisting in the development of consensus EMC standards for railway application. Few of these works have a direct impact and application to the design of a railway system as a whole. With the design and build of Light Rail Transport (LRT) costing between £15 million to £30 million per km route, there is a desire to integrate and apply EMC engineering right from the conceptual design stage of a railway design or modernisation project. This is more so, since in-situ EMC testing on a railway could cost as high as £100,000 per day (considering lost revenue, etc). Without a doubt, it is desirable to be able to compare different design solutions with respect to problems relating to electromagnetic coupling during the railway design phase. Currently this aspect is not covered in any international EMC standard - and perhaps, this is one area that cannot be subject to standardization but remains within the realm of best practice and engineering design.

Numerical and analytical tools therefore have a very valuable role to play, especially where the output from such would provide positive engineering input and reduce the cost of validation and system safety/analysis. The theoretical basis for evaluating the electromagnetic coupling in railway lines has its roots in power transmission system.

An objective of this research was the feasibility study of the application of a commercially available numerical tool, in particular one based on Transmission Line Modelling (TLM) to the analysis of railway electromagnetic coupling to nearby metallic structures. In this thesis, TLM has been applied to two cases to highlight the applicability and usefulness within railway applications.

The first case, involves the numerical modelling of a railway line with the view of being able to predict/estimate the electromagnetic fields at distances close to the railway line – thus being able to influence design decisions with respect to cable management system design, the installation of sensitive equipment in close proximity to the railway etc. The second case, involves the direct application of numerical techniques to the design and construction of concrete structures; this provides direct input to the application of global shielding techniques within railway systems, system safety analysis as well as direct application in the investigation of the impact of reinforced concrete slabs on the correct operation of audio frequency track circuits. In addition, the thesis includes an analysis of the analytical methods as they apply to railway applications

8.1 Analytical Methods – Railway Electromagnetic Coupling

The analytical method used to study the electromagnetic coupling to buried structures close to the railway is an iterative approach based on the transmission line theory. The process requires the determination of the:

- Rail current and potential;
- Inductively coupled currents and potential;
- Conductively coupled currents and potential; and
- The total interfering current – a combination of the conductively and inductively coupled current.

In applying this analytical process, some assumptions are made (i.e. such as the system parameters are evenly distributed over the whole length) however these assumptions do not hold true in operational railways. The analytical approach is applied by considering the two rails as one equivalent rail located midway between the two actual rails. This approach is only valid, provided it is not applied to the study of electromagnetic coupling from one rail to nearby buried metallic structures.

For the simple railway model where the continuous rails are the only metallic part of the return current, obtaining the relevant parameters (i.e. rail current and potential) is straightforward as long as the relevant parameters are known. The inclusion of booster transformers is possible provided the booster transformer is considered ideal. However, as the complexity of the railway model increases the application of the analytical method becomes difficult.

The analytical approach is best suited to the analysis of electromagnetic coupling to structures that are parallel to the railway track. For non-parallel

structures, the problem is solved by segmenting the problem space into smaller sections of parallel equivalence.

8.2 TLM Application – Railway Electromagnetic Coupling

The failure of the analytical method when applied to complex railway installations leads us to search for alternative methods that can be applied to assist in the railway system design. In this case, a commercially available tool is desirable as it removes the cost associated with code development and any safety analysis, which may be required before railway application acceptance. Analytically, circuit theory is applied to analyse the electromagnetic coupling, however the problem can equally be solved by applying electromagnetic field theory. In this case, Transmission Line Matrix (TLM) based on a commercially available code - Microstripes™ - is applied.

TLM was chosen because of its ability to analyse complicated structures. The flexibility and versatility of the method resides in the fact that the TLM mesh incorporates the properties of the electromagnetic fields and their interaction with the boundaries and material media.

There are a few challenges in applying numerical techniques to a railway line. An obvious problem faced with applying numerical techniques to railways is the large difference in dimensions in the problem space. The earth as well as the length of the railway is in the kilometre range whereas the conductors (i.e. rails, signalling and communication cables etc) have radii in the millimetre range and the ballast layer has dimensions in the metre range. Another issue is the modelling of semi-infinite elements such as earth and air and the ability to model booster transformers. In the commercially available tool used, it was not possible to model transformers. Finally, the total volume of the model in a three - dimensional TLM model must be meshed and included in

the calculation resulting in time consuming analysis. Initial simple railway models took approximately 50 days to run.

To reduce the computational resource demand, the TLM railway model is kept as simple as possible. To achieve this the length of the railway was limited, the ballast layer was removed, coarse meshing was applied to areas directly surrounding the physical model and the earth was simply modelled as a conductive layer. The rails are modelled as circular conductors and placed directly on the earth surface and radii of the conductors are kept identical with the exception of the catenary wire.

8.3 Analytical Method – Application to Concrete Modelling

Concrete is extensively used in the railway for a variety of application - as building materials to sleepers. The functionality of the concrete structure may have an impact on signalling compatibility if not managed effectively. For example, audio frequency track circuits or inductive loop train control systems tend to "loose" some of their operating current when installed over reinforced concrete structures. As a result these devices tend to be operated above their recommended operating parameters in reinforced concrete areas resulting in reduced life time and high maintenance cost.

The method applied to analyse the electromagnetic wave propagation through concrete structure is based on Schelkunoff's theory, which in effect is a transmission line model based on the assumption of a plane wave. Structural discontinuities in the concrete structure are not considered and the structure is considered isotropic and homogenous. The impact of moisture content on the ability of the concrete structure to attenuate electromagnetic waves was incorporated into the analysis via the relationship between the impedance, permittivity and permeability of a material. The global shielding expression

for shielding, incorporating the reflection, absorption and re-reflection terms, was modified to include the presence of reinforcing rods in the structure.

The resultant global expression was easily resolved using commercially available mathematical software – Mathematica™. The advantage of the analytical approach is the ease in which the impact of individual electrical parameters on the shielding effectiveness of the structure can be investigated and analysed.

8.4 Numerical Method – Application to Concrete Modelling

Applying TLM to determine the shielding effectiveness of concrete structures and to investigate the impact of individual parameters on the shielding effectiveness of concrete was a lot easier than its application to investigate the electromagnetic coupling of railway noise to buried metallic structures. The main problem related to the material definition applicable to concrete within the software package used. It was noted that specifying concrete as a simple dielectric material produced shielding data, which were in conflict with those, obtained analytically. Modelling concrete as a simple dielectric material results in an over estimation of the loss factor and did not account for energy losses due to the electrical conductivity of concrete. Most importantly, the simple dielectric model fails to describe the behaviour of concrete at low frequencies.

Because of the shortcomings of modelling concrete as simple dielectric material, it became necessary to explore complex material models within TLM. Microstripes™ has the ability to model complex dielectric materials that obey either Debye or Lorentz characteristics. Concrete was modelled as a dielectric material having Debye characteristics. Modelling concrete as a Debye material results in greater correlation between the analytical and numerical results. It is observed that there are slight differences between the

shielding effectiveness obtained from the numerical and analytical methods but that these differences are explained by the differences between the measured electrical parameters used in the analytical method and those obtained by fitting the dispersive model. The difference becomes more pronounced when analysing concrete structures having high moisture content.

Using the fitted parameters for concrete in both methods results in a good agreement between the shielding effectiveness data obtained. It is concluded that while the Debye model appears to model the behaviour of concrete accurately, the material model begins to fail when investigating the behaviour of concrete with high moisture content. This suggest the need to implement other material models such as Cole – Cole, however such models do not exist in Microstripes™.

This work has lead to the development of a material model for concrete that can be implemented in numerical simulators such as TLM. The output of this work is directly applicable to areas such as signalling design within the railway where the impact of concrete structures, particularly reinforced concrete structures, on the correct operation of sensitive train control system is not fully understood. Other areas of influence include the application of ground penetrating radar as a non-destructive test to assess the integrity of railway civil structures, where the attenuation properties of concrete is an important parameter.

8.5 Conclusions

The application of numerical simulators such as TLM to the design and upgrade of railway systems is viable. The application however depends largely

on the development and availability of suitable system models that can be used in commercially available numerical simulators.

TLM can be used effectively in the conceptual design phases of a railway system design, and where it can be used to influence design decisions and investigate design options. It can be used to study special cases – as in the case of the study of the electrical properties of concrete. With appropriates models, it can be used to identify causes of known interference and investigate the effectiveness of different solutions.

There are slight differences between the analytical and numerical methods, one of the differences relate to the input parameters used in both models. The analytical model requires impedance parameters whereas TLM (in effect an electromagnetic field model) requires dimensions and material properties as input. The impedance concept is not used in TLM other than the internal impedance of conductors – an internal processed parameter not visible to the user. The impedance used in the analytical method are impedances with earth return obtained through calculation, since the presence of earth return in the model makes it impossible to perform measurements.

Calculation of earth return impedance is often associated with Carsons's equation – it is possible to use Dubanton's formula (also known as the complex penetration model) to derive the impedance. Carson's equation contains two components: (1) the ideal component of the mutual impedance as it represents the mutual impedance when the earth is a perfect conductor, and (2) a correction term that accounts for the finite conductivity of the earth. This correction term contributes both resistive and inductive components to the mutual impedance and is frequently larger than the ideal component. The uncertainties due to the variations in earth resistivity are sometimes large than the errors due to the use of Carson's equation.

Similarly, in the second case study, the electrical properties of concrete are properties that are obtainable only through measurement and then used as input in the analytical and numerical code. As shown in the analysis, good agreement is obtained between the analytical and numerical model when the same baseline data is used.

8.6 Future Work

Some remarks can be made regarding the continuation of the research that was started for this thesis.

- The railway model implemented in TLM is very simple and does not include some key components of the railway, such the booster transformer. It would be beneficial to further enhance the model to include booster transformers, in order that a better picture is obtained for the leakage currents.
- The railway model implemented in TLM assumes above ground conditions and does not include the presence of a railway tunnel. The electromagnetic characteristics of a train in a tunnel is one of great interest. An enhanced model with a train in the tunnel should be developed. The tunnel could be modelled with the concrete material model developed in this thesis.
- It is desirable to characterise the electromagnetic profile of the railway, in terms of leakage current and electromagnetic field propagation when a train is moving.
- An improvement to the concrete material model, perhaps based on Cole - Cole, for use in TLM would be useful.

Appendix A

THIN WIRE APPROXIMATION – FORTRAN CODE

This appendix describes the sub routine used to compute the current distribution of a steel fibre inclusive in conductive concrete. The code uses Pocklington's Integral Equation.

A.1 Fortran Code

The sub-routine is written in Fortran and based on the code given in Page 737 of *Advanced Engineering Electromagnetic* by C.A. Balanis, published by John Wiley.

```
C**************************************************
C  THIS PROGRAM USES POCKLINGTON'S INTEGRAL EQUATIONS OF      *
C   ON A SYMMETRICAL DIPOLE, AND IT COMPUTES THE CURRENT
    DISTRIBTUION,                                             *
C INPUT IMPEDANCE, NORMALIZED AMPLITUDE RADIATION PATTERN,
    AND SCATTERING PATTERNS                                   *
C                                                             *
C  GEOMETRY                                                   *
C  HL - HALF OF THE DIPOLE LENGTH (IN WAVELENGTHS)            *
C  RA - RADIUS OF THE WIRE (IN WAVELENGTHS)                   *
C  NU - TOTAL NUMBER OF SUBSECTIONS (MUST BE AN ODD INTEGER)  *
C                                                             *
C  IOPT- OPTIONS TO USE POCKLINGTON'S FORMULATION OF          *
C TO SOLVE THE WIRE ANTENNA PROBLEM OR THE WIRE SCATTERER
PROBLEM.                                                      *
C                                                             *
```

```
C  IOPT=1 : ANTENNA PROBLEM                                          *
C   IOPT=2 : WIRE SCATTERING PROBLEM                                 *
C            *** IGNORE OPTION ISCAT WHEN IOPT=1 ****                *
C  ISCAT=1 , MONOSTATIC RADAR CROSS SECTON                           *
C  ISCAT=2, BISTATIC RADAR CROSS SECTION                             *
C  NEEDS TO SPECIFY INCIDENT ANGLE                                   *
C  IEX - OPTION TO USE EITHER MAGNETIC-FRILL GENERATOR OR DELTA
GAP
C                                                                    *
C          *** IGNORE OPTION IEX WHEN IOPT=2 ***                     *
C  IEX =1 : MAGNETIC-FRILL GENERATOR                                 *
C  IEX =2 : DELTA GAP                                                *
C                                                                    *
C      *** IGNORE POLRD, AND THETD WHEN IOPT-1 ***                   *
C  POLRD- ELECTRIC FIELD POLARIZATION RELATIVE TO THE PLANE OF *
C  INCIDENCE, WHICH IS DEFINED AS THE PLANE CONTAINING THE           *
C  INCIDENT WAVE VECTOR AND THE WIRE SCATTERER. REFER TO             *
C  FIGURE 7.23 FOR THE SCATTERER'S GEOMETRY (IN DEGREES).            *
C  THETD- THE INCIDENT ANGLE RELATIVE TO THE Z-AXIS (IN DEGREES*
C      *** THETD IS NEEDED FOR BISTATIC CASE ONLY ***                *
C                                                                    *
C  THIS PROGRAM USES PULSE EXPANSION FOR THE ELECTRIC CURRENT *
   MODE                                                              *
C  AND POINT-MATCHING THE ELECTRIC FIELD AT THE CENTER OF EACH*
C  WIRE SEGMENT.                                                     *
C                                                                    *
C********************************************** *******

C EXAMPLE A: HOW TO SPECIFY THE NUMBER OF SUBSECTIONS OF THE
   ANTENNA

C          OR SCATTERER. NM=21 FOR THIS EXAMPLE.

      PARAMETER ( NM=61, NMT=2*NM-1 )

      REAL LAMBDA,MU0,EPS1,EPS2,BETARE,BETAIM,ETARE,ETAIM

      COMMON/SIZE/HL,RA,DZ,ZM,ZN,NMH,LAMBDA,FREQ
```

```
      COMMON/CONST/BETA,ETA,RAD,J,PI
      COMPLEX ZMN(NMT) ,WA(NMT),CGA(NM) ,ZIN, J,CRT
      DIMENSION INDEX(NM),ETMM(181)
       EXTERNAL CGP
       DATA POLRD,THETD,ISCAT/0.0,0.0,0/

C     ********** CHOICE OF OUTPUT **********
C
          OPEN(UNIT=2,FILE='RESULTS.dat',STATUS='NEW')
         OPEN(UNIT=3,FILE='PWRSinp.dat',STATUS='OLD')

C    EXAMPLE B: HOW TO SPECIFY THE ANTENNA PROBLEM USING
MAGNETIC
   FRILL
C       IOPT=1
C       IEX=1
C    EXAMPLE C: HOW TO SPECIFY THE ANTENNA PROBLEM USING DELTA
GAP
C      IOPT=1
C      IEX=2
C EXAMPLE D: HOW TO SPECIFY THE MONOSTATIC SCATTERING PROBLEM
C      IOPT=2
       ISCAT=1
C    THE ANGLES OF INCIDENCE AND POLARIZATION ARE READ FROM A
FILE
CC     POLRD=0.0
CC    THETAINC=90.0
```

```
C    READ SOME DATA FROM THE INPUT FILE
READ                                                    (3,*,ERR=9999)
EPS1,EPS2,BETARE,BETAIM,ETARE,ETAIM,THETAINC,POLRD
C    IEX=1
C     EXAMPLE E: HOW TO SPECIFY THE BISTATIC SCATTERING PROBLEM
C     AT A POLARIZATION ANGLE OF 45 DEGREES,
C     AND AN INCIDENT ANGLE OF 60 DEGREES
C     IOPT=2
C     ISCAT=2
C     POLRD=45.0
C     THETD=30.0
C THE PRESET EXAMPLE HERE IS THE WIRE ANTENNA PROBLEM OF
   MAGNETIC
C    FRILL GENERATOR MODEL
CCC      IOPT=1
CCC      IEX=1
C . . SOME CONSTANTS
         PI=3.14159265
         MU0=4.*PI*1.E-7
         EPS0=8.854*1.E-12
         RAD=PI/180.
         J=CMPLX(0.,1.)
C        FREQUENCY and WAVELENGTH
         FREQ=500.0*1.E6
C . .    IN FREE SPACE
```

```
C       LAMBDA=1./SQRT(MU0*EPS0)/FREQ
C       BETA=2.0*PI/LAMBDA
C       ETA=120.*PI
C . . IN CONCRETE
CCC     EPS1=4.61982
CCC     EPS2=0.143723

LAMBDA=1/SQRT(MU0)/SQRT(0.5*(SQRT((EPS1*EPS0)**2+(EPS2*EPS0)**2)
      +(EPS1*EPS0)))/FREQ
C . . BETA IS THE COMPLEX PROPAGATION CONSTANT IN CONCRETE AND
ETA
    IS THE CONCRETE COMPLEX IMPEDANCE.
C . . THEY NEED TO BE CALCULATED BY MATHEMATICA AND INSERTED
HERE
     FOR EACH NEW MOISTURE CONTENT OR FREQUENCY.
CCC     BETA=CMPLX(0.350313,22.5263)
CCC     ETA=CMPLX(175.212,2.72478)
        BETA=CMPLX(BETARE,BETAIM)
        ETA=CMPLX(ETARE,ETAIM)
       WRITE (6,46) MU0,EPS0
       WRITE(6,48) FREQ,LAMBDA
C . . GEOMETRY DATA
C . . EXAMPLE: DIPOLE HALF LENGTH OF 0.235 WAVELENGTHS
C . . AND WIRE RADIUS OF 0.005 WAVELENGTHS.
       HL=30./2.*1E-3
       RA=.5/2.*1E-3
      NMH=0.5*(NM+1)
       DZ=2. *HL/NM
```

```
      IF(IOPT.EQ.1) THEN
      WRITE(6,50) HL,RA
      IF(IEX.EQ.1) WRITE(6,100)
      IF(IEX.EQ.2) WRITE(6,102)
      ELSE
      WRITE(6,52) HL,RA
      ENDIF
      WRITE(6,54) NM
C . . THE IMPEDANCE MATRIX HAS A TOEPLITZ PROPERTY, THEREFORE ONLY
C . . NM ELEMENTS NEED TO BE COMPUTED, AND THE MATRIX IS FILLED I N
C . . A FORM THAT CAN BE SOLVED BY A TOEPLITZ MATRIX SOLVING
      SUBROUTINE
      ZM=HL-0.5*DZ
      B=0.5*DZ
      A=-0.5*DZ
      DO 4 I=1,NM
      ZN=HL-(I-0.5)*DZ
      CALL CSINT(CGP,A,B,79,CRT)
      ZMN(I)=CRT
      IF (I .EQ. 1) GOTO 4
      ZMN(NM+I-1)=CRT
4     CONTINUE
      IF(IOPT.EQ.2.AND.ISCAT.EQ.1) GOTO 60
      IF(IOPT.EQ.1) THEN
      RB=2.3*RA
```

```
      TLAB=2.*ALOG(2.3)
      DO 10 I=1,NM
      ZI=HL-(I-0.5)*DZ
      R1=BETA*SQRT(ZI*ZI+RA*RA)
      R2=BETA*SQRT(ZI*ZI+RB*RB)
      IF(IEX.EQ.1) THEN
      CGA(I)=-J*BETA**2/(ETA*TLAB)*(CEXP(-J*R1)/R1-CEXP(-J*R2)/R2)
      ELSE
        IF(IEX.NE.2) WRITE(6,999)
        IF(I.NE.NMH) THEN
        CGA(I)=0.
        ELSE
       CGA(I)=-J*BETA/(ETA*DZ)
       ENDIF
       END IF
10     CONTINUE
       CALL TSLZ(ZMN,CGA,WA,NM)
C . . OUTPUT THE CURRENT DISTRIBUTION ALONG OF THE DIPOLE
       WRITE(6,104)
       DO 12 I=1,NMH
       XI=HL-(I-. 5)*DZ
      YI=CABS(CGA(I))
      WRITE(6,106) I, XI , CGA(I) , YI
12     CONTINUE
C . . COMPUTATION OF THE INPUT IMPEDANCE
       ZIN=1./CGA(NMH)
```

```
      WRITE(6,108) ZIN
C . . COMPUTATION OF AMPLITUDE RADIATION PATTERN OF THE
ANTENNA
      CALL PATN(CGA,NM,ETMM,IOPT)
      WRITE(6,110)
      DO 14 I=1,181
      XI=I-1.
14    WRITE(6,112) XI, ETMM(I)
      ELSE
C . . WIRE SCATTERER PROBLEM, BISTATIC CASE
      IF(IOPT.NE.2) WRITE(6,999)
      IF(ISCAT.NE.2) WRITE(6,999)
      CTH=COS(THETD*RAD)
      STH=SIN(THETD*RAD)
      CSPL=COS(POLRD*RAD)
      DO 15 I=1,NM
      Z1=HL- (I-0.5)*DZ
15      CGA(I)=-J*BETA/ETA*CSPL*STH*CEXP(J*BETA*ZI*CTH)
C . .     NOW SOLVE FOR THE CURRENT DISTRIBUTION
          CALL TSLZ(ZMN,CGA,WA,NM)
C . . COMPUTE THE PATTERN
          WRITE(6,120)
          WRITE(6,122) THETD,POLRD
          DO 20 I=1, NM
          XI=HL-(I-0.5)*DZ
          YI=CABS(CGA(I))
```

```
          WRITE(6,124) XI,CGA(I),YI
20        CONTINUE
C . . COMPUTATION OF BISTATIC RCS PATTERNS
          CALL PATN(CGA,NM,ETMM,IOPT)
          WRITE(6,126)
          DO 40 I=1,181 XI=I-1.
          WRITE(6,128) XI,ETMM(I)
40        CONTINUE
          ENDIF
          GOTO 200
C . . THE MONOSTATIC CASE
C . . THIS IS THE CASE WE ARE INTERESTED IN
60   WRITE(6,140)
     DO 70 M=1,91
     THETA=(M-1.)*RAD
     CTH=COS(THETA)
     STH=SIN(THETA)
    CSPL=COS(POLRD*RAD)
     DO 62 I=1,NM
    ZI=HL-(I-0.5)*DZ
C  62     CGA(I)=-J*BETA/ETA*CSPL*STH*CEXP(J*BETA*ZI*CTH)
 62              CGA(I)=-J*2.*PI*FREQ*CMPLX(EPS1,-EPS2)*EPS0*CSPL*STH*CEXP
    (J*BETA*ZI*CTH)
      CALL TSLZ(ZMN,CGA,WA,NM)
     IF(THETA.EQ.THETAINC*RAD) THEN
      WRITE(2,122) THETA/RAD,POLRD
```

```
      DO 320 I=1, NM
      XI=HL-(I-0.5)*DZ
     YI=CABS(CGA(I))
     WRITE(2,124) XI,CGA(I),YI
320   CONTINUE
      ENDIF
      IF(ABS(CTH).LE.1.E-3) THEN
      FT=1.
      ELSE
      FT=SIN(BETA*DZ*CTH*.5)/(BETA*DZ*CTH*.5)
      ENDIF
      CRT=0.
      DO 64 I=1 ,NM
     ZI=HL-(I-.5)*DZ
    CRT=CRT+CEXP(J*BETA*ZI*CTH)*FT*CGA(I)*DZ
64    CONTINUE
      PTT=CABS(CRT)*STH*STH*ETA*0.5
     PTT=PTT*PTT*BETA*2.
     IF(PTT.LE.1.E-10) PTT=1.E-10
     PTT=10. *ALOG10(PTT)
        ETMM(M)=PTT
70      ETMM(182-M)=PTT
        WRITE(6,142) POLRD
        WRITE(6,144)
        DO 72 I=1,181
       XI=I-1
```

```
72      WRITE(6,146) XI , ETMM(I)
46    FORMAT(15X, 'SOME CONSTANTS'//5X, 'MU0= ', E12.4,' (H/m)', 4X , 'EPS0=',
       E12.4,' (F/m)'/)
48    FORMAT(15X, 'INITIAL SETTINGS'//5X, 'FREQ = ', E12.4, ' (Hz)',4X,
       WAVELENGTH=',E12.4,' (m)'/)

50      FORMAT(15X, 'WIRE ANTENNA PR0BLEM'//5X, 'LENGTH = 2 X ', F6.4, '
(m)',                                                          4X,
      'RADIUS OF THE WIRE=',F6.4,' (m) '/)
52     FORMAT(15X,'WIRE SCATTERER PROBLEM'//5X,'LENGTH = 2 X ' , F 6.4 , '
(m)',
      4X,'RADIUS OF THE WIRE=',F6.4,' (m) '/)
54    FORMAT(15X,'NUMBER OF SUBSECTIONS = ' ,I3/)
100   FORMAT(5X, 'POCKLINGTON"S EQUATION AND MAGNETIC FRILL
       MODEL'/)
102    FORMAT(5X,'POCKLINGTON"S EQUATION AND DELTA GAP MODEL'/)
104    FORMAT(10X,'CURRENT DISTRIBUTION ALONG ONE HALF OF THE
       DIPOLE'/8X,'POSITION Z',3X,'REAL
PART',3X,'IMAGINARY',3X,'MAGNITUDE'/)
106    FORMAT(3X,I3,4X,F6.4,5X,F9.6,3X,F9.6,3X,F9.6)
108     FORMAT(/3X,'INPUT IMPEDANCE = ' , F 7.1 , ' + J' , F 7.1 , ' (OMS)')
110    FORMAT(/3X,'RADIATION POWER PATTERN VS OBSERVATION ANGLE
       THETA'//3X,'THETA ( IN DEGREES)',2X,'POWER ( IN DB)')
112    FORMAT(8X,F6.1,8X,F8.2)
120          FORMAT(4X,'BISTATIC WIRE SCATTERER PROBLEM WITH
POCKLINGT0N"S
       ',' EQUATION'//)
122    FORMAT(8X,'#INCIDENT ANGLE=',F5.1,' DEGREES,
POLARIZATION=',F5.1,
 ' DEGREEES'//10X,'#CURRENT DISTRIBUTION ALONG THE
```

```
DIPOLE'//8X,'#POSITION Z', 3X,'REAL
PART',3X,'IMAGINARY',3X,'MAGNITUDE'/)
C 124   FORMAT(10X,F6.4,5X,F9.6,3X,F9.6,3X,F9.6)
124     FORMAT(10X,F6.4,5X,E12.4,5X,E12.4,5X,E12.4)
126   FORMAT(/4X,'BISTATIC RADAR CROSS SECTION PATTERN VS
      OBSERVATION', ' ANGLE THETA '//8X,'THETA(IN DEGREES) ',2X,'RCS
      (IN DBSM)')
128     FORMAT(12X,F6.1,8X,F10.2)
140   FORMAT(4X,'MONOSTATIC WIRE SCATTERER PROBLEM WITH
      POCKLINGTON"S',' EQUATION'/)
142   FORMAT(4X,'THE POLARIZATION TO THE PLANE OF INCIDENCE = ' ,
      F 5.1 , ' DEGREES '/)
144   FORMAT ( 14X ,' THE MONOSTATIC RADAR CROSS SECTION PATTERN'//
      10X, ' INCIDENT ANGLE (THETA) ' ,5X, 'RCS IN (DBSM) ' )
146     FORMAT(20X,F7.2,15X,F10.2)
500     FORMAT(E12.4,/,E12.4,/,E12.4,/,E12.4,/,E12.4,/,E12.4)
999   FORMAT(5X,'******WARNING: NO SUCH OPTION. CHOOSE A VALID
      OPTION'/20X,'AND TRY AGAIN.')
200     STOP
C
C     ********** ERROR CONDITIONS **********
C
9999      WRITE(6,10000)
10000   FORMAT(/,3X,'***** ERROR *****',/,3X
     $    ,'INPUT DATA ARE NOT OF THE RIGHT FORMAT',/)

        END
C..
```

```
      COMPLEX FUNCTION CGP(Z)
C..   POKLINGTON'S KERNEL
      COMMON/SIZE/HL,RA,DZ,ZM,ZN,NMH,LAMBDA,FREQ
      COMMON/CONST/BETA , ETA, RAD , J,PI
      COMPLEX J
      Z1=ZN-ZM +Z
      R=SQRT(RA*RA+Z1*Z1)
      CGP=CEXP(-J*BETA*R)*((1.+J*BETA*R)*(2.*R*R-
3.*RA*RA)+(BETA*RA*R)**2)/
      (4. *PI*R**5)
      RETURN
      END
C.
      SUBROUTINE PATN(CGA,NM,ETMM,IOPT)
C.. THE SUBROUTINE TO COMPUTE THE RADIATION PATTERN
      COMMON/SIZE/HL,RA,DZ,ZM,ZN,NMH,LAMBDA,FREQ
      COMMON/CONST/BETA,ETA,RAD,J,PI
      COMPLEX CGA(NM),J,CRT
     DIMENSION ETMM(181)
     DO 4 I=1,181
     THETA=(I-1.)*RAD
     CTH=COS(THETA)
     STH=SIN(THETA)
     IF(ABS(CTH).LE.1.E-3) THEN
     FT=1.
    ELSE
```

```
      FT=SIN(BETA*DZ*CTH*. 5)/(BETA*DZ*CTH*. 5 )
      ENDIF
            CRT=0.
            DO 2 M=1,NM
            ZM=HL-(M-. 5) *DZ
            CRT=CRT+CEXP(J*BETA*ZM*CTH)*FT*CGA(M)*DZ
2           CONTINUE
            PTT=CABS(CRT)*STH*STH*ETA*0.5
4           ETMM(I)=PTT
            IF(IOPT.EQ.1) THEN
           AMAX=ETMM(1)
            DO 6 I=2.181
            IF(ETMM(I).GT.AMAX) AMAX=ETMM(I)
6           CONTINUE
            DO 8 I=1,181
            PTT=ETMM(I)/AMAX
            IF(PTT. LE. 1. E-5) PTT=1.E-5
8           ETMM(I)=20.*ALOG10(PTT)
           ELSE
            DO 10 I=1,181
            PTT=ETMM(I)**2*BETA*2.
           IF(PTT.LT.1.E-10) PTT=1.E-10
10         ETMM(I)= 10.*A LOG10(PTT)
            ENDIF
           RETURN
           END
```

```
C*********************************************** ******
**
C     SUBROUTINE TS L
      NETLIB
C     INPUT :
C     (C)A(2*M - 1)
C     THE FIRST ROW OF THE T-MATRIX FOLLOWED BY ITS FIRST COLUMN
C          BEGINNING WITH THE SECOND ELEMENT. ON RETURN A IS
UNALTERED.
C     (C)B(M)
C     THE RIGHT HAND SIDE VECTOR B.
C     (C)WA(2*M-2)
C     A WORK AREA VECTOR
C     ORDER OF MATRIX A.
C     OUTPUT
C     (C)B(M)
C     THE SOLUTION VECTOR.
C     PURPOSE:
C     SOLVE A SYSTEM OF EQUATIONS DESCRIBED BY A TOEPLITZ MATRIX.
C     A * X = B
C     SUBROUTINES AND FUNCTIONS:
C     TOEPLITZ PACKAGE . . . TSLZ1
C*********************************************** ******
*
      SUBROUTINE TSLZ(A,B,WA,M)
      INTEGER M
     COMPLEX A(2*M-1),B(M),WA(2*M-2)
```

```
      CALL TSLZ1(A,A(M+1),B,B,WA,WA(M-1),M)
      RETURN
      END
C..   SUBROUTINE TSLZ1(A1,A2,B,X,C1,C2,M)
      INTEGER M
      COMPLEX A1(M) ,A2(M-1),B(M),X(M),C1(M-1) ,C2(M-1)
      INTEGER I1,I2,N,N1,N2
      COMPLEX R1,R2,R3,R5,R6
      R1 = A1(1)
      X(1)=B(1)/R1
      IF (M .EQ. 1) GOTO 80
      DO 70 N = 2 , M
      N1=N-1
      N2 = N - 2
      R5 = A2(N1)
      R6 = A1(N)
      IF (N .EQ. 2) GOTO 20
      C1(N1) = R2
      DO 10 I1 = 1, N2
      I2 = N - I1
          R5 = R5 + A2(I1)*C1(I2)
          R6 = R6 + A1(I1+1) * C2(I1)
10        CONTINUE
20        CONTINUE
          R2 = -R5/R1
          R3 = -R6/R1
```

```
      R1 = R1 + R5*R3
      IF (N .EQ. 2) GOTO 40
      R6 = C2(1)
      C2(N1) = (0.0D0,0.0D0)
      DO 30 I1 = 2 , N1
      R5 = C2(I1)
      C2(I1) = C1(I1)*R3 + R6
      C1(I1) = C1(I1) + R6*R2
      R6 = R5
30    CONTINUE
40    CONTINUE
      C2(1) = R3
      R5 = (0.0D0,0.0D0)
      DO 50 I1 = 1, N1
      I2 = N - I1
      R5 = R5 + A2(I1) * X(I2)
50    CONTINUE
      R6 = (B(N) - R5)/R1
      DO 60 I1 = 1, N1
      X(I1) = X(I1) + C2(I1)*R6
60    CONTINUE
      X(N) = R6
70    CONTINUE
80    CONTINUE
      RETURN
      END
```

```
C..   SUBROUTINE CSINT(CF,XL,XU,N,CRT)
C..   FAST ALGORITHM FORM OF THE SIMPSON'S INTEGRAL ROUTINE
      IMPLICIT COMPLEX (C)
      CRT=CF(XL)+CF(XU)
      HD=(XU-XL)/(N+1)
      DO 20 I=1 ,N
      XI=XL+I*HD
      IF(MOD(I,2) . NE. 0) THEN
     CRT=CRT+4. *CF(XI)
     ELSE
     CRT=CRT+2.*CF(XI)
     ENDIF
20   CONTINUE
     CRT=CRT*HD*0.33333333
     RETURN
     END
```